



SIMÃO FREITAS GONÇALVES

Bachelor of Biomedical Engineering

**DEVELOPMENT OF AN UPPER LIMB
MYOELECTRIC PROTHESIS IN
FLEXIBLE/HYBRID MATERIAL,
FOR APPLICATION IN YOUNG PATIENTS**

DISSERTATION SUBMITTED IN PARTIAL FULFILLMENT OF THE
REQUIREMENTS FOR THE DEGREE OF MASTER OF SCIENCE IN
BIOMEDICAL ENGINEERING

MASTER IN BIOMEDICAL ENGINEERING

NOVA University Lisbon
march, 2023



DEVELOPMENT OF AN UPPER LIMB MYOELECTRIC PROTHESIS IN FLEXIBLE/HYBRID MATERIAL, FOR APPLICATION IN YOUNG PATIENTS

DISSERTATION SUBMITTED IN PARTIAL FULFILLMENT OF THE REQUIREMENTS
FOR THE DEGREE OF MASTER OF SCIENCE IN BIOMEDICAL ENGINEERING

SIMÃO FREITAS GONÇALVES

Bachelor of Biomedical Engineering

Adviser: Bruno Alexandre Rodrigues Simões Soares

Associate Professor, NOVA University Lisbon

Co-adviser: Nuno Miguel de Pinto Lobo Matela

Associate Professor, Faculty of Sciences of the University of Lisbon

Development of an Upper Limb Myoelectric Prosthesis in Flexible/Hybrid Material, for Application in Young Patients

Copyright © Simão Freitas Gonçalves, NOVA School of Science and Technology, NOVA University Lisbon.

The NOVA School of Science and Technology and the NOVA University Lisbon have the right, perpetual and without geographical boundaries, to file and publish this dissertation through printed copies reproduced on paper or on digital form, or by any other means known or that may be invented, and to disseminate through scientific repositories and admit its copying and distribution for non-commercial, educational or research purposes, as long as credit is given to the author and editor.

To my family and many friends.

Acknowledgements

The path to this point was not easy, but working on this thesis was an exciting and exceptional experience and the best way to finish this last chapter of my academic life. It was a remarkable journey full of setbacks, mistakes, acknowledgements and resilience. However, knowing this thesis can help contribute to the scientific community and affect many people in the future, kept me motivated and focused on this work as well as on giving my best.

This work would not be possible without the support of my supervisors, Prof. Dr. Bruno Soares, Prof. Dr. Nuno Matela and Prof. Dr^a Cláudia Quaresma. I would like to express my gratitude for their professionalism, understanding, guidance and assistance during this journey.

Secondly, I would like to thank to my professors that challenged me to push further and to learn more, influenced and guided me in my academic life.

At last, I would like to thank my family and friends, especially my parents, for their emotional support during this journey. Thank you for giving me the encouragement I needed through these five years.

Thank you!

*“Ability is what you ´re capable of doing.
Motivation determines what you do. Attitude
determines how well you do it.” (Lou Holtz)*

Abstract

With the recent developments in the Additive Manufacturing (AM) industry, new methods of prostheses production have taken over the prosthetic industry. These new prostheses models produced using 3-Dimensional (3D)-printing methods solve some of the issues of the most common prostheses, such as cost and weight, but, despite their growth, still present high rejection rates, especially in children. These rejections are mostly related to the low levels of anthropomorphism and limitations in terms of functionality associated to 3D printed prostheses. The main goal of this study was to develop an aesthetically appealing 3D printed myoelectric prosthesis for a four year old child with a transverse metacarpal total deficiency.

The development of the prosthesis was based on the assessment and improvement of current 3D printable prosthetic models, and the integration of a myoelectric classifier and the electronic components into the model. The whole prosthesis was designed using a combination of the *Fusion 360 CAD* and *SolidWorks CAD 2021* softwares, and produced using *The Original Prusa i3 MK3S* with polyactic acid (PLA) or *Filaflex* filaments. The prosthesis was designed through an iterative process, where several prototypes were developed in order to optimise its appearance and functionality. Some printed models were subjected to pull tests, that evaluated its flexibility and allowed the development of the electronic sector of the prosthesis.

The developed prosthesis possessed a high level of anthropomorphism and functionality, consisting of a solution that is quite similar to the human hand and was able to simulate the intended movements, although with some limitations. Additionally, the device was relatively cheap and light when compared to existing 3D-printed myoelectric prostheses.

Although this thesis has some limitations, it certainly contributed to clarify many of the doubts that still exist in the scientific community. Hopefully, it will help to further develop the prosthetic industry.

Keywords: Additive Manufacturing, 3D modelling, upper limb prosthesis, myoelectric prosthesis, flexible materials, servomotors

Resumo

Nos últimos anos, o desenvolvimento de técnicas de Manufatura Aditiva (MA) tem permitido a evolução nos métodos de produção de próteses. Esses novos modelos de próteses produzidos usando métodos de impressão 3D resolvem alguns dos problemas das próteses mais comuns no mercado, como custo e peso, mas, apesar destes avanços, ainda apresenta altas taxas de rejeição, principalmente em crianças. Essas taxas de rejeição estão muitas vezes relacionadas com os baixos níveis de antropomorfismo e funcionalidade destes modelos. O principal objetivo deste estudo tornou-se então desenvolver uma prótese mioelétrica esteticamente atraente, produzida através de impressão 3D, para uma criança de quatro anos e com deficiência total do metacarpo transversal.

O desenvolvimento da prótese deu-se por meio da avaliação dos modelos atuais de próteses produzidos por impressão 3D, melhoria das suas características e integração de um classificador mioelétrico e os componentes eletrônicos associados. A prótese foi toda projetada usando uma combinação dos softwares *Fusion 360 CAD* e *SolidWorks CAD 2021* e produzido utilizando a *The Original Prusa i3 MK3S* e filamentos de PLA ou *Filaflex*. A prótese foi concebida através de um processo iterativo, onde vários protótipos foram desenvolvidos de forma a otimizar a sua aparência e funcionalidade. Alguns dos modelos impressos foram submetidos a testes de tração, de forma a avaliar a sua flexibilidade e desenvolver as componentes eletrônicas da prótese.

A prótese desenvolvida possuía um alto nível de antropomorfismo e funcionalidade, obtendo-se uma solução bastante semelhante à mão humana capaz de simular, embora com algumas limitações, os movimentos pretendidos. Além disso, o dispositivo é relativamente barato e leve quando comparado com outros modelos de próteses produzidos por impressão 3D.

Embora o protótipo final tenha algumas limitações, certamente contribuiu para o desenvolvimento do modelo prótico e esclarece alguns dos problemas em modelos antigos. Espera-se que este estudo ajude a aprofundar e desenvolver a indústria das próteses.

Palavras-chave: Manufatura Aditiva, modelação 3D, prótese de membro superior, prótese mioelétrica, materiais flexíveis, servomotores

Contents

List of Figures	xix
List of Tables	xxv
Glossary	xxvii
Acronyms	xxix
1 Introduction	1
1.1 Objectives	2
2 Clinical Background	5
2.1 Upper Limb Anatomy	5
2.2 Upper Limb Pathologies	7
2.2.1 Congenital Malformation	7
2.2.2 Amputation and Trauma	7
2.3 Current Prosthetic Solutions	9
2.3.1 Passive Prosthesis	9
2.3.2 Body-Powered Prosthesis	11
2.3.3 Electrical Prosthesis	11
2.3.4 Myoelectric Prosthesis	11
2.3.5 User Needs	12
3 Additive Manufacturing	15
3.1 Additive Manufacturing Methods	16
3.2 Fused Deposition Modeling Method	18
4 Electromyography as an Input of Myoelectric Control	21
4.1 Signal Acquisition Using Surface EMG	22
4.1.1 EMG Electrode Placement and Signal Acquisition Technique . .	24
4.2 Electromyography as an Input of Myoelectric Control	24

5	State of Art	27
5.1	Early History of Artificial Limbs	27
5.2	Overall Analysis of Current Prosthetic Devices	29
6	Concept Development	35
6.1	Introduction to the Study	35
6.2	Methodology	35
6.2.1	Prosthesis Design	36
6.2.2	Tuning of the Printing Parameters	39
6.2.3	Pull Tests	41
6.2.4	Integrating Hardware and Software for Myoelectric Control	42
6.2.5	Prosthesis Assembly	44
6.2.6	Prosthesis Evaluation	50
7	Results and Discussion	53
7.1	Prosthesis Design	53
7.1.1	Fingers Design	54
7.1.2	Wrist Region Design	59
7.1.3	Metacarpal Region Design	62
7.2	Tuning of the Printing Parameters	68
7.2.1	Influence of Layer Orientation	69
7.2.2	Switching Printing Parameters Mid Print	69
7.2.3	Pull Tests	70
7.3	Integrated Hardware and Software for Myoelectric Control	74
7.3.1	EMG Signal Acquisition and Processing	75
7.3.2	Electronic Integration for Myoelectric Control	80
7.4	Motor Powered Components	84
7.4.1	Parameters Identification of the Servomotor	84
7.5	Prosthesis Assembly and Functionality	91
7.6	Prosthesis Evaluation	99
7.6.1	Prosthesis Characteristics	101
7.6.2	System Usability Scale Assessment	102
8	Conclusion	105
8.1	Summary of the Study Achievements	105
8.2	Future Work	107
	Bibliography	109
	Appendices	
A	Additional Details on the Concept Development	117

B Filament Technical Data Sheet	119
C Recommended Printing Parameters	123
D Pull Tests	127
E System Usability Scale	143
F Prosthesis Costs	149

List of Figures

2.1	Upper Limb Bone Structure [16]	5
2.2	Upper Limb Movements: (a) Abduction and Adduction of the arm, (b) Flexion of the arm, (c) Internal and External rotation, (d) Flexion of the forearm [16]	6
2.3	Wrist Movements: (a) Radial deviation, (b) Ulnar deviation, (c) Wrist extension, (d) Wrist flexion, (e) Finger extension, (f) Finger flexion, (g) Supination, (h) Pronation [16]	6
2.4	Grasp Movements: (A) Pentadigital grip, (B) Petradigital grip, (C) Tridigital grip [16]	7
2.5	Amniotic Band Syndrome [22]	9
2.6	Amputation Levels of the Upper Limb [17]	10
2.7	Passive Prosthesis of the Upper Limb [24]	10
2.8	e-NABLE Body-Powered Prosthesis of the Upper Limb [13]	11
2.9	Electric Prosthesis Structure [27]	12
2.10	Myoelectric Prosthesis [26]	12
3.1	3D Printing Mechanism [33]	15
3.2	Sterolithography Method [34]	16
3.3	Selective Laser Sintering Method [35]	17
3.4	Fused Deposition Modeling Method [36]	17
3.5	Binder Jetting Method [37]	18
3.6	PolyJet Method [38]	18
3.7	Structure of the 3D Printer <i>Original Prusa i3 MK3S+</i> : 1. Extruder motor; 2. Filament; 3. Filament Support; 4. Fan; 5. Extruder; 6. Motherboard; 7. Heating bed support; 8. Control Panel; 9. <i>Reset</i> Button; 10-11. Control Buttons; 12. Magnetic heating bed. [42]	19
4.1	Diagram of the sliding filament theory [46].	22
4.2	Diagram of surface Electromyography (EMG) signal acquisition method [27].	23
4.3	Diagram of ideal electrode placement in regards to the orientation of the muscle fibers [55].	24

5.1	Egyptian prosthetic toe believed to be one of the earliest prosthetic devices made [57].	27
5.2	Medieval artificial limbs that allowed amputees to continue their fighting careers [57].	28
5.3	<i>e-Nable</i> Project Prosthesis Models [60]	30
5.4	Nazree ´s Prosthetic Hand [61].	30
5.5	Design details of the components of the body-powered hand prosthesis developed by F. Pinheiro [62]: (a) anterior view of the hand body; (b) top view of the hand body; (c) inner design of the finger.	31
5.6	Main developed prosthesis by Ana Oliveira ´s thesis [63]: (a) anterior view; (b) posterior view.	32
5.7	Example of the measurement process of the child ´s upper limbs [63]: (a) first position; (b) second position; (c) third position.	32
5.8	Upper limb ´s extremities replicas made with plaster [63]: (a) Left extremity with a transverse metacarpal total deficiency; (b) Dorsal (left) and palmar (right) views of the healthy right healthy hand.	33
5.9	<i>Ottobock</i> Prosthesis Models [64]	33
6.1	Methodology flowchart	37
6.2	Modification process of the design file: (a) mesh representation; (b) mesh representation after reducing the number of faces to under 10 000; (c) body representation.	38
6.3	Tested printing settings of <i>PrusaSlicer</i> software.	40
6.4	Tested printer settings of <i>PrusaSlicer</i> software	40
6.5	Tested filament settings of <i>PrusaSlicer</i> software.	41
6.6	Pull tests setup used in this and Ana Oliveira ´s study [63].	42
6.7	Illustration of the acquired movements [69].	43
6.8	Prosthesis components for its assembly.	45
6.9	Process of wiring of the fingers.	46
6.10	Process of connecting the fingers to the metacarpal piece and wiring of the metacarpal region.	46
6.11	Process of connecting the fingers to the servomotors, whilst passing through the metacarpal region piece.	47
6.12	Process of assembling the pins that connect the metacarpal region structure to the forearm gauntlet.	48
6.13	Exploded view of the prosthesis.	48
6.14	Interfacing a single servomotor with an Arduino Uno.	49
6.15	Interfacing servomotors with Arduino board.	49
6.16	Interfacing HC-05 Bluetooth Module with Arduino Uno.	50
6.17	Circuit diagram used in the prosthesis prototype.	50

7.1	Comparison between the plaster replicas (above) and the <i>.stl</i> files resulting from the 3D scanning procedure (below) [63]: (a) left upper limb’s extremity; (b) posterior view of the right sound hand; (c) anterior view of the right sound hand.	54
7.2	Main developed prosthesis by Ana Oliveira’s thesis [63]: (a) anterior view; (b) posterior view.	55
7.3	Inner design of the final model prototype used in Ana Oliveira’s study: cut along the sagittal plane of the index finger (left) and shape of the designed phalanges (right) [63].	55
7.4	Result of the pull test used in the final prototype’s combination of features [63].	56
7.5	Final finger model prototype.	57
7.6	Final fitting mechanism model prototype: different transversal sections of the segments that compose this fitting mechanism.	58
7.7	Final fitting hole prototype of the metacarpal region: test cube and test cube with a cut along the sagittal plane of the finger.	58
7.8	Final thumb model prototype.	59
7.9	Original forearm design of the final prototype from Ana Oliveira’s study [63].	60
7.10	Partial design of the <i>Phoenix Hand v2</i>	60
7.11	Design of the prototypes for the gripper box.	61
7.12	Simulation of the behaviour of the prosthesis when force is applied [73].	61
7.13	Draft of the metacarpal region structure, inspired in the <i>Nazree’s Prosthetic Hand</i> . Segments 1 to 3 would be articulated to simulate the motion of the metacarpal region while gripping.	62
7.14	Design of the first prototype of the metacarpal region from Ana Oliveira’s study [63].	63
7.15	Design of the second prototype of the metacarpal region from Ana Oliveira’s study [63].	64
7.16	Final metacarpal region prototype from Ana Oliveira’s study [63].	64
7.17	Different views of the design of the final metacarpal region prototype from Ana Oliveira’s study [63].	65
7.18	Dimensions for the servomotor support system in the metacarpal region prototype.	66
7.19	Design of the metacarpal region prototype.	67
7.20	Different views of the design of the metacarpal region prototype.	67
7.21	Design of the metacarpal region prototype with a cut along the sagittal plane.	68
7.22	Results of the influence of layer orientation tests.	69
7.23	Results of the switching parameters tests.	70
7.24	Picture of the pull test setup.	71
7.25	Behaviour of the model printed with <i>Filaflex 60A</i> and 25% infill.	72
7.26	Behaviour of the model printed with <i>Filaflex 60A</i> and 50% infill.	72
7.27	<i>BIOPAC Model MP-36</i> acquisition unit by ©BIOPAC [74].	76

7.28	Picture of the original acquisition electrodes position.	76
7.29	Original acquisition electrodes position.	77
7.30	<i>Biopac Student Lab</i> ® file using the old electrodes position.	77
7.31	New acquisition electrodes position.	78
7.32	<i>Biopac Student Lab</i> ® file using the new electrodes position.	78
7.33	Main muscles responsible for finger flexion.	79
7.34	<i>Flexor digitorum profundus</i> muscle [77].	80
7.35	<i>Flexor pollicis longus</i> muscle [78].	80
7.36	Scheme of the classification stages of Ema Lopes' classifier [68].	81
7.37	<i>Python</i> script to control an Arduino.	82
7.38	Arduino <i>sketch</i> to control servomotors movement.	83
7.39	Electric signal control servomotor [79].	84
7.40	<i>Tower Pro SG90-360°</i> servomotor and dimensions [80].	85
7.41	Design of the first prototype with five <i>Tower Pro SG90-360°</i> servos.	86
7.42	Whippletree mechanism assembly: (a) the strings connect the fingers and are inserted in distal-proximal order, then passed through the whippletree holes and inserted by doing the inverse path; (b) the fingers are fitted in the metacarpal region after being connected; (c) the index connects to the middle finger and the string passes through the whippletree external hole, while the middle connects to the ring finger and passes the string through the inner hole [63].	87
7.43	Design of the second prototype with three <i>Tower Pro SG90-360°</i> servos.	88
7.44	<i>Tower Pro MG995-360°</i> servomotor and dimensions [84].	89
7.45	Alternative for the <i>Tower Pro MG995-360°</i> servomotor.	90
7.46	Design of the third prototype with a <i>Tower Pro SG90-360°</i> servo and a <i>Tower Pro MG995-360°</i> servo.	90
7.47	Printed components for the final prosthesis prototype.	91
7.48	Bottom view of the printed thumb for the final prosthesis prototype.	92
7.49	Printed index finger for the final prosthesis prototype.	93
7.50	Printed components for the wrist region of the final prosthesis prototype.	94
7.51	Fitting of the pins in the metacarpal region: (a) the pins are fitted from the inside of the stump-prosthesis interface in the counterbored holes; (b) pins after being fitted in the metacarpal region.	94
7.52	Suggestions of how to use a dual extruder printer for printing certain prosthesis pieces.	95
7.53	Isometric view of the <i>E2 3D Printer</i> by ©Raise3D [89].	96
7.54	Examples of prints made with the <i>E2 3D Printer</i> using two different filaments [90].	96
7.55	Final prosthesis model.	97
7.56	Printable components of the prosthesis fully assembled.	97
7.57	Electronic circuit used in the prosthesis model.	98

7.58 Gripping movement of the final prosthesis prototype.	98
7.59 Index pointing movement of the final prosthesis prototype.	99
7.60 Process necessary every time the prosthesis is scaled: (a) original model, (b) scaled model, (c) scaled model with the servomotor support system.	100
A.1 Extended methodology flowchart	118
C.1 Print Settings parameters used in the <i>PrusaSlicer</i> software.	124
C.2 Filament Settings parameters used in the <i>PrusaSlicer</i> software.	125

List of Tables

2.1	Forearm Muscles and their Functions [17].	8
2.2	Advantages and Disadvantages of Existing Types of Prosthesis [28].	13
5.1	Advantages and Disadvantages of Current Prosthesis Models using 3D Printing [59]	29
6.1	Comparative Analysis of the Work Done in Ana Oliveira and Ema Lopes' Thesis and the Current Research.	36
7.1	Mechanical properties of the materials used during this study.	73
7.2	<i>Tower Pro SG90-360°</i> servomotor specifications [80].	85
7.3	<i>Tower Pro MG995-360°</i> servomotor specifications [84].	89
7.4	Material cost, mass and total printing time of the final prosthesis prototype.	101
D.1	Pull tests results of the model printed with <i>Filaflex 60A</i> and 25% infill	135
D.2	Predicted behaviour of the model printed with <i>Filaflex 60A</i> and 25% infill	135
D.3	Pull tests results of the model printed with <i>Filaflex 60A</i> and 30% infill	136
D.4	Predicted behaviour of the model printed with <i>Filaflex 60A</i> and 30% infill	136
D.5	Pull tests results of the model printed with <i>Filaflex 60A</i> and 40% infill	137
D.6	Predicted behaviour of the model printed with <i>Filaflex 60A</i> and 40% infill	137
D.7	Pull tests results of the model printed with <i>Filaflex 60A</i> and 50% infill	138
D.8	Predicted behaviour of the model printed with <i>Filaflex 60A</i> and 50% infill	138
D.9	Pull tests results of the model printed with <i>Filaflex 70A</i> and 25% infill	139
D.10	Predicted behaviour of the model printed with <i>Filaflex 70A</i> and 25% infill	139
D.11	Pull tests results of the model printed with <i>Filaflex 70A</i> and 30% infill	140
D.12	Predicted behaviour of the model printed with <i>Filaflex 70A</i> and 30% infill	140
D.13	Pull tests results of the model printed with <i>Filaflex 70A</i> and 40% infill	141
D.14	Predicted behaviour of the model printed with <i>Filaflex 70A</i> and 40% infill	141
F.1	Discriminated cost of the printing components for the final prototype of the prosthesis.	150

F.2	Discriminated cost of the electronic components for the final prototype of the prosthesis.	150
F.3	Discriminated cost of the extra material required for the final prototype of the prosthesis.	150

Glossary

<i>Machine Learning</i>	branch of the broader field of artificial intelligence that makes use of statistical models to develop predictions 2, 76
<i>open-source</i>	Computer software with its source code released and licensed under an open source license in which copyright provides the right to study, modify and distribute the software for free to anyone and for any purpose 2, 28, 29, 106
<i>anatomy</i>	The science that studies the structure of the body of living beings, including it's systems, organs and tissues 5
<i>bilateral motor coordination</i>	Ability to use the right and left sides of the body together, either at the same time or in alternating movements 1
<i>biomechanics</i>	The study of biological systems, particularly their structure and function, using methods derived from mechanics, which is concerned with the effects that forces have on the motion of bodies 5
<i>myoelectric</i>	relating to, or utilizing electricity generated by muscle xi, 2, 11, 13, 22, 24, 25, 27, 33–35, 37, 53, 59, 74, 75, 99–101, 103, 105–108
<i>myology</i>	The study of the muscular system, including the study of the structure, function and diseases of muscle 5
<i>sarcomere</i>	The smallest functional unit of the striated muscle tissue. 21

Acronyms

2D	2-Dimensional 15
3D	3-Dimensional xi, xxi, xxv, 2, 11, 15–19, 27–29, 35, 37, 53, 54, 62, 95, 99, 101–103, 106, 107
ABS	acrylonitrile butadiene styrene 18
AM	Additive Manufacturing xi, 2, 15, 16, 18, 27, 28, 35, 53, 105, 107, 108
ATP	Adenosine Triphosphate 21
CAD	Computer-Aided Design 15, 38
DC	direct current 11
DfAM	Designing for Additive Manufacturing 36
EMG	Electromyography xix, 22–25, 36, 75, 76, 78–80, 100, 105, 106
FCT NOVA Technology	NOVA School of Science 95
FDM	Fused Deposition Modeling 17–19, 28, 29, 69
MVC	Maximal Voluntary Contraction 43
PET-G	polyethylene terephthalate glycol 39
PLA	polylactic acid xi, 18, 37, 39, 62, 65, 68, 92–94, 102, 108
RXD	Receive Serial Data 49
SLA	Stereolithography 16
SLS	Selective Laser Sintering 16
SPP	Serial Port Protocol 81

STL	Standard Tessellation Language 15
SUS	System Usability Scale 50, 51, 102, 103
TXD	Transmit Serial Data 49

Introduction

The hands are one of the most important anatomical structures in the human body, they play a key role in perceiving tactile sensations, performing basic day-to-day activities and even establishing interpersonal communication through sign language [2]–[4]. The motor properties of these extremities will define a person's ability to carry out activities in their daily lives. Thus, the absence of this anatomical structure, whether that is partial or complete, has a major influence on the patient's quality of life, impairing their level of autonomy and their psychological state [5].

In 2019, around 2 million people were living with an amputated limb, with around 35% living without an upper limb [6]. In Portugal alone, between 2000 and 2015, more than 1 000 upper limb amputations were performed [7]. In the adult population, most new cases of loss of a limb stem mainly from trauma, however, in the pediatric population, the occurrence of congenital malformation is the main reason for the absence or loss of a limb. Epidemiological studies have estimated that the overall incidence of these malformations can range from 3.4 to 21.5 per 1000 births, depending on the country of region [8], [9].

During their formative years, patients tend to face various mental and social problems related to their upper limb deficiency, which can develop into cases of depression and social isolation [10]. In addition to their mental health damage, it can also lead to a significant negative impact on the muscular development of the affected limb and on its bilateral motor coordination [5]. The use of prostheses at a young age can help restore partial functionality and overcome some of the difficulties encountered. In the long term, the use of prostheses also promotes better muscle development, bi-manual activity, symmetrical growth and development of manual dexterity [11], [12]. It is thus justifiable the importance of developing new models of prostheses and their application in young patients.

Up until recently, prosthetic innovation did not belong in an attractive industry due to its high development costs and relatively low market demand, originating the production of exclusively more sophisticated prosthetic models with above-expected prices. The cost of a common commercial upper limb body-powered prosthesis can vary between

4.000€ and 10.000€, while the cost of a commercial upper limb electric prosthesis can vary between 25.000€ and 75.000€ [4]. The development of the AM industry was the main catalyst of the prosthetic industry and the driver of new charity projects, such as the *e-Nable* project.

The *e-Nable* project is a project developed by a worldwide online community of volunteers who collaborate in the development of low-cost models of body-powered prosthetic upper limbs, using new 3D printing methods [13]. All models developed are free and *open-source*.

Despite the recent developments achieved in the *e-Nable* project, the prosthetic models continue to have a very high rejection rate, in both children and adults. The prostheses use bright colours and look similar to superhero hands in order to increase the acceptance rate of children. However, this customization ends up contributing to a higher rejection rate in the long term, as many of the children consider prostheses as toys and not an essential good. In the case of teenagers and adults, the childlike appearance makes the use of the prostheses less appealing [14]. In addition to appearance, there are other aspects that have a negative influence on the acceptance rate of these prostheses, such as their rigidity, which promotes discomfort, and the discrepancy between the functionality of the prostheses and the natural functionality of the human upper limb [15].

Addressing these limitations and needs could revolutionize the prosthetic industry and the lives of amputees and children. Therefore, there is a need to develop more sophisticated, customizable and more realistic models that ensure comfort, low cost and optimized functionality.

1.1 Objectives

The main objective of this study is based on the development of a functional myoelectric, low-cost, highly customizable and realistic upper limb prosthesis made from flexible material and new 3D printing methods.

By replacing the rigid material, normally used in 3D printing, with a flexible material, it is intended to obtain a prototype that simulates to its best the characteristics of the human hand with a more comfortable and aesthetically appealing design. Upgrading from a body-powered prosthesis to a myoelectric prosthesis aims to improve significantly the levels of functionality. The upgrades can not compromise significantly other factors such as weight, cost and ease of repair.

In order to achieve this objective, this study was divided into two parts. In the first phase, it was necessary to analyze the state of the art of existing prostheses and re-design the prosthetic models made available by the *e-Nable* project with the ideal prostheses on of flexible material and printing parameters. In the second phase of development, a deeper understanding of myoelectric signal acquisition, processing and classification through *Machine Learning* was made in order to make the prosthetic model electronic. This dissertation follows on from two other dissertations. The thesis previously developed

had the objectives of creating a signal acquisition and classification system and developing a new prosthesis prototype using flexible material. The objectives of this thesis were fulfilled to a certain degree, however, their prototypes had low functionality levels and did not fulfil all the patients' needs. The aim of this work is to combine both prototypes developed in the previous studies, improve the prosthetic model and move from the prototype phase to the final product, whilst developing a *scaling* methodology for patients of different ages and genders.

The research work described in this dissertation was carried out in accordance with the norms established in the ethics code of Universidade Nova de Lisboa. The work described and the material presented in this dissertation, with the exceptions clearly indicated, constitute original work carried out by the author.”

Clinical Background

In this chapter, the fundamental concepts of anatomy, biomechanics and myology of the upper limb and different associated pathologies are discussed in order to have a better understanding of the subject in question. Additionally, the different types of prosthesis available for the upper limb are described and there is a brief discussion on the main aspects that the prosthetic field needs to improve.

2.1 Upper Limb Anatomy

The upper limb is divided in three different parts. The first one is the arm, which goes from the shoulder to the elbow. The second part is the forearm, which goes from the elbow to the wrist. The final part is the hand, which goes from the wrist to the fingers. The bones that make the upper limb can be observed in Figure 2.1.

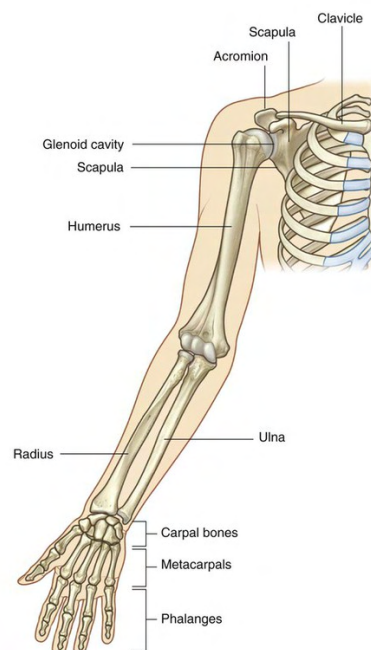


Figure 2.1: Upper Limb Bone Structure [16]

Losing a hand can have a significant impact in one's life. Only through the use of a prosthesis can the lost limb be substituted and some of the basic functionality can be restored. For that reason, it is crucial to develop a prosthesis model capable of simulating the movements of the arm. There are six fundamental movements that need to be analysed: flexion, extension, abduction, adduction, supination and pronation. It is possible to analyse these types of movements of the upper limb in Figure 2.2 and the main movements capable of being made by the wrist in Figure 2.3.

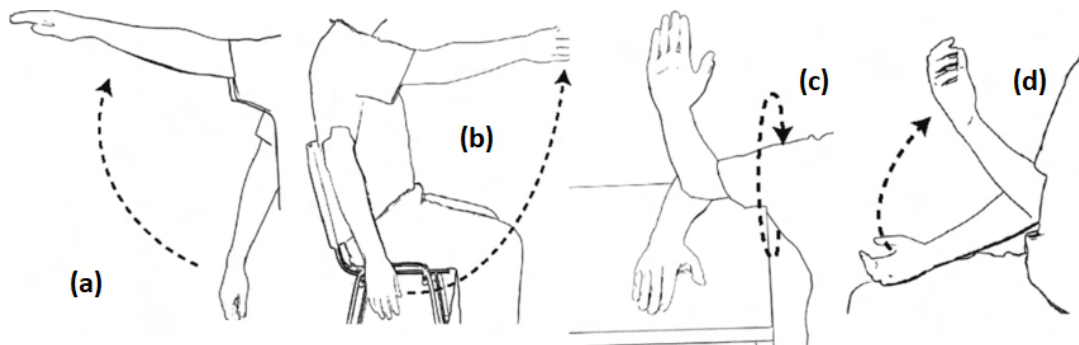


Figure 2.2: Upper Limb Movements: (a) Abduction and Adduction of the arm, (b) Flexion of the arm, (c) Internal and External rotation, (d) Flexion of the forearm [16]

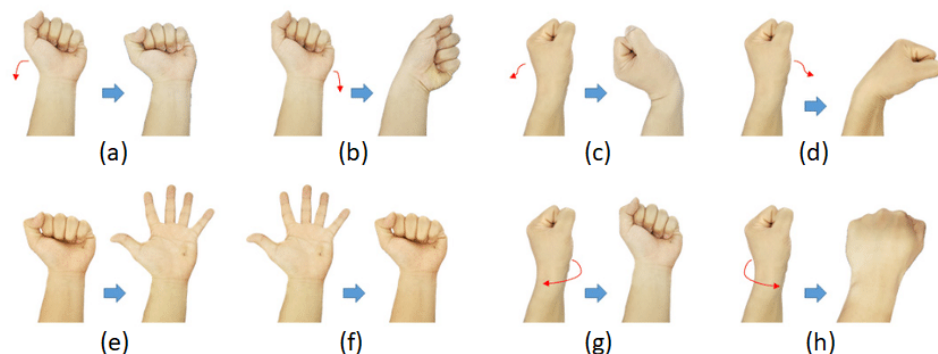


Figure 2.3: Wrist Movements: (a) Radial deviation, (b) Ulnar deviation, (c) Wrist extension, (d) Wrist flexion, (e) Finger extension, (f) Finger flexion, (g) Supination, (h) Pronation [16]

Most daily activities demand, beyond the movement of the upper limb and its wrist, the action of grabbing onto objects through the usage of the fingers, as shown in Figure 2.4. The action of grabbing onto objects demands high levels of precision. The main elements involved in the positioning of the fingers are the wrist, the metacarpophalangeal and interphalangeal joints. The object is grabbed using essentially the thumb, the index finger and the middle finger [16].

In this study, there is only a need to study the muscles responsible for the movement of grabbing since that is the action the developed prototype is trying to mimic. Due to limitations in the equipment used, the collection of the myoelectric signals can only be

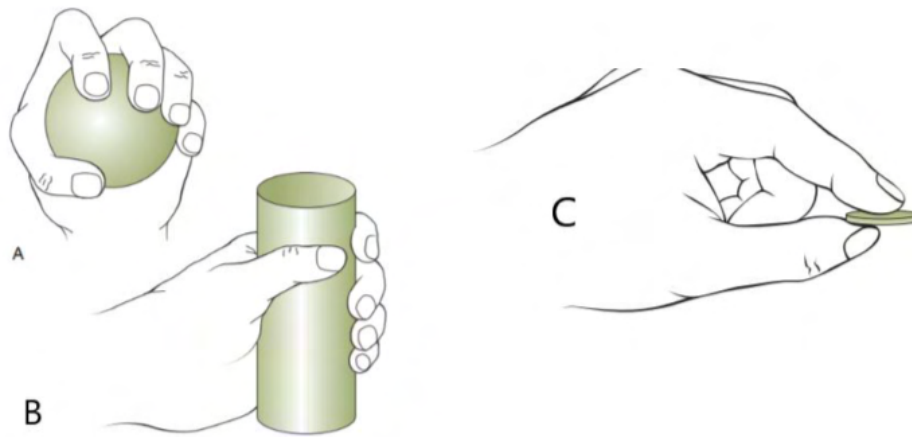


Figure 2.4: Grasp Movements: (A) Pentadigital grip, (B) Petradigital grip, (C) Tridigital grip [16]

achieved by one source, chosen to be the forearm. On Table 2.1 it is possible to see the main muscles of the forearm involved in it's movement and the hand's movement.

2.2 Upper Limb Pathologies

2.2.1 Congenital Malformation

There is a possibility of physical anomalies of the upper limbs occurring from the moment the limb begins formatting during pregnancy, between the fourth and eighth week after fertilization. This type of structural or functional changes present from birth are called structural congenital malformations [18], [19].

The presence of these anomalies is not related to any specific cause, however there are certain factors that increase the probability of these problems developing. Since this type of anomalies originate from genetic problems, it is believed that factors that contribute to the increase in chromosomal anomalies, such as diabetes, exposure to radiation, alcohol and drug consumption, are common in cases of congenital malformation [18], [19]. There is a higher prevalence of cases with this type of malformation in developing countries, which may be related to the lower level of access to primary health care [19].

Another frequent cause of cases of structural malformations is the presence of amniotic bands in the uterine cavity. This condition gives rise to what is called amniotic band syndrome. This syndrome is associated with the appearance of fibrous bands that wrap around the various parts of the fetus in the uterus, leading to a blockage of blood flow, which can lead to tissue necrosis of the affected limb [20], [21].

2.2.2 Amputation and Trauma

Traumatic events or severe illnesses can also lead to partial or total loss of an upper limb. In developing countries, the main cause of upper limb loss in adulthood is accidents that

Table 2.1: Forearm Muscles and their Functions [17].

Forearm Muscles	Action
Anterior Forearm Muscles	
Pronator Teres Muscle	forearm pronation and flexion
Flexor Carpo Radialis Muscle	assists flexion and abduction of the hand
Palmaris Longus Muscle	flexion of the hand and tense the palmar aponeurosis
Flexor Carpi Ulnaris Muscle	assists in flexion and adduction of the hand
Flexor Digitorum Superficialis Muscle	flexion of the proximal and metacarpophalangeal phalanges
Flexor Digitorum Profundus Muscle	distal interphalangeal flexion
Flexor Pollicis Longus Muscle	thumb phalanx flexion
Pronator Quadratus Muscle	forearm pronation
Lateral Forearm Muscles	
Brachioradialis Muscle	forearm flexion and pronation
Extensor Carpi Radialis Longus Muscle	hand extension and abduction
Extensor Carpi Radialis Brevis Muscle	hand extension and abduction
Supinator Muscle	forearm supination
Posterior Forearm Muscles	
Extensor Digitorum Muscle	finger extension
Extensor Digiti Minimi Muscle	extension of the 5th finger
Extensor Carpi Ulnaris Muscle	hand extension and adduction
Anconeus Muscle	forearm extension
Abductor Pollicis Longus Muscle	thumb extension and abduction
Extensor Pollicis Brevis Muscle	extension of the metacarpophalangeal and carpometacarpal joints
Extensor Hallucis Longus Muscle	extension of the inter and metacarpophalangeal joints
Extensor Indicis Muscle	extension of the metacarpophalangeal and interphalangeal joints of the index finger

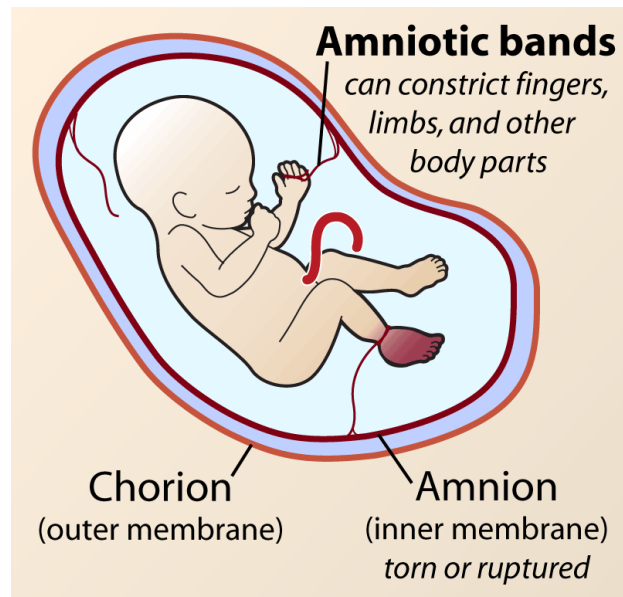


Figure 2.5: Amniotic Band Syndrome [22]

can lead to untreated infections, while in developed countries the main cause is due to vascular disorders [16], [23].

Depending on the level of amputation, upper limb amputation can be classified as scapulothoracic disarticulation, shoulder disarticulation, transhumeral amputation, transradial amputation, elbow disarticulation, forearm amputation, wrist disarticulation, intercarpal disarticulation, carpophalangeal amputation, interphalangeal amputation or amputation at the level of phalanges, as shown in Figure 2.6.

2.3 Current Prosthetic Solutions

The current prosthesis model can be classified as passive prostheses or active prostheses. Passive prostheses can be further subcategorized into static or dynamic prostheses. Static prostheses serve only for aesthetic purposes, dynamic prostheses allow the patient to recover some of the lost activities and grasp lightweight objects, using internal mechanisms to control their movements, and active prostheses as electrical mechanisms as a way of controlling actions [24]–[26].

2.3.1 Passive Prosthesis

Passive prostheses are devices that replace a missing limb or body part, but do not have the ability to move on their own, as shown in Figure 2.7. They are typically made of lightweight and durable materials such as plastic, metal and silicone. They provide cosmetic appearance, support and balance [24].

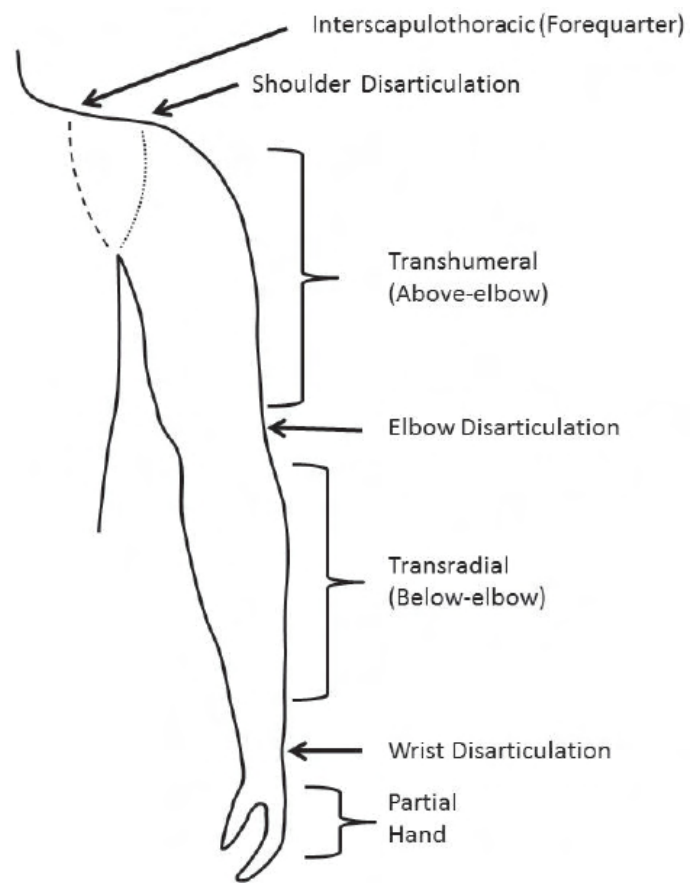


Figure 2.6: Amputation Levels of the Upper Limb [17]



Figure 2.7: Passive Prosthesis of the Upper Limb [24]

2.3.2 Body-Powered Prosthesis

Body-powered prostheses use user movements to perform basic actions [25], [26]. Currently, most of these types of prostheses are developed using 3D-printing techniques, which leads to a lower product price.

These prostheses use a combination of non-elastic wires and elastic wires to allow for certain movements. Non-elastic wires will connect certain regions of the prosthesis to healthy parts of the residual limb (hand or elbow). The bending of the healthy structure will imply a consequent movement of the prosthesis structure. Elastic threads are used to simulate extension movements and cause resistance in certain regions, such as phalanges, as shown in Figure 2.8 [26].

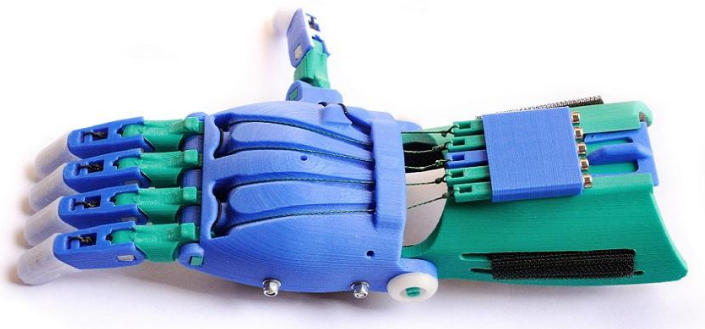


Figure 2.8: e-NABLE Body-Powered Prosthesis of the Upper Limb [13]

2.3.3 Electrical Prosthesis

The introduction of servomotors, microcontrollers and sensors in prostheses gave rise to a new category, electrical prostheses. This type of prosthetic model is characterized by its resemblance to robotic hands, using high levels of technology to carry out basic movements, as shown in Figure 2.9.

This type of prosthesis, despite its innovations, has certain limitations imposed by the use of conventional direct current (DC) electric motors [26]. Although this model generates a lower rejection rate, it is possible to identify several limitations with regard to noise, slowness of movements and limitations in the strenght of movements.

2.3.4 Myoelectric Prosthesis

Myoelectric prostheses belong to a sub-category of electrical prostheses. Like electrical prostheses, this model uses servomotors and microcontrollers to carry out movements, however it stands out due to the fact that the input is received by a myoelectric signal, generated by muscle activation, as shown in Figure 2.10 [25], [26]. These are more advanced devices that use a combination of electrical signals from the user's own muscles and

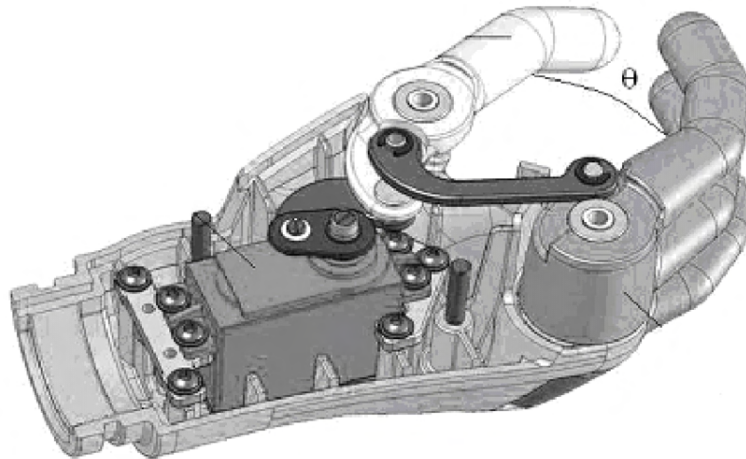


Figure 2.9: Electric Prosthesis Structure [27]

sophisticated electronics to control the movements of the prosthesis. They are designed to offer improved functionality, appearance and comfort compared to passive prostheses.

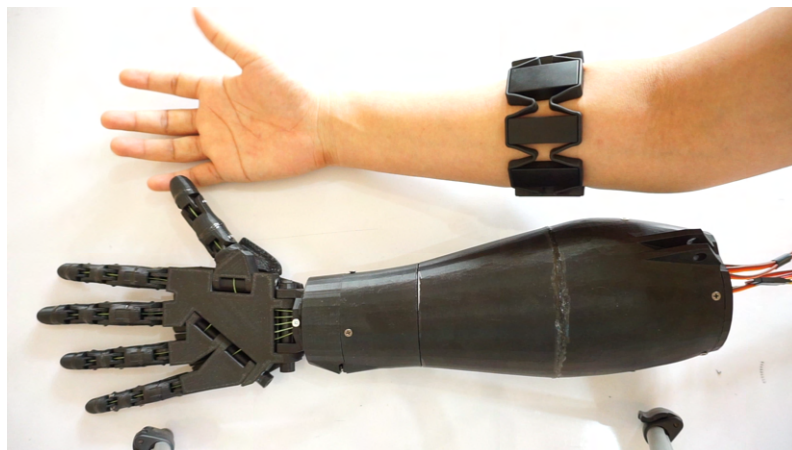


Figure 2.10: Myoelectric Prosthesis [26]

These devices are a promising technology that can offer improved functionality and appearance for individuals with missing limbs or body parts.

2.3.5 User Needs

Despite all the recent technological advances, the models currently on the market have a very high rejection rate. There is then a need to consider the opinions of users in order to improve the models.

Regardless of the age or user's skill level, a key aspect of the model is its ease of use. Next, the factors considered most important are size and weight. Other important factors to highlight are appearance, functionality and strength of movements [28], [29].

The prostheses currently on the market were developed with the aim of improving the user's bi-manual function and providing a better life. However, regardless

2.3. CURRENT PROSTHETIC SOLUTIONS

of the type of prosthesis used, its users are able to identify flaws in the type of prosthesis chosen. as shown in Table 2.2 [28].

Table 2.2: Advantages and Disadvantages of Existing Types of Prosthesis [28].

Prosthesis Type	Advantages	Disadvantages
Passive	aesthetically appealing, cheap, comfortable	does not have any level of functionality
Body-Powered	simplicity to use, weight, cost-effectiveness	user dependent, low strength, low sensory feedback
Electric	more intuitive and natural response	noise, price, weight, dependent on batteries and myoelectric signals, slow control

Additive Manufacturing

Additive Manufacturing (AM), better known as 3D printing, encompasses a group of technologies with the aim of producing objects from digital models [30]–[33]. Currently, there are already several models, each with specific characteristics for the production of parts, but all types of 3D printing follow the same ideology. These objects are built using a 3D Computer-Aided Design (CAD) [30].

CAD files, resulting from CAD software, contain the solid virtual description of the model and its geometry and size [32], [33]. With the model ready, the CAD file is exported in a Standard Tessellation Language (STL) format. This file format produces a triangular representation of the surface of the object that contains the spatial coordinates of the triangles that, together, produce the design of the object [33]. The STL file is then submitted to a 3D printing software which converts the 3D model into a combination of 2-Dimensional (2D) cross-sectional series, which correspond to the print layers. Consequently, the 3D printer will have access to a set of instructions that indicate the values of coordinates that the extruder needs to follow to print the desired model, as we can see in Figure 3.1 [31], [33].

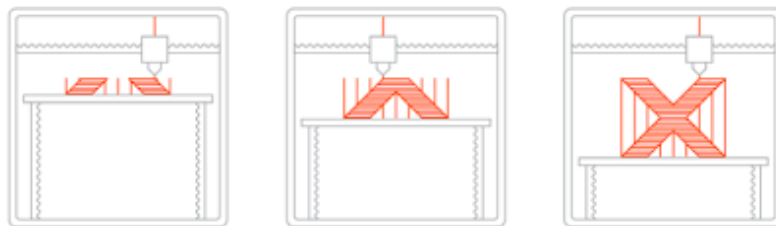


Figure 3.1: 3D Printing Mechanism [33]

3.1 Additive Manufacturing Methods

AM is an ever-evolving technology. The five main methods of AM are:

- **Sterolithography (SLA)**- is a type of 3D printing technology that uses a laser to cure photopolymer resin, which is a type of liquid plastic that hardens when exposed to light. The laser is directed onto a flat platform immersed in the resin, where it cures and solidifies the resin into a solid layer. The platform then moves downward by a small increment, and the laser cures the next layer. This process is repeated until the entire object is built up layer by layer, as shown in Figure 3.2 [34].

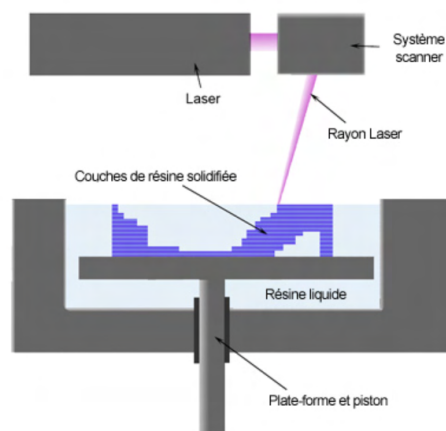


Figure 3.2: Sterolithography Method [34]

SLA has several advantages over other 3D printing processes, including the ability to produce high-resolution, intricate objects with smooth surface finishes, and the ability to use a wide range of materials, including transparent and flexible materials. The process is also fast, making it well-suited for rapid prototyping and small-batch production.

However, SLA also has some disadvantages, such as the need to support structures to hold up overhanging parts of the object during printing, and the potential of warping and deformation due to the high curing temperatures involved in the process. Additionally, SLA objects are typically more brittle than objects made with other 3D printing methods, and they may also be more porous, making them less suitable for applications that require high strength or water resistance.

- **Selective Laser Sintering (SLS)**- 3D printing process that uses a laser to fuse together fine powder particles layer by layer to form a solid object. The powder is spread evenly over a flat platform, and the laser is directed onto specific areas of the powder, fusing the particles together and building up the object layer by layer, as shown in Figure 3.3 [35].

This method allows for the ability to produce complex, multi-part objects with intricate internal structures, and use a wide range of materials, including metals,

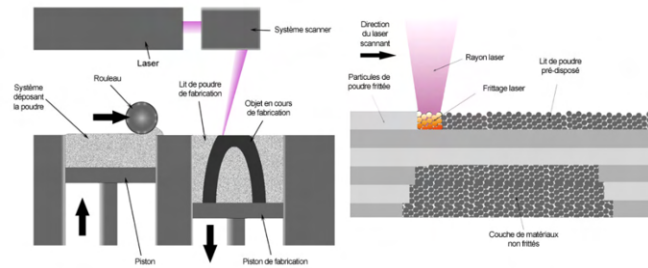


Figure 3.3: Selective Laser Sintering Method [35]

plastics and ceramics. The process also eliminates the need for support structures, as the surrounding powder acts as a support for the object during printing.

Be that as it may, it still requires for post-processing in order to remove excess powder and to smooth the surface finish of the object, and the potential for porosity in the object can occur due to the open structure of the powder bed.

- **Fused Deposition Modeling (FDM)**- most common 3D printing process that uses melted plastic filament to build up an object layer by layer, as shown in Figure 3.4. A more in depth explanation into the FDM printing method is described in Chapter 3.2.

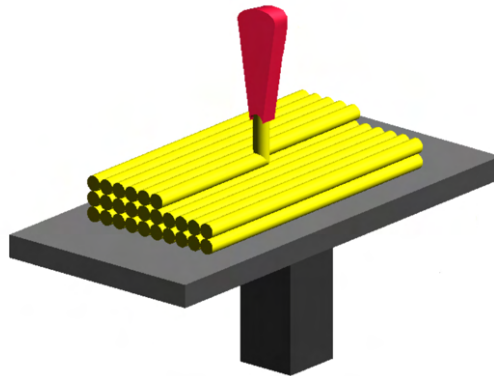


Figure 3.4: Fused Deposition Modeling Method [36]

- **Binder Jetting**- process that uses a jetting system to deposit a binder material onto a bed of powder, as shown in Figure 3.5. The binder material binds the powder particles together to form a solid layer, the process is repeated until the entire object is built up. The excess powder is then removed, leaving behind the final 3D printed object. This method is known for its ability to produce high-resolution objects with intricate details [37];
- **PolyJet or Material Jetting**- process that makes use of liquid photopolymers resin and a print head to build objects layer by layer. It works by jetting small droplets of liquid resin onto a build platform and using UV light to cure and solidify the resin

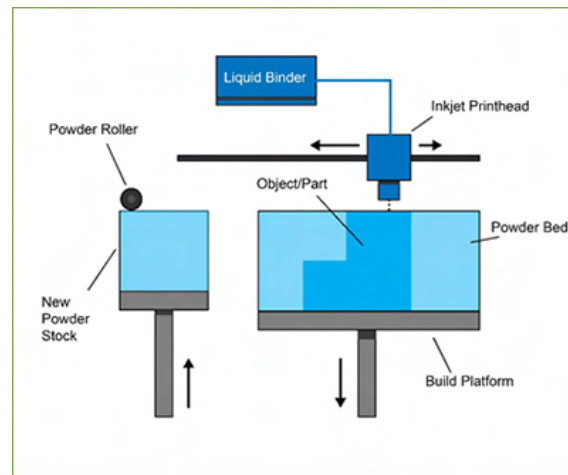


Figure 3.5: Binder Jetting Method [37]

into the desired shape. Material jetting is known for producing high-resolution, accurate and detailed parts with a smooth surface finish [38].

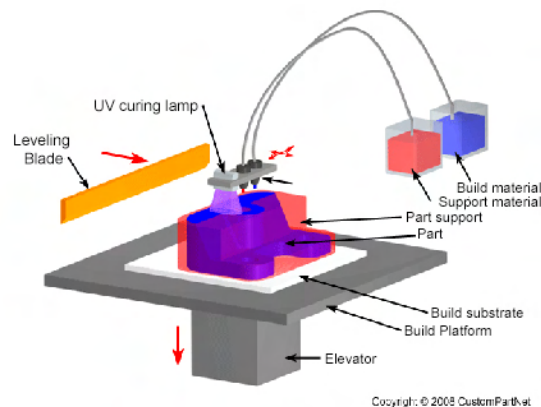


Figure 3.6: PolyJet Method [38]

3.2 Fused Deposition Modeling Method

AM techniques have evolved exponentially, the most common being the FDM technique. This technique is characterized by its layer-by-layer printing, where an extruder moves along a printing plate and deposits melted plastic filament in the desired position [36]. The filament is typically made of thermoplastic materials such as acrylonitrile butadiene styrene (ABS) or PLA. Some of the newer 3D printers may have more than one extruder, which allows the ability to print with more than one material [39].

The filament is fed into a heated extruder head, which melts the plastic and deposits it onto a flat build platform in the desired shape. The build platform then moves downward by a small increment and the extruder head deposits the next layer of plastic on top. This process is repeated until the entire object is built up [40], [41]. FDM machines can produce objects with a high level of accuracy and with a wide range of material options, including

flexible and rigid materials. An example of a FDM 3D printer and its components is shown in Figure 3.7.

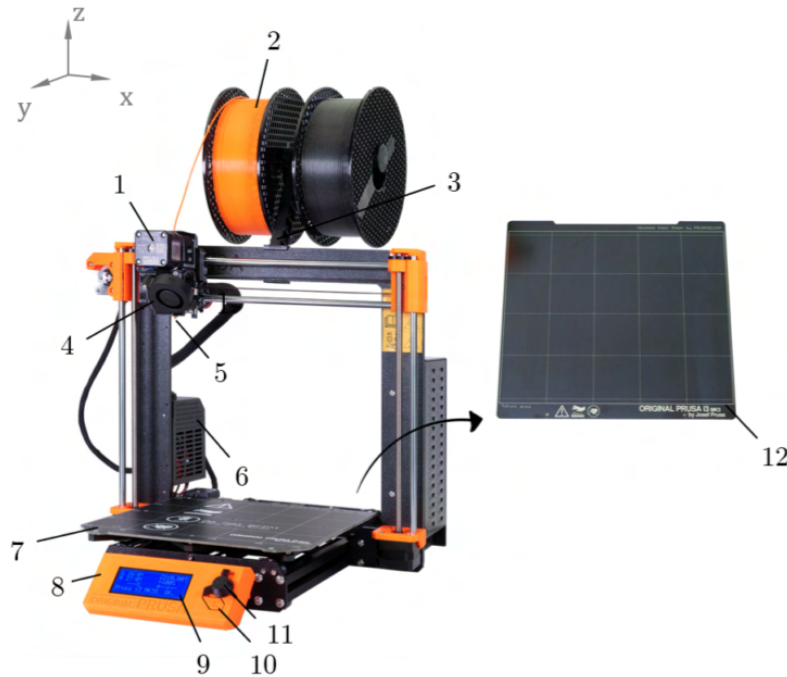


Figure 3.7: Structure of the 3D Printer *Original Prusa i3 MK3S+*: 1. Extruder motor; 2. Filament; 3. Filament Support; 4. Fan; 5. Extruder; 6. Motherboard; 7. Heating bed support; 8. Control Panel; 9. *Reset* Button; 10-11. Control Buttons; 12. Magnetic heating bed. [42]

FDM has several advantages over other 3D printing methods. One of the main advantages is its accessibility and ease of use. FDM machines are widely available and relatively affordable, making them well suited for both personal and commercial use. Additionally, FDM is a relatively fast 3D printing process, making it well suited for low-volume production and rapid prototyping [40].

Another advantage is the strength and durability of the objects it produces. FDM objects are typically stronger and more durable than objects produced by other 3D printing methods, and they have a wide range of material options, including materials that are flame-resistant, UV-resistant and heat-resistant [40], [41], [43].

However, there are also some limitations when using this printing process. The potential for visible layer lines on the surface of the object is still present and the need for support structures to hold up overhanging parts of the objects during printing affects printing quality. Additionally, FDM objects may have a lower dimensional accuracy and surface finish compared to objects made with other 3D printing methods.

Electromyography as an Input of Myoelectric Control

The movements and stabilization of the upper limb are generated by specialized cells that produce muscle contraction. It is vital to understand the process of muscle contraction in order to better simulate the arm movements.

The event of muscle contraction is a complex process that involves a series of physiological and biochemical events that result in the shortening of the muscle fibres. The process starts when a nerve impulse, also known as an action potential reaches the muscle fibre via motor neuron. The motor neuron releases a neurotransmitter at the motor endplate, the junction between the nerve and the muscle fiber [44]. The neurotransmitter binds to specific receptors on the cell membrane of the muscle fibre, causing an influx of positively charged ions, such as sodium, into the muscle fibre. This leads to depolarization of the cell membrane and triggers a series of events known as the sliding filament theory [44], [45].

The sliding filament theory states that during contraction, the thin filaments, made of actin, slide over the thick filaments, made of myosin, shortening the sarcomere and thus the overall muscle fibre, as shown in Figure 4.1. The myosin filaments have small projections, called cross-bridges, that attach to the actin filaments, generating force as they move [46].

To contract the muscle, Adenosine Triphosphate (ATP) is hydrolyzed, releasing energy that allows the myosin heads to pivot and bind to the actin filament. The myosin heads then use the energy from the ATP to move along the actin filament and generate force.

Once the nerve impulse stops, the muscle relaxes. The release of acetylcholine from the motor endplate stops, allowing the breakdown of acetylcholine and the reuptake of positively charged ions, restoring the resting potential of the sarcolemma and ending contraction [44], [45].

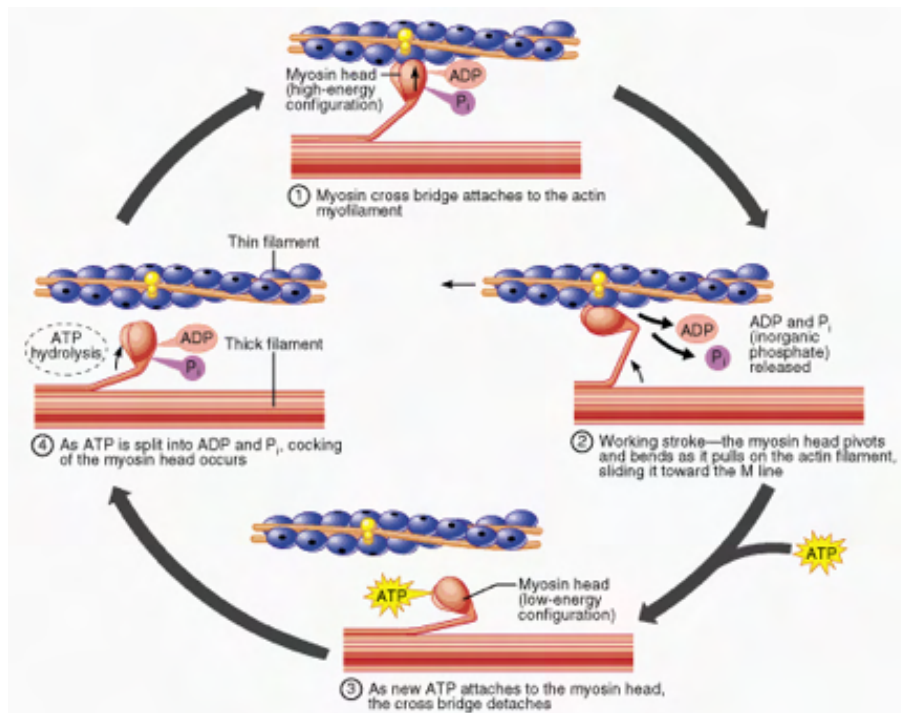


Figure 4.1: Diagram of the sliding filament theory [46].

4.1 Signal Acquisition Using Surface EMG

In order to monitor these electrical activities of the muscle motor units, it is used methods of EMG. There are two ways of measuring myoelectric signals: through needles (invasive process) or surface electrodes (non-invasive procedure). The raw myoelectric signal's amplitude ranges from -5 to 5 mV with a 10-500 Hz frequency range [47]. The amplitude of the measured signal is extremely sensitive to a series of intrinsic and extrinsic factors. The most common intrinsic factors that can impact signal acquisition are the muscular fibre composition, the muscle fibre diameter, the distance between the active fibres and the amount of tissue between the muscle surface and the electrodes [47], [48]. Extrinsic factors are those that affect during the moment of acquisition. The most common ones are the electrodes' configuration, the electrodes placement, sweating or temperature of the patient [49].

Another common and influential phenomenon that occurs during signal acquisition is the crosstalk phenomenon. The phenomenon refers to the interference between signals from two or more muscles that are being measured simultaneously. This can occur in several ways, such as *conductive crosstalk*, *electrode migration* or *electromagnetic interference*. This phenomenon is more significant during surface EMG acquisition.

Conductive crosstalk occurs when the electrical activity from one muscle is picked up by the electrodes of another muscle, leading to an overlap of the signals. This can occur when the electrodes are positioned too close to each other or when the electrical signals from one muscle are strong enough to reach the electrodes of the other muscle. *Electrode*

migration occurs when electrodes are not securely attached to the skin or not positioned correctly, leading to the recording of signals that do not correspond to the intended muscle. *Electromagnetic interference* occurs when external sources of electromagnetic energy interfere with the EMG signals. This can lead to artifacts or noise in the EMG signals, leading to incorrect conclusions about the muscle activity [50]–[52].

It is important to minimize crosstalk in EMG as it can affect the accuracy of the measurements and lead to incorrect conclusions about muscle activity. Minimizing crosstalk requires careful attention to electrode placement, skin preparation and reducing electromagnetic interference [50].

Surface EMG uses electrodes placed on the skin surface in order to measure the electrical activity of muscles, as shown in Figure 4.2. The electrical signals generated by the muscles are recorded through these electrodes, providing information about the muscle activity. It is important to use high-quality equipment and techniques for surface EMG acquisition to obtain accurate and reliable signals. Proper electrode placement, signal amplification and data analysis are crucial for obtaining meaningful information about the muscle activity.

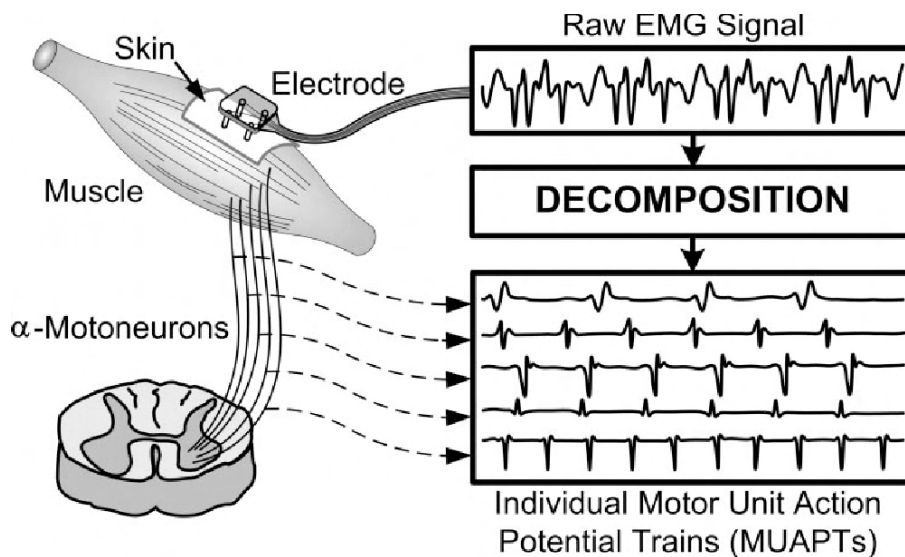


Figure 4.2: Diagram of surface EMG signal acquisition method [27].

Using surface EMG acquisition methods is more desirable due to it being non-invasive, which means it does not require any penetration of the skin or insertion of electrodes, making it less painful and less risky for patients. It also is a relatively simple and cost-effective technique, making it a valuable tool for monitoring muscle activity in clinical and research settings. Nevertheless it has its limitations, such as, the quality of the signal obtained is depended on the quality of the skin-electrode interface. Factors such as skin moisture, skin impedance and electrode placement can affect the quality of the signals. Small muscle tremors, body movements can also interfere with the accuracy of the signal by producing movement artifacts [53].

4.1.1 EMG Electrode Placement and Signal Acquisition Technique

In order to obtain better EMG signal, the electrode placement is an important factor to consider. The ideal electrode placement will depend on several factors, including the muscle being studied, the specific goal of the EMG measurement and the equipment used. However, there are some general guidelines that can be followed to improve electrode placement.

The electrodes should always be placed over the muscle belly. This will ensure that the maximum number of muscle fibres are being recorded, which will result in higher signal amplitudes. The orientation of the muscle fibres should also be considered. The electrodes should be placed parallel to the muscle fibers, as shown in Figure 4.3. This helps reduce the effects of movement artifacts and ensure that the signal is not contaminated by noise or artifacts [54].



Figure 4.3: Diagram of ideal electrode placement in regards to the orientation of the muscle fibers [55].

The skin should also be properly prepared prior to electrode placement, including cleaning and drying the skin, since it influences the skin-electrode interface [54].

By following established guidelines and techniques for electrode placement, it is possible to obtain accurate and meaningful information about muscle activity in surface EMG acquisition.

4.2 Electromyography as an Input of Myoelectric Control

A way of controlling prosthetic devices or other assistive technology is by using methods of myoelectric control. These methods use the electrical signals generated by the muscles to operate the devices.

The use of myoelectric control is common for upper limb prosthesis, where the user moves specific muscles to control specific actions of the prosthetic device. For example, contracting the biceps muscle may trigger the prosthetic hand to close, while relaxing the biceps muscle may cause the hand to open.

To use myoelectric control methods, electrodes are placed on the skin over the muscle that the user wants to control the prosthetic device with. The EMG signals generated by these muscles are transmitted to a control unit, which processes the signals and converts them into control signal inputs for the prosthetic device.

These methods have several advantages over other control methods. For example, it allows users to control the device in a more intuitive way using their own muscle movements. It also offers improved functionality, as users can control multiple degrees of freedom in the prosthetic device, such as grasping and wrist rotation. Additionally, it also provides greater customization options, allowing users to tailor the control of the device to their individual needs [56]. However, there are also limitations to myoelectric control. The user requires some residual muscle control in order to generate the EMG signals required for control. Additionally, detecting fine EMG signals can be challenging, and proper electrode placement and signal processing algorithms are crucial for effective myoelectric control [52], [53].

This chapter describes the main technological advances in the prosthetic field through AM techniques. In particular, a literature review of devices printed in 3D using flexible materials and prototypes that use techniques for collecting and processing myoelectric signals will be carried out.

5.1 Early History of Artificial Limbs

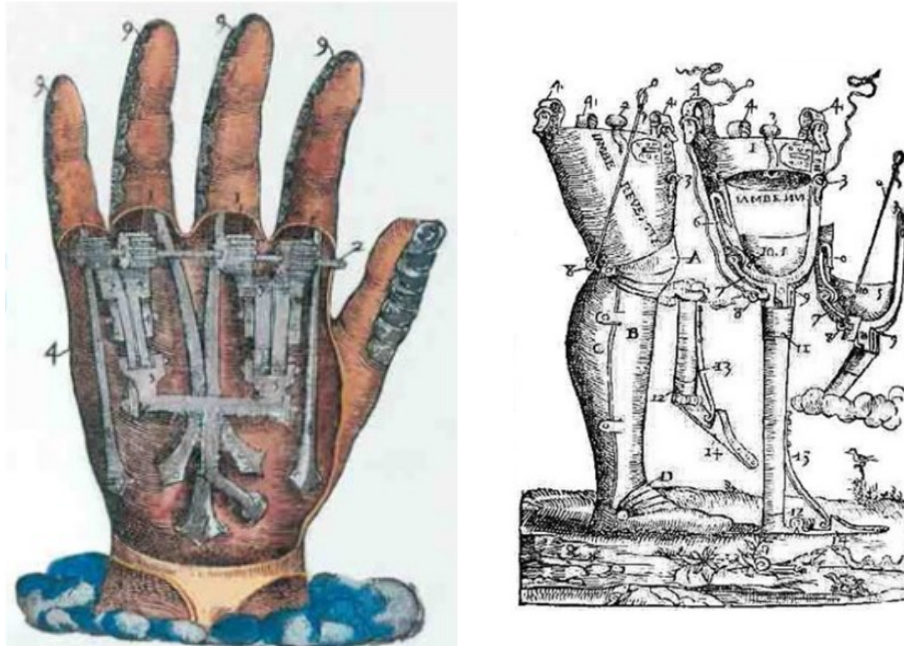
One of the earliest functional prosthetic body parts is thought to be an example of artificial toes from Ancient Egypt, shown in Figure 5.1. Since the early stages of prosthetic development, the importance of using prostheses not only as decorative devices but also as a functional device was noticeable, with this prototype being developed with the aim of helping carry some of the user's body weight and being responsible for forward propulsion [57].



Figure 5.1: Egyptian prosthetic toe believed to be one of the earliest prosthetic devices made [57].

In general, artificial limbs development moved forward during the Rome and Greek civilizations with the aim of allowing wearers who had lost a limb to continue a fighting

career. The artificial fingers could be used to grasp a shield, hold reins or even a quill. Figure 5.2 shows two different medieval designs of prosthetic devices with a low level of functionality, allowing the user to prolong his fighting career.



(a) Medieval design of a prosthetic hand.

(b) Medieval design of a prosthetic leg.

Figure 5.2: Medieval artificial limbs that allowed amputees to continue their fighting careers [57].

Centuries later, the huge number of casualties in the American Civil War caused the demand for artificial limbs to skyrocket. Many veterans turned to design their own prostheses as a response to the limiting capabilities of the limbs on offer. Over time, the constant improvements in medicine and the need for better models enabled several enhancements in the prosthetic field [57], [58].

Medicine has been benefiting from several technological fields, including AM. AM has been used in several fields, such as materials and mechanical engineering, computer technology, electronics and medicine. Various AM techniques have been developed with FDM in particular becoming the highlight of 3D printing, since it allowed for low-cost production of complex geometries with a high accuracy [40], [41], [43].

Many of these techniques were patented and only with the expiration of these patents in the last decade, manufactures were allowed to develop new cheaper and more accessible 3D printers, signalling the beginning of the new phase of prosthetic development [41]. With this new accessibility, communities started to form and a wide variety of *open-source* prototypes started to be shared around and available through the internet.

5.2 Overall Analysis of Current Prosthetic Devices

The use of 3D printing methods with these new prostheses models allowed production considering user's needs and high customization. As described in Chapter 2.3.5, prosthetic manufacturers should be sensitive to this user's needs. Hence, any progress made in the prosthetic field should be made considering these needs.

The use of 3D printing and FDM techniques in prosthetic and clinical manufacturing has promoted the development of new models of prostheses capable of satisfying some of the needs of their users. The table 5.1 shows the main advantages and drawbacks of using 3D printing techniques to produce prosthetic prototypes.

Table 5.1: Advantages and Disadvantages of Current Prosthesis Models using 3D Printing [59]

Advantages	Disadvantages
lightweight and easy to use	limb function does not necessarily improve
low cost compared to prosthetic models available on the market	most of the materials used are thermoplastic, i.e. sensitive to high temperatures
easy assembly, which allows replacement of damaged parts	requires access to a 3D printer to replace damaged parts
appealing appearances for children	unappealing appearance for adults
devices promote a social life in children	devices too fragile to be used in all kinds of daily activities
free, <i>open-source</i> and customizable templates	lack of medical validation

Most prostheses have similar designs, consisting of models with finger flexion capability and an anthropomorphic appearance. The *Raptor Reloaded* and the *Phoenix Hand v2* model are two examples of types of available prostheses, shown in Figure 5.3 [60]. Both models were developed by the *e-Nable* project.

All components that make up the models are printed in 3D. It is composed by 3D-printed snap pins, a modular tensioning system (composed by elastic bands and fishing line) and it can have Velcro or leather palm enclosures. The tensioning system closes the fingers through the flexion of the wrist, therefore requiring the amputee to have the function of the wrist. These models are cheap to produce and easy to assemble.

Another worth mentioning prosthetic device, due to its significant advances, is the *Nazree's Prosthetic Hand*, shown in Figure 5.4. This prosthesis's metacarpal design is composed by three segments that follow the shape of the human hand's creases, allowing the simulation of the gripping motion.

This device has a hidden whippletree mechanism that connects all the fingers using a single cable. Moreover, this prototype can be covered by a silicon glove to appear even more like a human hand.

In 2018, F. Pinheiro developed a new prototype for a non-customized body-powered



(a) *Raptor Reloaded* Prosthesis

(b) *Phoenix Hand v2* Prosthesis

Figure 5.3: *e-Nable* Project Prosthesis Models [60]

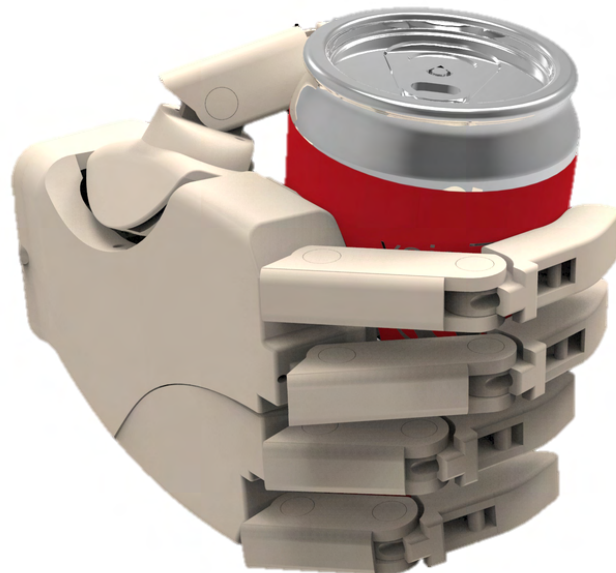


Figure 5.4: Nazree's Prosthetic Hand [61].

prosthesis, which combined pieces made from flexible or stiff materials, shown in Figure 5.5. This prototype attempted to develop a more appealing and realistic design by avoiding the exposure of the actuation of cables and hinges and with a more realistic approach to the piece's design [62].

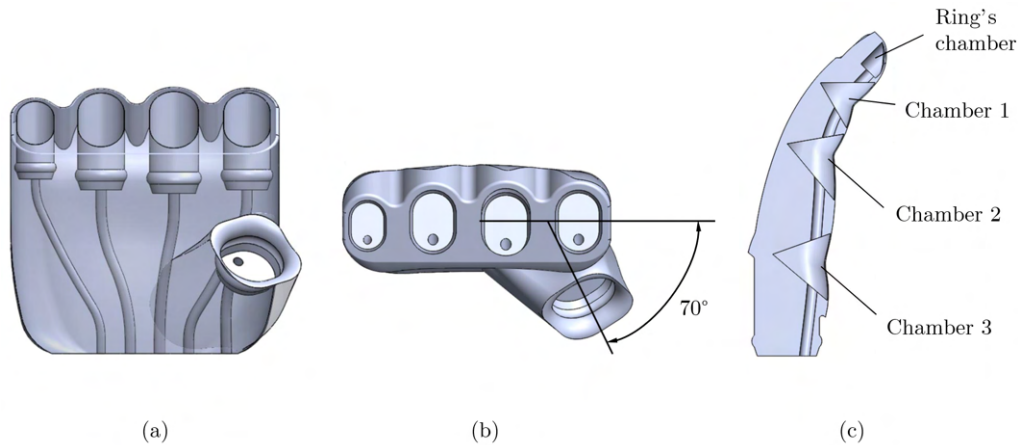


Figure 5.5: Design details of the components of the body-powered hand prosthesis developed by F. Pinheiro [62]: (a) anterior view of the hand body; (b) top view of the hand body; (c) inner design of the finger.

Despite F. Pinheiro's prototype being one of the better ones, the fingers' design as well as the thumb position still needed revision, in order to give the prosthesis a more natural look. These adjustments needed to be done without compromising the prosthesis' functionality. Also, the remaining design of the prosthesis should also be improved in terms of anthropomorphic shape. Thus, there was a need to improve the cosmetic appearance of 3D-printed body-powered prostheses, without compromising the other user's needs such as comfort, lightweights, low-cost and functionality. Flexible materials were thought to be the key to solving some of the referred issues since they allowed them to achieve a more realistic appearance and establish some sensory feedback.

Ana Oliveira's study in 2021, intended to solve some of these problems [63]. In the end, the study ended with the prototype shown in Figure 5.6.

This prototype achieved a high level of customization due to the developed protocol that measured and assessed the anatomical features of both limbs' extremities. It is expected to use this same protocol for any new prosthesis developed with this new model. This developed method consists of simple measurements and body casting of both limbs' extremities, providing different types of information, from single to three-dimensional data.

The first procedure consists of measuring the child's upper limbs. It starts with the collection of personal data and the clinical background of the child. This form is inspired by the one used during the measurements sessions in the *Patient Innovation* program, more specifically in the "*Dar a Mão*" project. Then, both limbs are measured according to the measurements guide from the *e-Nable* project, where some photos were taken on



Figure 5.6: Main developed prosthesis by Ana Oliveira's thesis [63]: (a) anterior view; (b) posterior view.

millimeter paper placed under the child's limbs for reference. In order to facilitate this process, a coin is placed in the picture for better dimensional reference. An example of the measurement process is shown in Figure 5.7.

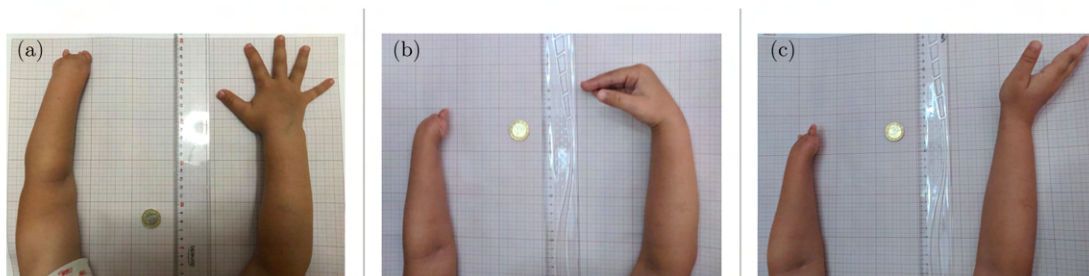


Figure 5.7: Example of the measurement process of the child's upper limbs [63]: (a) first position; (b) second position; (c) third position.

The second procedure consists of body-casting of both limbs. Before starting the procedure, the child's limbs should be greased with baby oil. Then, the limbs are immersed in a solution of alginate, a biopolymer obtained from brown seaweed. This specific alginate is *Orthoprint*, by ©Zhermack. After solidifying, the limbs are removed and cleaned, and the mould is filled with a plaster solution. After the plaster is set and dry, the alginate is removed, and the resulting replicas are obtained, as shown in Figure 5.8.

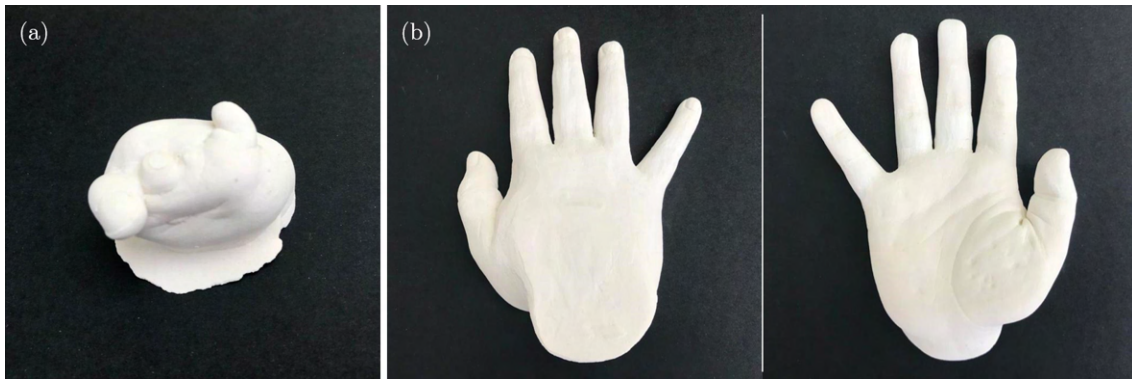


Figure 5.8: Upper limb's extremities replicas made with plaster [63]: (a) Left extremity with a transverse metacarpal total deficiency; (b) Dorsal (left) and palmar (right) views of the healthy right healthy hand.

With the measurements and body-cast replicas, it is possible to extract enough information to adapt the prosthesis to the patient's dimensions. This high level of customization is similar to the *Patient Innovation's* prosthesis, which is considered of high level.

Ana Oliveira's prototype presented a huge upgrade from the previous prototypes but it had some limitations in terms of functionality. For that reason, this prototype was the starting point for this study.

In terms of myoelectric prostheses, there are several industries specialized in the development of new models. A company worth mentioning is the German company *Ottobock*, whose most popular models are the *BeBionic Hand* and the *Michelangelo's Arm* [64], shown in Figure 5.9.



(a) *BeBionic Hand* [65] Prosthesis

(b) *Michelangelo's Arm* [66] Prosthesis

Figure 5.9: *Ottobock* Prosthesis Models [64]

In both cases, it was essential to produce a comfortable, intuitive model that uses

fourteen different grip patterns and hand movements. The performance of individual motors in each finger allows natural and coordinated movements. These prostheses have a control proportional to the strength of the muscles that regulate the speed of movement.

Some of the newer models available use advanced sensors and algorithms to provide improved control and dexterity. Additionally, these are commercially available prosthetic hands that can be customized to match a person's skin tone. Nevertheless, it is important to keep in mind that myoelectric prostheses require regular maintenance and battery replacement, and may not be suitable for individuals with certain medical conditions.

Current prosthetic models provide significant advancements in the field of artificial limbs, offering improved functionality and a more natural feel to the user. However, they are also a considerable financial investment, and it's important to carefully consider all factors before choosing a myoelectric prosthesis.

Concept Development

This chapter describes the clinical case in which this study is based on, as well as the methodology used to develop a customised 3D myoelectric prosthesis using AM and a low-cost and simple myoelectric controller where the input is the user's intention, acquired with one single channel acquisition. The idea is to produce a functional and simple device, similar to the biological hand that can simulate three different hand gestures - Rest Position, Spherical Grip and Index Finger Pointing. Given that the prosthesis was developed through an iterative process, where the results of a given prototype influenced the methodology used in the following, most details are present in Chapter 7.

6.1 Introduction to the Study

The prosthesis device developed during this study was based on a single clinical case. Since one of the main goals of this study consisted in customising the developed prosthesis, addressing more than one clinical case would be far too time-consuming for the duration of this work.

This study was a continuation and combination of two previous studies developed by the colleagues Ana Oliveira and Ema Lopes, so all the information of the patient was withdrawn from those studies. The clinical case was of a four-year-old (at the time of the measuring session) with a left transverse metacarpal total deficiency caused by amniotic band syndrome. Table 6.1 shows a comparative analysis of the work done in Ana Oliveira and Ema Lopes' thesis and the current research.

6.2 Methodology

The methodology applied in this study was inspired by the Product Design and Development methodology [67]. The first step was defining the goals of this study through the identification of the main flaws in most upper limb prosthetic devices, as described in Chapters 2 and 5 and the limitations of the previous models developed during Ana Oliveira's and Ema Lopes's study [63], [68]. Afterwards, the main user's needs were

Table 6.1: Comparative Analysis of the Work Done in Ana Oliveira and Ema Lopes' Thesis and the Current Research.

Previous Research	Current Research
design of the fingers	re-design of the fingers with the addition of elliptic holes in the interphalangeal joints
design of the wrist region	re-design of the wrist region by testing the addition of the servomotor support system
design of the metacarpal region	re-design of the metacarpal region with the addition of the servomotor support system and update of the wiring system
tuning of the printing parameters	further research into tuning the printing parameters
pull tests to determine ideal parameters whilst using <i>Filaflex 82A</i>	pull tests to determine ideal parameters whilst using <i>Filaflex 60A</i> and <i>70A</i>
development of a EMG signal classifier	implementation of the EMG signal classifier into the prototype
	research into the ideal electrode position for better EMG signal acquisition
	development of the electronic components responsible for the movement of the prosthesis

taken into consideration in order to determine the specifications and alterations of the present prosthesis. Finally, the main concepts used to develop the prosthesis were generated on these specifications.

The concept selection phases were performed aiming for a high level of customization and functionality, whilst maintaining its simplicity and low price. During this phase, several prototypes were designed and tested. For the EMG signal processing and classification phase the main goal was further to develop Ema Lopes' s EMG signal classifier by investigating new electrode positions and their effects and improving the classification performance by decreasing the number and complexity of the acquired movements.

Finally, the whole prosthesis was evaluated in order to identify possible improvement points for the future. Figure 6.1 presents the short version of the flowchart that illustrates the development process of the prosthesis. Appendix A presents a more detailed and thorough description of the used methodology.

6.2.1 Prosthesis Design

One of the main goals of this study is to design a highly customised prosthesis. The design of the prosthetic device was made considering the Designing for Additive Manufacturing

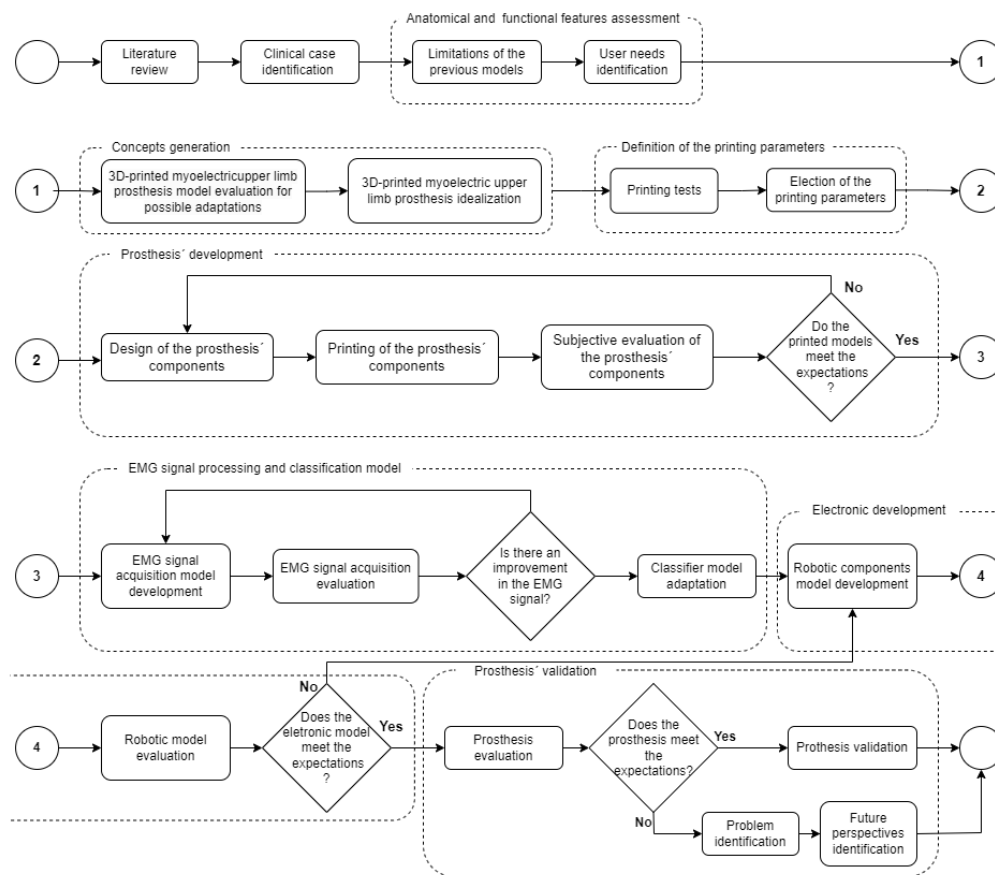


Figure 6.1: Methodology flowchart

(DfAM) principles, aiming to achieve the best results when printing the different models that compose the prosthesis.

The prosthesis' design is composed of different components that can be segmented into three different parts: the fingers, the metacarpal region and the wrist region. The entire design was originally made during Ana Oliveira's study, considering the extrusion width and height, so the designed walls could be a multiple of those values. The printing position was also a considered factor as well as the existence of support structures, that were avoided whenever possible. When working with more common, non-flexible materials, such as *PLA*, support systems do not affect the surface quality of the model, but when working with *Filalfex*, due to its flexibility, support systems lower the surface quality and for that reason should be avoided. These factors were considered of extreme importance and were kept in mind during any alteration to the original model. Ana Oliveira's prosthesis model is an easy-to-build prototype with a good level of functionality, where all parts can be 3D-printed, which allows for a short time to market and a high level of customization. However, one of the aims of this study is to upgrade from a body-powered prosthesis to a myoelectric one. Thus, it was necessary to update some parts and design new ones in order to be compatible with the electronic components

without compromising the prosthesis weight and associated cost.

The whole prosthesis was designed using a combination of *Fusion 360 CAD* software (version 2.0.10940) by ©Autodesk for simpler updates in the design and the *SolidWorks CAD 2021* software by ©Solidworks for more complicated designs and updates. The *.stl* files resulting from the original model developed during Ana Oliveira’s study, were imported to the CAD software and then modified in order to improve the original models and adapt the model to the new electronic components, whilst preserving the anatomical features of the child and allowing the most customization of the prosthesis as possible.

Since all the original *.stl* original files were shared through the *Fusion Projects* hub, it was possible to download them in a variety of formats. For the simpler designs and updates, the file was downloaded directly in a *.stl* file format, which was used for the *Fusion 360 CAD* software and required a change in its representation from a *mesh* to a *body*, (*Brep*), so it could be modified. This format also allowed for a reduction of the computational burden of dealing with a huge number of faces. The number of faces was reduced up to a maximum recommended number of 10 000 faces, before doing the conversion. Figure 6.2 shows an example of the process from the resulting *mesh* to the final customizable *body* representation. No re-scaling was used during the development of the prosthesis.

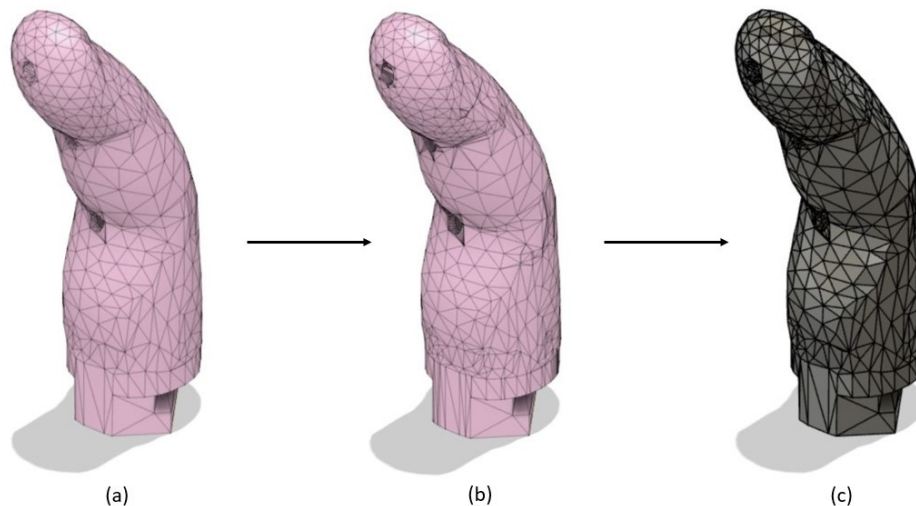


Figure 6.2: Modification process of the design file: (a) mesh representation; (b) mesh representation after reducing the number of faces to under 10 000; (c) body representation.

For the bigger files and more complicated designs and updates, the *SolidWorks CAD 2021* software was preferable since it allowed for more complex alterations. The best way found to export the file from *Fusion Projects* hub to the *SolidWorks* software, was by exporting the file in a *.stp* file format. This file format was compatible with the *SolidWorks*

software but did not allow for a reduction of the number of faces since it directly opened the file in a *body* representation. This process required a bigger computational burden but did not present any difficulties during the development of this study.

6.2.2 Tuning of the Printing Parameters

The developed prosthesis is composed of a combination of flexible and rigid materials. In the beginning stages of this process, in order to test the adequate material for the final prototypes, several models of the index finger were printed using *Filaflex 60A* and *Filaflex 70A*. In the later stages of the study, the fingers, metacarpal and wrist regions were printed using *Filaflex 60A*, whilst the wrist pins were printed using *PLA*. Some of the pieces designed during this study were printed using *polyethylene terephthalate glycol (PET-G)*, before being printed using the flexible filament, due to the abundance of *PET-G* and the shortage of *Filaflex* in the laboratory. This allowed for testing to see if the developed pieces designed in *SolidWorks* and *Fusion 360 CAD* were printable.

Through the design of the fingers, several printing tests were made in order to determine the printing parameters of *Filaflex* that would lead to the best printing quality and desirable behaviour. Due to being from the same manufacturer, there was no need to distinguish the printing parameters for the *Filaflex 60A* and *Filaflex 70A*. A desirable printing quality implies a model printed with the fewest defects, such as bad adhesion between layers, excess of extruded materials or void formations, smooth surfaces, among others. A desirable functionality means a print model capable of simulating the flexibility and behaviour found in the human hand.

During this study, all prints were achieved using *The Original Prusa i3 MK3S+* by ©Prusa Research. The printing parameters were defined using the corresponding slicing software, the *PrusaSlicer* software (version 2.5.0).

The filament technical data sheet for the filaments used, provided by Recreus, this filament's manufacture, is shown in Appendix B. It was advised to test small variations in the parameters since the printer model could influence the print quality. The main variables that were tested were: the number of printing walls, the infill, the printing speed, the amount of extruded material and the retraction speed. Figures 6.3, 6.4 and 6.5 present the printing parameters that were changed during these tests. Each branch of these figures correspond to the setting tabs of the *PrusaSlicer* software. The printing position and its influence were also tested.

The search for the ideal parameters was obtained through an iterative process where the visual features of the model resulting from tests with certain sets of printing parameters were taken in consideration. In each test, a single printing parameter was adjusted from the previous.

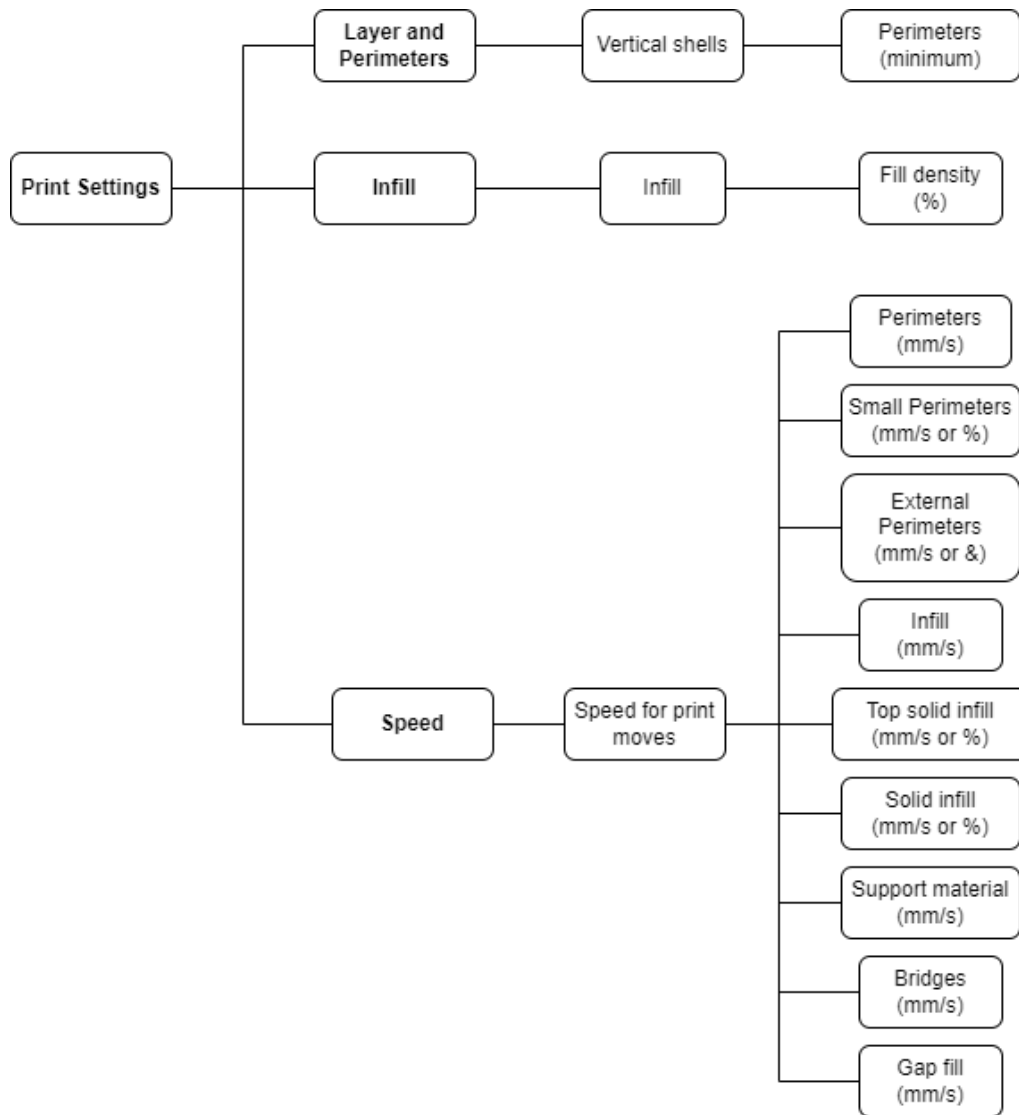


Figure 6.3: Tested printing settings of *PrusaSlicer* software.

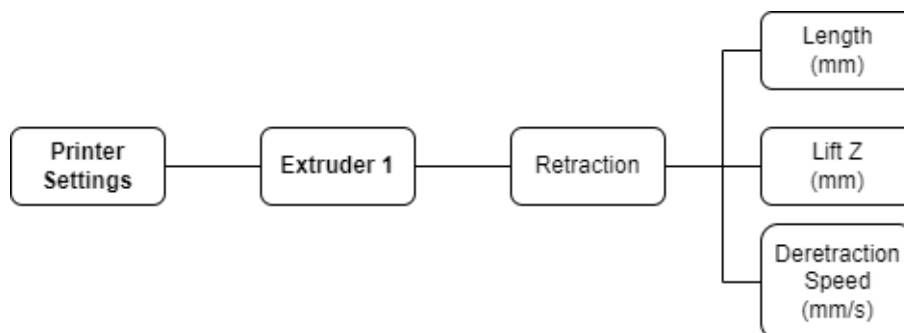


Figure 6.4: Tested printer settings of *PrusaSlicer* software

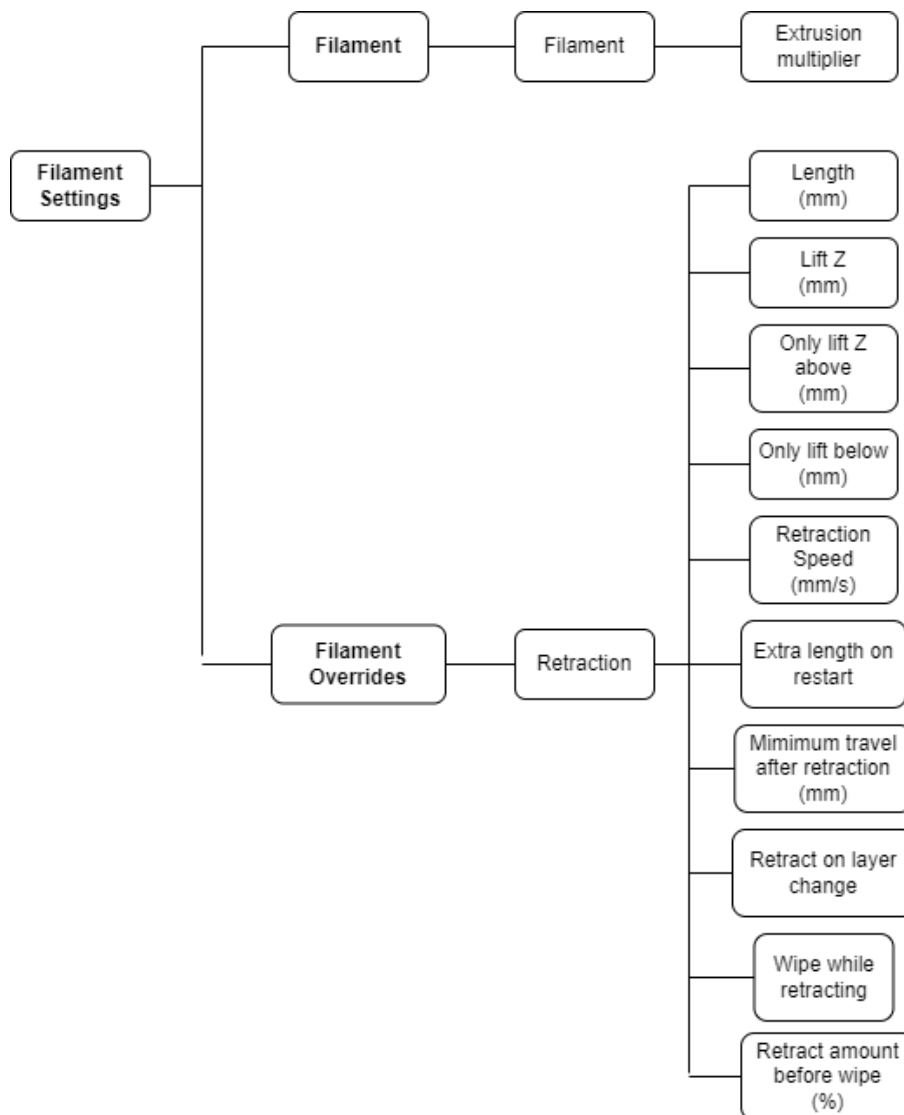


Figure 6.5: Tested filament settings of *PrusaSlicer* software.

6.2.3 Pull Tests

During the design of the fingers, several models were developed and, in order to evaluate each's performance, several tests were performed. These tests aimed to evaluate the level of functionality (i.e., the force applied in order to produce a full finger flexion). While printing quality was assessed subjectively by looking at the obtained object and its surface, these tests allowed quantifying the force necessary for the finger model to complete a full finger flexion. Therefore, a protocol was necessary in order to measure the force needed to bend each finger model. During Ana Oliveira's study a protocol was developed in order to evaluate the level of functionality of the finger pieces printed using *Filaflex 82A* [63]. In this study, the same protocol was followed in order to evaluate finger pieces printed using new materials, *Filaflex 60A* and *Filaflex 70A*. The protocol used and the consequent results are made available in Appendix D.

The finger model under test was placed in a support system fixed to an elevated

structure. This finger would have a nylon string tied to the tip of the finger and pass through the finger so that it could be pulled vertically. A dynamometer was placed below and tied to the string in order to measure the force applied to the finger. To the other extremity of the dynamometer, a tissue bag, where metallic cylinders could be placed, was tied, causing the finger to bend. Consequently, the fingertip would suffer a displacement that was later measured with a dial gauge. The contact point of the dial gauge was in contact with a horizontal tab fitted to the top of the dynamometer. Hence, when the finger flexed, the dynamometer would move accordingly. This process was repeated with increasingly more weight in the tissue bag until full flexion was achieved, which corresponded to a displacement of 20 mm. Figure 6.6 schematizes the setup of the described procedure.

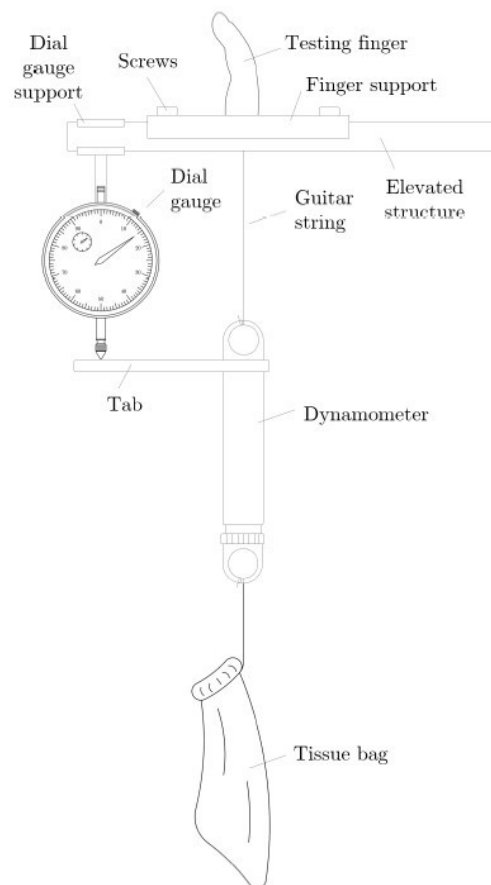


Figure 6.6: Pull tests setup used in this and Ana Oliveira's study [63].

6.2.4 Integrating Hardware and Software for Myoelectric Control

In order to improve the *EMG* signal acquisition process it was important to follow the same protocol followed by Ema Lopes' study [68]. Ema Lopes developed an acquisition protocol that was approved by the Ethical Committee of the Faculty of Science of the University of Lisbon before experimenting with it in June 2021. This protocol was

followed by forty-five healthy volunteers without any known neurological or physical pathological conditions. The protocol and study achieved positive results but there were concerns about the placement of the electrodes in the forearm. This study followed the same protocol developed by Ema Lopes but tested different placements for the electrodes and their influences in two different volunteers.

6.2.4.1 Experimental protocol

This experiment was divided into one training portion and a real-time acquisition that soon followed. The volunteer performed three gestures separated by rest intervals in order to avoid muscle fatigue. Since the main goal was recognition of specific movements, between sets of movements, the volunteer's forearm was laid down on the back of the hand in order to avoid fatiguing positions. During the training session, it was initiated the calibration phase established the rest and Maximal Voluntary Contraction (MVC) for all exercises.

After practising the exercises and calibrating the equipment, the protocol of the main study was followed. The number of repetitions and the exercise order were not randomised in order to trigger an unconscious reaction on part of the volunteer. The three exercises requested to be performed, shown in Figure 6.7, were the following:

1. In the first exercise (spherical grip), the volunteer was asked to perform the movement of grabbing a spherical tennis ball.
2. In the second exercise (tripod grip), the volunteer had to perform the movement of pressing the thumb and the first and second fingers together.
3. In the final exercise (index finger flexion), the volunteer had to perform the movement of flexion of the index finger.

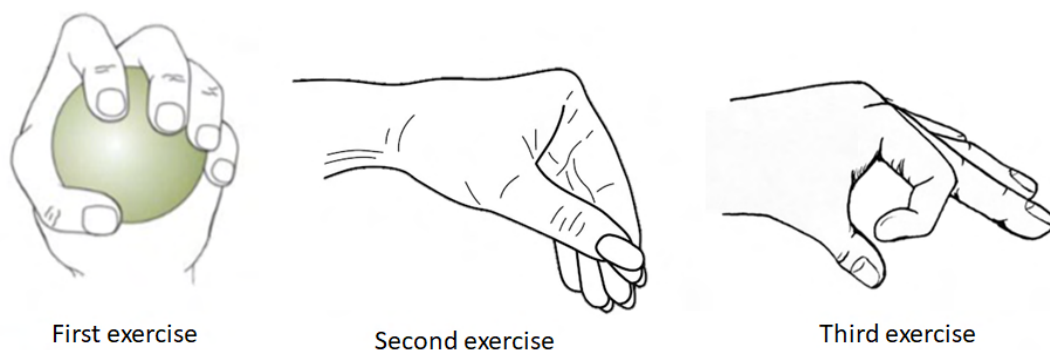


Figure 6.7: Illustration of the acquired movements [69].

Before starting acquisition it is recommended to clean the sweat of the volunteer's skin with alcohol, which is a crucial step to improve the quality of the acquisition and the reduction of possible artefacts [70].

The used protocol during the acquisition was:

1. The volunteer was asked to sit down in a chair in a comfortable position. It was necessary to maintain an upright body posture with an angle of 90 degrees between the elbow and the table.
2. During the training stage, the electrodes were positioned and it was tested if the signal was being detected through the display panel. The electrode's position was marked in order to ensure the electrodes were in the same position in case one of them moved or fell.
3. The acquisition started.
4. The first movement of picking up a ball (spherical grip) was performed. The volunteer reached for the tennis ball, which was placed on the table, held the ball for 2 seconds and then dropped it.
5. Afterwards the tripod grip movement was performed. The thumb, index and middle finger were pulled together, held for 2 seconds and then the volunteer went back to the resting position.
6. Finally, the finger flexion movement was performed for 2 seconds before returning to the resting position.
7. Each exercise was repeated ten times in a total time of 40 seconds.
8. The acquisition was repeated with both arms, dominant and non-dominant.
9. The data was saved and the acquisition ended.

In this study, the acquisitions process was repeated several times by two volunteers, each of them with a different electrodes' placement.

6.2.5 Prosthesis Assembly

The prosthesis was assembled after completing the component's design, printing and testing. Several prototypes were partially assembled but only the final model was assembled till the end. These partial assemblies allowed for a better understanding of what aspects were important to update. Only the final model was fully assembled in order to save the low resources, especially the servomotors.

The assembly process remains basically the same during the whole study, with the evaluation of the prototype not having a significant influence in the assembly process.

The assembly is a long process, taking up about four hours time. It is not a difficult process but a meticulous one, especially when wiring the fingers and the metacarpal region. Figure 6.8 presents the main components and materials needed to assemble the prosthetic device.

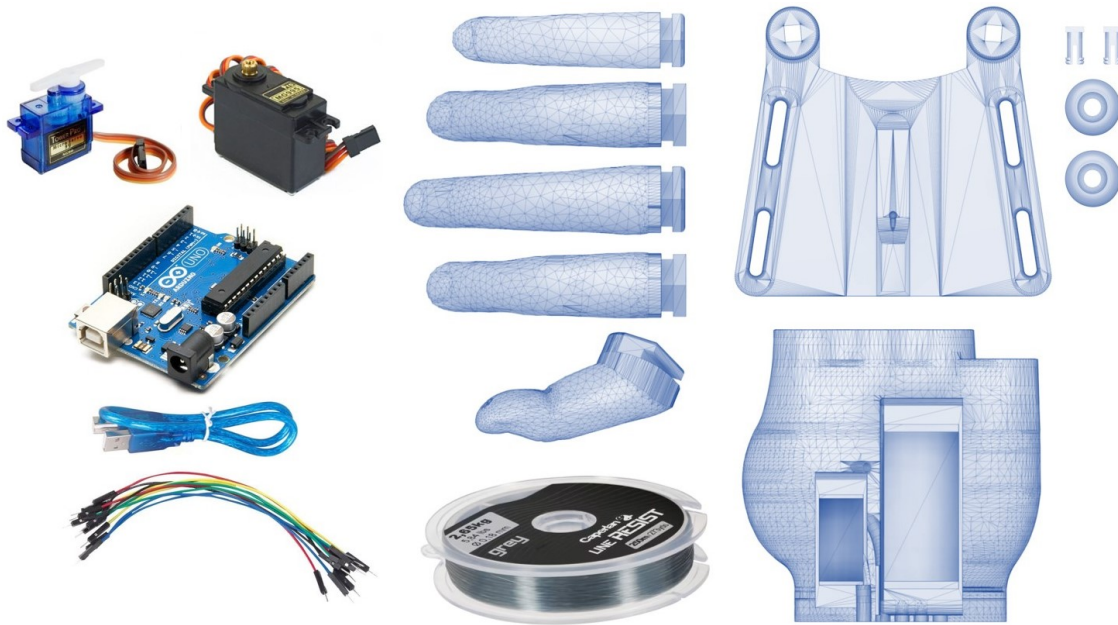


Figure 6.8: Prostheses components for its assembly.

The development of the fitting mechanism during this study facilitates significantly the assembly of the prosthesis. There is no need for extra pins in order to connect most pieces, as they connect directly, allowing for an easy assembly and substitution of individual pieces.

6.2.5.1 Assembly of the Prosthesis Device

The first step of the assembly is the wiring of the fingers. The fingers' assembly require special attention, since it connected the fingers straight to the servomotors. The index finger is connected solely to the smaller and weaker servo whilst the rest of the fingers are connected to the more powerful servomotor. In all fingers, a 0.20 mm nylon string is inserted in a distal-proximal order. The process of passing the wire through the finger's wire canal is helped by the use of a needle. The wire should be tied to the needle and then passed through the canal whilst using the interphalangeal joint holes as checkpoints, pulling the wire with it. The steps of wiring the fingers are shown in Figure 6.9.

With all fingers wired, the next step is connecting the fingers to the metacarpal region. This is achieved through the developed fitting mechanism that directly connects the proximal part of the fingers to the distal part of the metacarpal region piece. Figure 6.10 illustrates the process of connecting the metacarpal region to the fingers and following the wiring process.

After every finger is connected to the metacarpal region piece, the servomotors can be fitted into the metacarpal piece. Each servo is directly fitted to its specific place and afterwards, the wires connected to the fingers are rolled into the servo. This connects every component of the prosthesis and allows the prosthesis to perform some specific

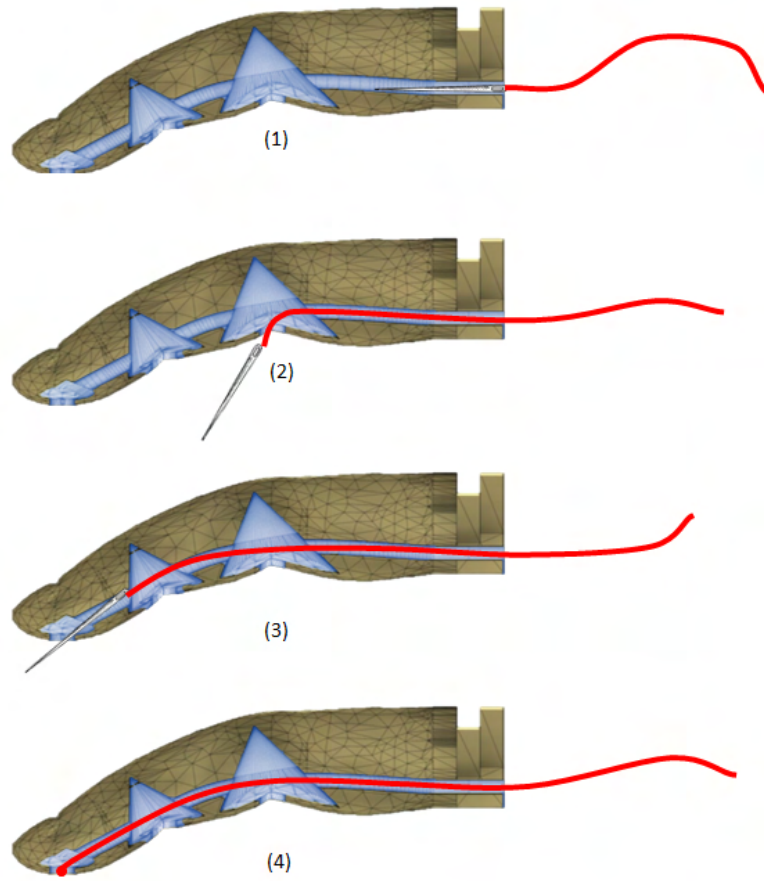


Figure 6.9: Process of wiring of the fingers.

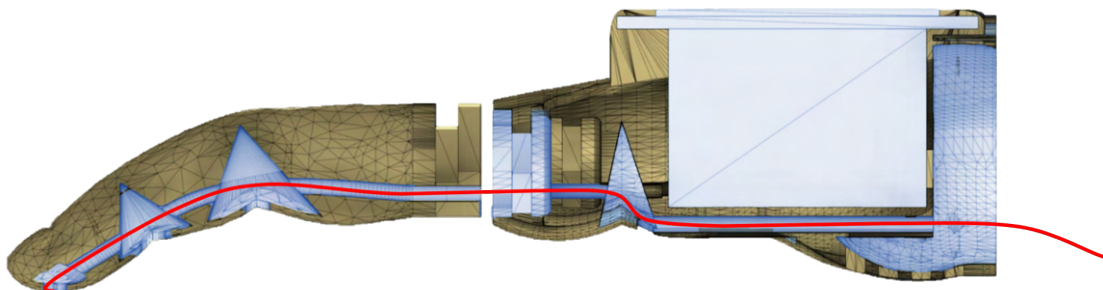


Figure 6.10: Process of connecting the fingers to the metacarpal piece and wiring of the metacarpal region.

movements. Figure 6.11 shows the complete wiring system that connects the fingers to the servomotors, whilst passing through the metacarpal region piece. The process of connecting to the servomotor requires special attention. Each wire is connected individually but afterwards, they all must have the same tension as the other ones connected to the same servomotor. This is important in order for the fingers to all flex the same quantity during the movement.

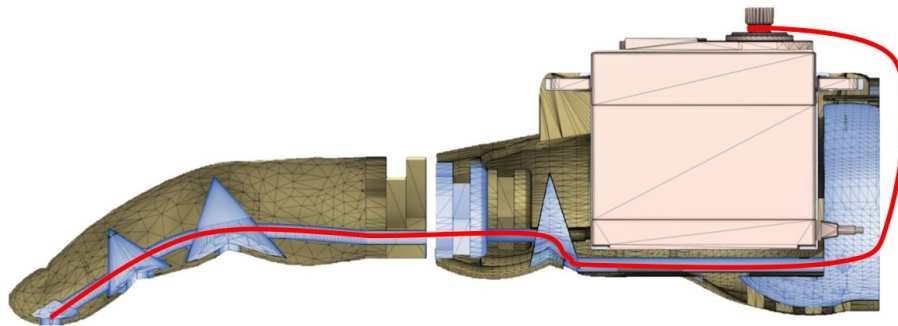


Figure 6.11: Process of connecting the fingers to the servomotors, whilst passing through the metacarpal region piece.

The final step is the connection of the metacarpal region structure to the forearm gauntlet. It starts with the insertion of the wrist pins. The pins of this prosthesis present no differences from the ones of the previous model. The pins are inserted from the inside of the stump-prosthesis interface. Figure 6.12 shows the design of the metacarpal region as well as its pins and how to insert them. After assembling the mode pins, the gauntlet can be connected and locked in place with the pin caps.

For better understanding on the assembly of the printable components of the prosthesis, Figure 6.13 shows the exploded view of the prosthesis.

By this stage, the prosthetic model is already assembled but there still is necessary to connect the servomotors to the electronic components, so that it can receive the classifier output and perform the intended movements.

6.2.5.2 Assembly of the Electronic Components

Interfacing a single servomotor with an Arduino UNO is a simple process that only requires the connection of three wires to the Arduino supply pins, as shown in Figure 6.14. There is no need for an external power supply since the Arduino is capable of powering a single servomotor.

Connecting multiple servomotors with an Arduino seems an easy process but only connecting the servos to the Arduino supply pins, as shown in Figure 6.15(a), will not work properly due to the lack of enough current to drive all the motors. It is necessary to

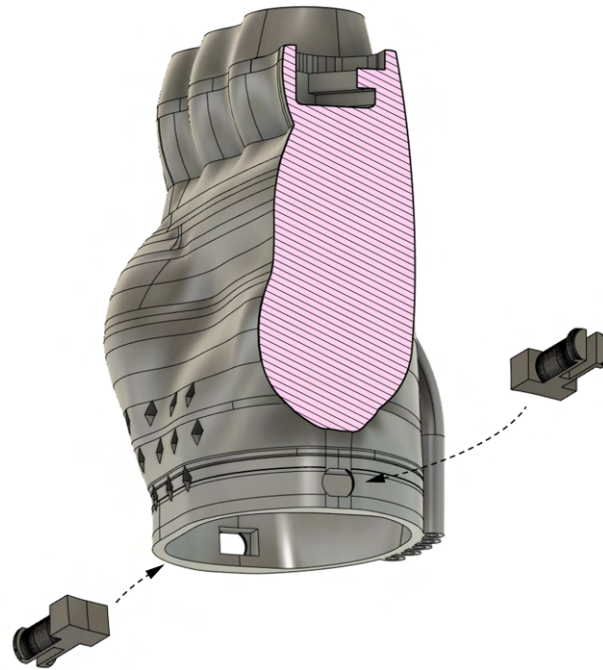


Figure 6.12: Process of assembling the pins that connect the metacarpal region structure to the forearm gauntlet.

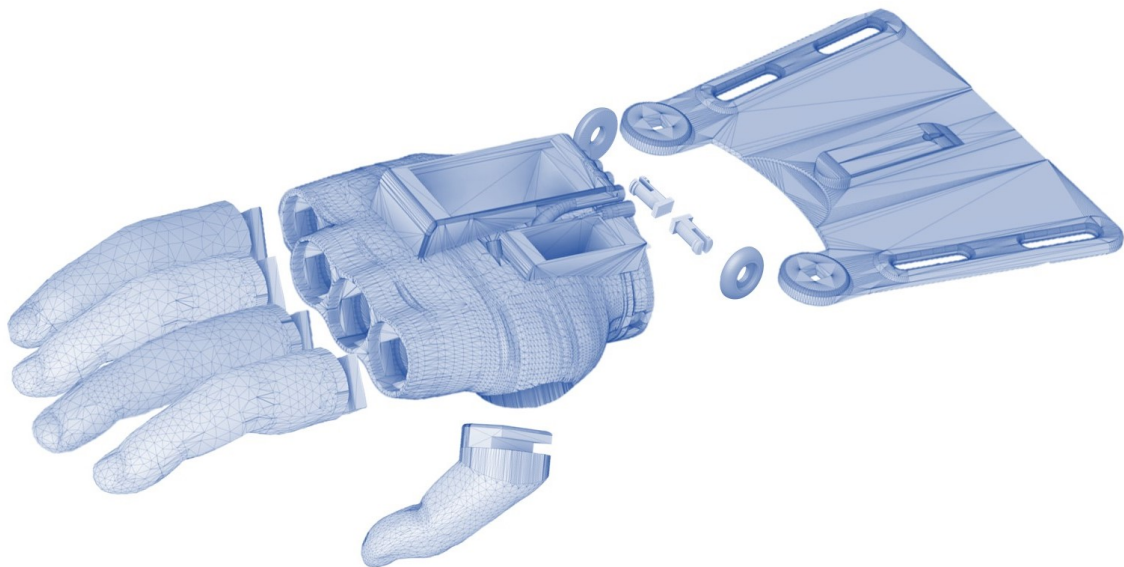


Figure 6.13: Exploded view of the prosthesis.

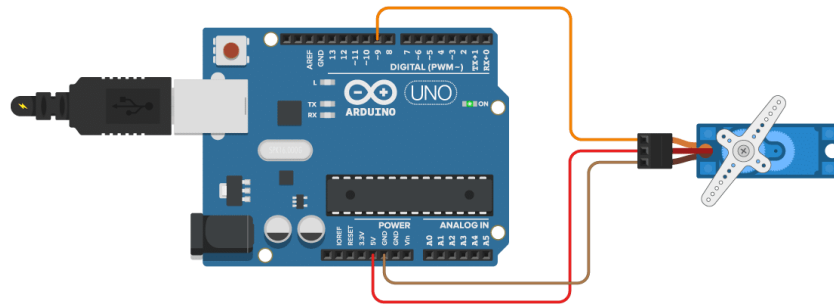
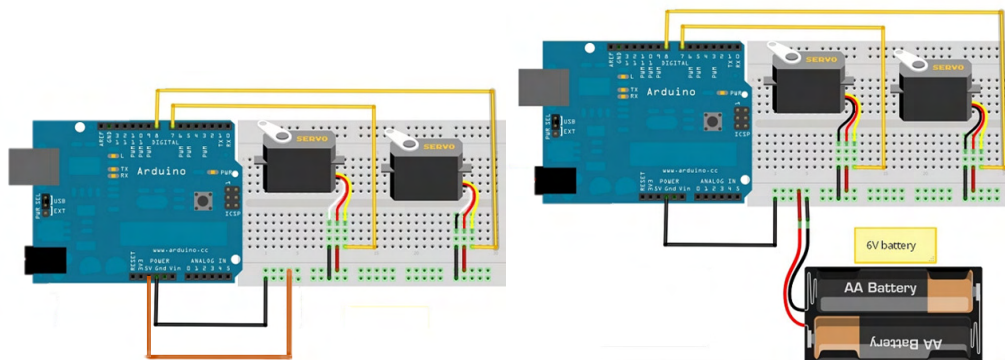


Figure 6.14: Interfacing a single servomotor with an Arduino Uno.

use a separate power supply for the motors either it be from some adapters (5V 2A) or from a combination of batteries, as shown in Figure 6.15(b).



(a) Interfacing servomotors with Arduino board and no external power supply. (b) Interfacing servomotors and an external power supply with Arduino board.

Figure 6.15: Interfacing servomotors with Arduino board.

In order to achieve a wireless connection between the computer and the Arduino, it is necessary to use a Bluetooth module transmitter, such as the HC-05 Bluetooth module. The HC-05 requires a connection of four pins, the power supply connected to a 5V pin, the ground connected to the GND pin and Transmit Serial Data (TXD) and Receive Serial Data (RXD) pins connected to the Arduino supply pins. Afterwards, it is essential to connect the Bluetooth module to the computer. This is achieved by searching for BT devices in the *Bluetooth connections* tab in the computer *Settings* and connecting to the device called "HC-05". The standard PIN code is 1234.

For this study, it is necessary to connect a total of two servomotors to the *Arduino UNO R3*. Figure 6.17 shows the circuit diagram of the electronic components used in the assembly of this prosthesis. In order to power the prosthesis, more specifically the servos and the Arduino board, it is used an external power supply a 6V at 500 mA/h battery pack of four alkaline batteries and a 9V battery, respectively. This battery pack generates

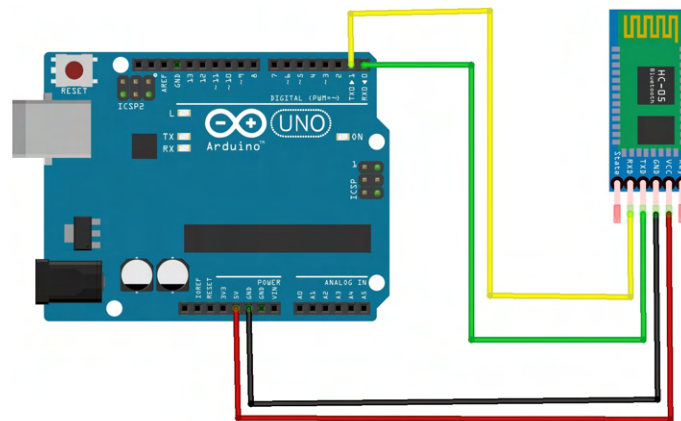


Figure 6.16: Interfacing HC-05 Bluetooth Module with Arduino Uno.

enough energy to power all the electronic components for a short period of time.

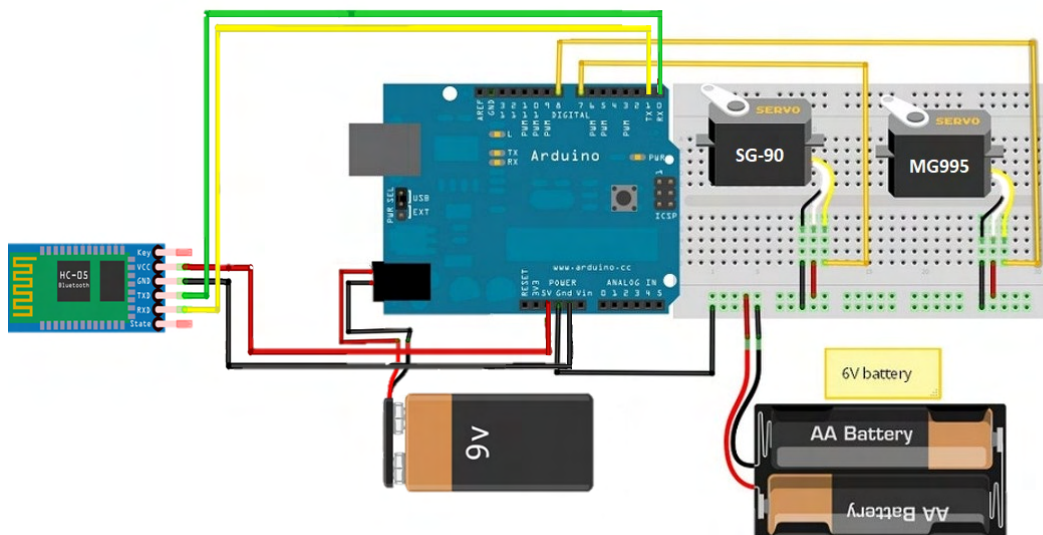


Figure 6.17: Circuit diagram used in the prosthesis prototype.

6.2.6 Prosthesis Evaluation

The evaluation of the prosthesis was made after the assembly of the final prototype. The device is evaluated in terms of functionality and cosmetic appearance. The development costs, the total printing time and their weight were also assessed. It was not possible to present the resulting prosthesis to the child and his family. This did not allow the measurement of their level of satisfaction through the System Usability Scale (SUS). This tool was developed in order to measure the usability of a wide variety of products or services. The responses of the user to the SUS survey are converted to a score and calculated to a

mathematical value. With this score in mind, it is possible to confirm if the prosthesis has meet the expectations. Due to its importance, since it was not possible to present the survey to the patient or his/her family, the survey was still answered in order to properly evaluate the cosmetic appearance, functionally, and overall usability.

The SUS is composed of ten questions with five response options that go from "Strongly agree" to "Strongly disagree", which correspond to a score from 5 to 1, respectively. These responses are converted to a score calculated according to the equations 6.1, 6.2 and 6.3, which κ is the score of the question φ . The score's scale ranges from 0 to 100. A score above 68 is considered to be above average and what is expected [71], [72].

$$a = \sum_{i=1}^5 \kappa_{2i-1} - 5 \quad (6.1)$$

$$b = 25 - \sum_{i=1}^5 \kappa_{2i} \quad (6.2)$$

$$SUS_{score} = (a + b) \times 2.5 \quad (6.3)$$

Besides the standard 10 questions that compose the SUS, Ana Oliveira decided to add ten additional questions that would help have a better understanding of the features necessary to improve. These additional questions were also answered in this study.

These questions follow the logic of the SUS questions and are specific to the developed prostheses in this study. Since this second questionnaire is similar in terms of positive and negative connotation to the SUS questions, this questionnaire was evaluated using the same formulas. Appendix E presents the new survey and its responses.

Results and Discussion

Developing prosthesis devices that meet basic user needs whilst maintaining an aesthetic appeal has been extremely challenging due to the high costs of production and development. New AM techniques have solved many of these main problems in the prosthesis field, leading to more affordable, accessible, lighter and customizable devices.

Capturing the anatomical features is crucial to develop customised prosthetic devices and may be the key to reducing the rejection rate of these devices, especially at younger ages. Combining methods of 3D scanning with AM has been key in turning this final objective feasible.

This study aims to present the development of a new model of a 3D-printed myoelectric customizable prosthesis suitable for young children in a fast development phase. This chapter presents and discusses the many trials and results of the development of this new prosthetic model, in which several prototypes and created concepts are analysed. Some suggestions for further improvements are also presented.

7.1 Prosthesis Design

Since the main goal of this prosthesis is capturing the anatomical features in order to make it the most realistic, the base prototype used is of one developed with the help of a child patient with amniotic band syndrome during Ana Oliveira's study [63]. This patient was an integral part of the development of this prosthesis since the final product is developed towards patients like the one in question.

In order to develop a prototype that would fit the patient's needs, a computer-readable representation of the child's upper limb extremities was essential. This was achieved in Ana Oliveira's study, using a method of 3D scanning plaster replicas of the patient's extremities [63]. Figure 7.1 shows the accuracy of the representations resulting from the 3D scanning of the body-casting replicas obtain during the measuring session.

With the computer representation of the upper limbs, and after many different iterations of prototypes, a final body-powered upper arm prosthesis was achieved by Ana

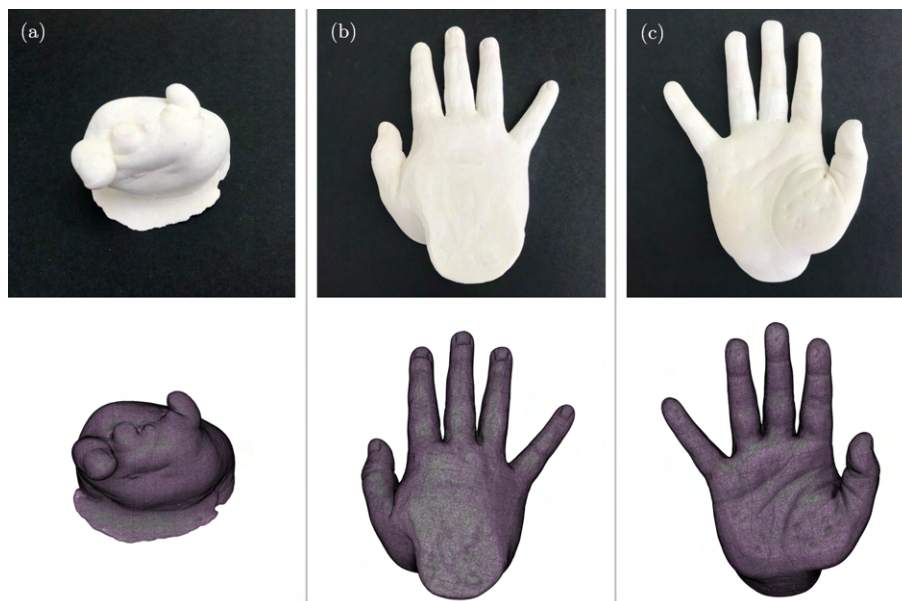


Figure 7.1: Comparison between the plaster replicas (above) and the *.stl* files resulting from the 3D scanning procedure (below) [63]: (a) left upper limb's extremity; (b) posterior view of the right sound hand; (c) anterior view of the right sound hand.

Oliveira, as shown in Figure 7.2 [63]. Regarding the cosmetic appearance, it was considered to be successful in its development, it presented a high level of anthropomorphism, thanks to the use of flexible filament and different infill percentages to mimic the hand's bones, and some protuberances that simulated the hand creases and knuckles, creating the idea of a real hand, especially when compared to other 3D-printed prosthesis. Nevertheless, in regard to certain parameters, it lacked some fundamental aspects and needed some upgrading in order to improve the prototype. Additionally, the prototype was initially developed to be body-powered so it needs some upgrading in order to be compatible with the electric components required for its new functionality.

7.1.1 Fingers Design

The fingers were the components that require the most attention since they are the components that require the most in-depth study. In order to produce the ideal finger design, a deeper understanding of its behaviour to *Filaflex* is required, so in-depth research into previous studies was made [62], [63].

Ana Oliveira's study tested the behaviour of a variety of prototypes in order to reach the optimal one. A combination of pull tests were made, in which variations in the wire holes' position, chambers' angles and curvature of the fingers were studied. After a further evaluation on the advances made in Ana Oliveira's study, it was concluded that the combination of features resulted in a high level of functionality and should continue as the prototype selected as the final model. Figure 7.3 shows the design of the final model prototype, which was modelled for the remaining fingers. The results of the tests,



Figure 7.2: Main developed prosthesis by Ana Oliveira's thesis [63]: (a) anterior view; (b) posterior view.

performed in order to study the influence of the chamber angles, that present the best results are also displayed in Figure 7.4.

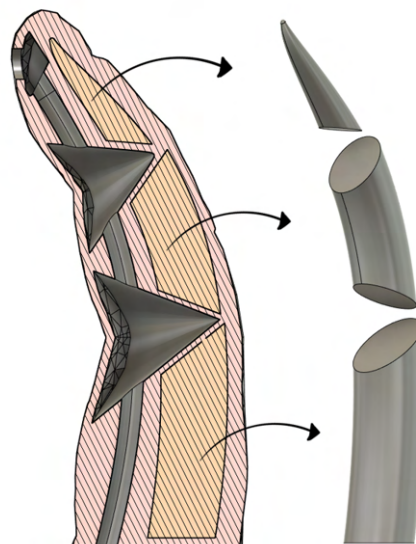


Figure 7.3: Inner design of the final model prototype used in Ana Oliveira's study: cut along the sagittal plane of the index finger (left) and shape of the designed phalanges (right) [63].

Although the functionality levels were up to par and required no update, when it came to the ease of assembly and repair, it lack in a significant way. For Ana Oliveira's study, the finger prototype had less flexibility so it required a guitar string to assembly the

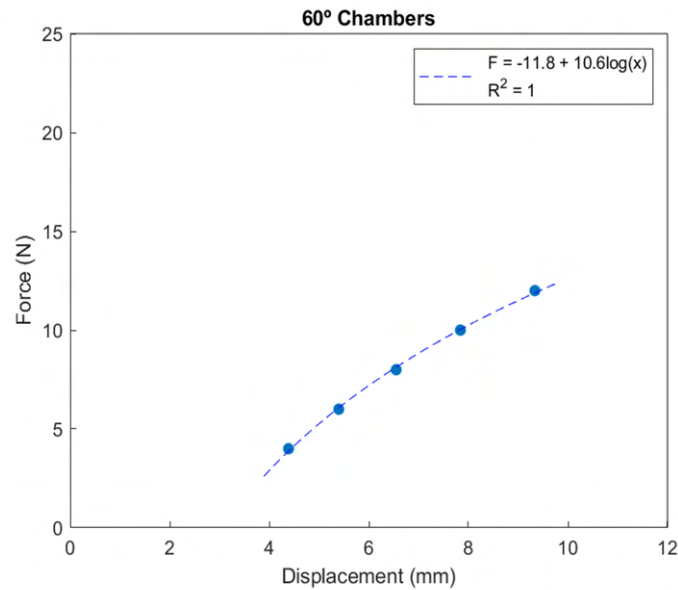


Figure 7.4: Result of the pull test used in the final prototype's combination of features [63].

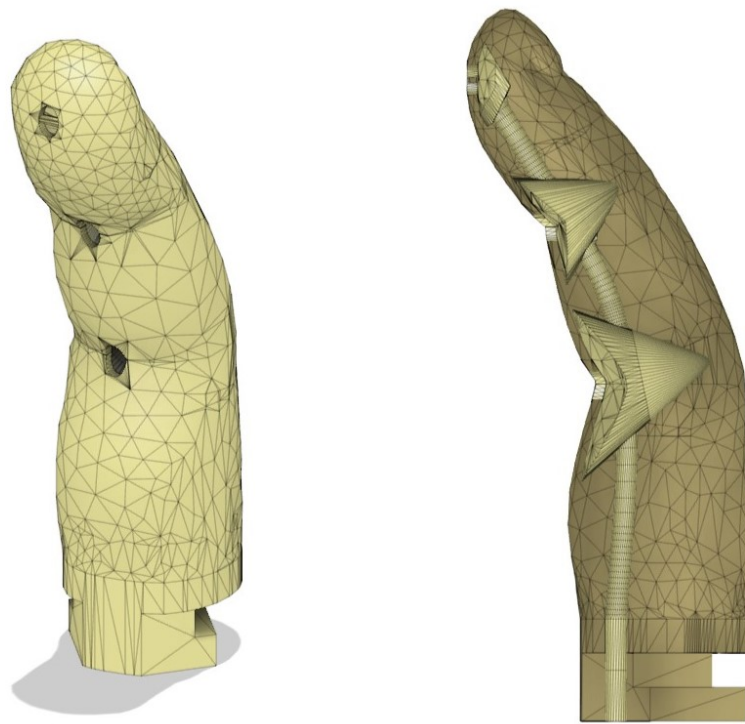
finger to the metacarpal region, but in this newer iteration of the prototype, the fingers become more flexible so the guitar string should be substituted for a cheaper, lighter and less rigid material.

The material chosen for this substitution was a nylon string, due to its high resistance to tension, elasticity and memory. With this substitution a new problem appears, this new material is significantly less rigid than the material used previously which causes the string can get blocked in the debris found in the phalanges tunnels and when going through its chambers, it can curl up on itself.

The new filament used and its high flexibility can increase the difficulty of clearing the phalanges tunnels, so it becomes more difficult to find a new, reliable option that also decreases the price of production and increases the ease of the string passing through. After a variety of prototypes, it was concluded the easiest way of overcoming this problem was adding elliptic holes in the interphalangeal joints that work as *checkpoints*, so the person responsible for the assembly of the prosthesis can help guide the string through the tunnel and chambers. This *checkpoints* are shown in Figure 7.5. With this method, the functionality of the prototype is not affected while, it becomes relatively easier to assemble and repair.

An important aspect of the finger model design is its fitting mechanism, which is responsible for fixing the fingers to the metacarpal region. Its assembly must be simple, so the fingers can easily to fixed or removed in case of need of repairs, however, it must have a system that prevents the separation of the fingers from the metacarpal region when the prosthesis is being actuated.

The final prototype developed in Ana Oliveira's study, at first glance, seemed to



(a) Design of the final model prototype.

(b) Inner design of the final prototype.

Figure 7.5: Final finger model prototype.

work as expected, and after a few tests, it was confirmed this model needed no further alterations [63]. This model used a diamond-shaped segment with rounded bottom edges in order to fix the fingers to the metacarpal region. This model is shown in Figure 7.6 and its fitting hole is shown in Figure 7.7. As desired, the finger can easily be fixed and its removal offers some resistance, needed during the operation of the prosthesis, but not enough to make its removal difficult.

The design of the index finger was the design that set the base for the development of the design of the remaining fingers. For that reason, it required the most time invested. The thumb present design process presented some differences from the other fingers due to its different morphology, as shown in Figure 7.8, but Ana Oliveira's study's chosen methodology and respective values gave showed great results in mimicking the behaviour of a real thumb [63]. The main problem with this design comes in its printing quality, that decreases due to its morphology, Despite all efforts printing quality, is still not desirable but has increased significantly.

With all these alterations made, the fingers have not only shown a higher level of anthropomorphism and maintained the anatomical features of the child's fingers, but also made the assembly an easier process. Thus, the final methodology could be easily applied to other children's fingers in order to design highly customised prostheses, increasing their long-term usage.

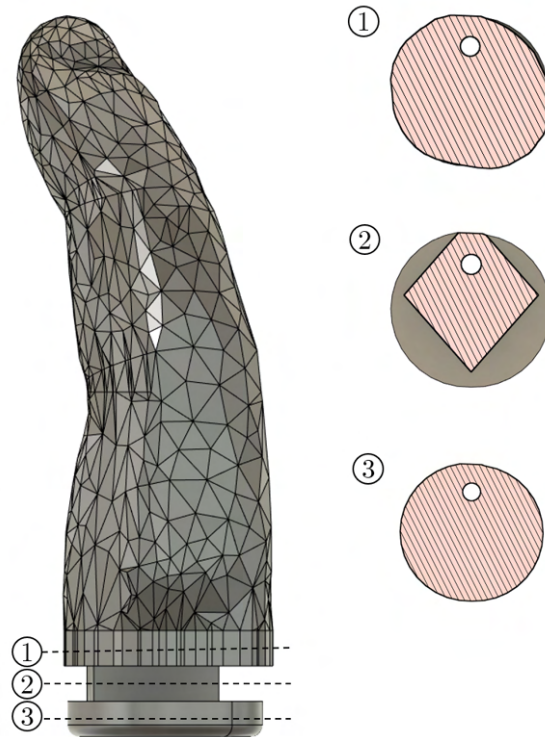


Figure 7.6: Final fitting mechanism model prototype: different transversal sections of the segments that compose this fitting mechanism.

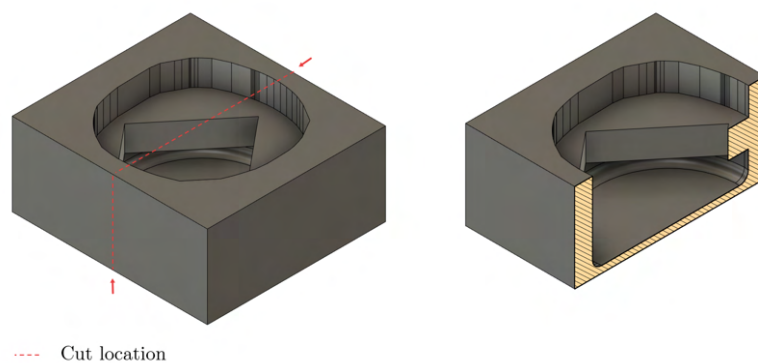


Figure 7.7: Final fitting hole prototype of the metacarpal region: test cube and test cube with a cut along the sagittal plane of the finger.

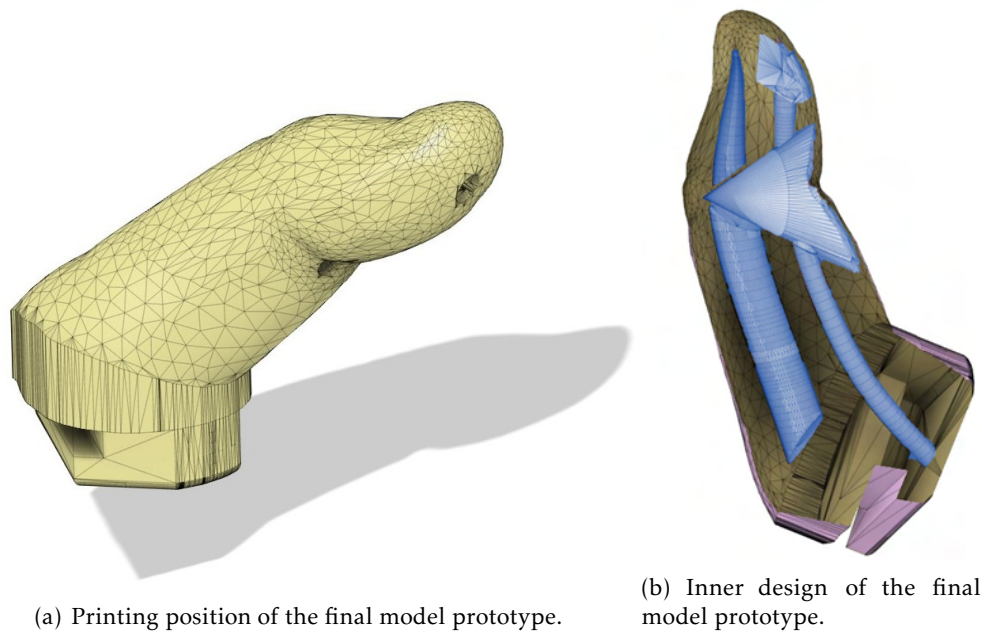


Figure 7.8: Final thumb model prototype.

7.1.2 Wrist Region Design

During Ana Oliveira's study, the wrist design was the simpler stage in the whole process of development, as all the components that were used are from other prostheses [63]. Since the initial idea was to use a whippletree mechanism, all the used components were from *Phoenix Hand v2*, as shown in Figure 7.9, even though the tension system of the main prosthesis was from the *Raptor Reloaded* prosthesis. However, this fact had no further influence as the gauntlet, the thermo pins, their caps and the retention clip are the same for both prostheses. The only modification initially made was the re-sizing of the components in order to match the other components.

In terms of printing parameters, this region of the prosthesis should be printed using the most flexible material available in order to increase comfort as much as possible. In order to evaluate the comfort, it was not possible to consider data from practical tests. The ideal printing parameters and infill percentage were achieved through trial and error. After testing several forearm prints with different printing parameters, it was concluded the ideal prototype was achieved whilst using *Filaflex 60A* and an infill of 20%, since this was the print that adapted better to the forearm and maintained a certain level of rigidness so it can be properly connected to the metacarpal region.

Turning the body-powered prosthesis into a myoelectric prosthesis means there was a need to make a few alterations in the design model. The main addition was adding a support system for the servomotors used to power the movements of the prosthesis.

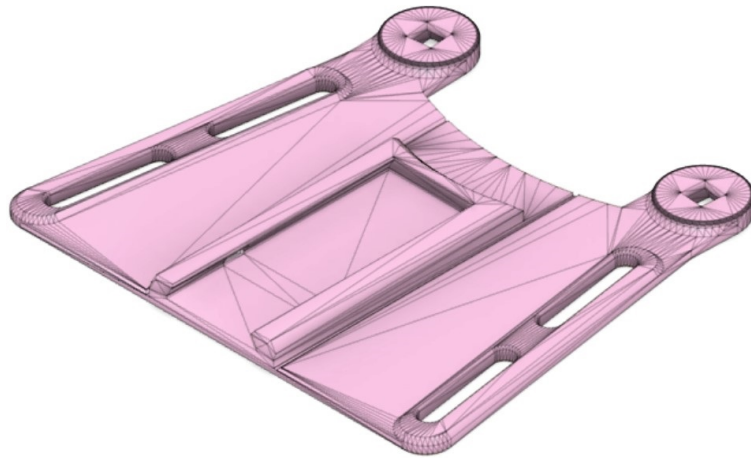
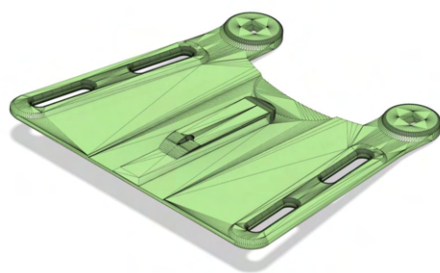


Figure 7.9: Original forearm design of the final prototype from Ana Oliveira's study [63].

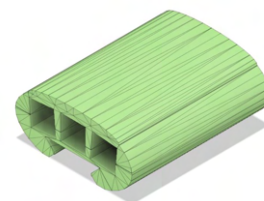
7.1.2.1 Addition of the Servomotor Support System Prototype

At first glance, the wrist region of the prosthesis seemed the most logical for the location of the servomotors support system, but after further evaluation it showed that it did not have a lot of areas to organize the servos in an efficient way.

For that reason, the first prototypes developed were inspired by the *Phoenix Hand v2* model used in the *e-Nable* project. The *Phoenix Hand v2* design uses a gripper box that attaches to the gauntlet, as shown in Figure 7.10. This gripper box is responsible for the tension that powers the movement of the body-powered *Phoenix Hand v2* prosthesis.



(a) Design of the *Phoenix Hand v2*'s gauntlet.

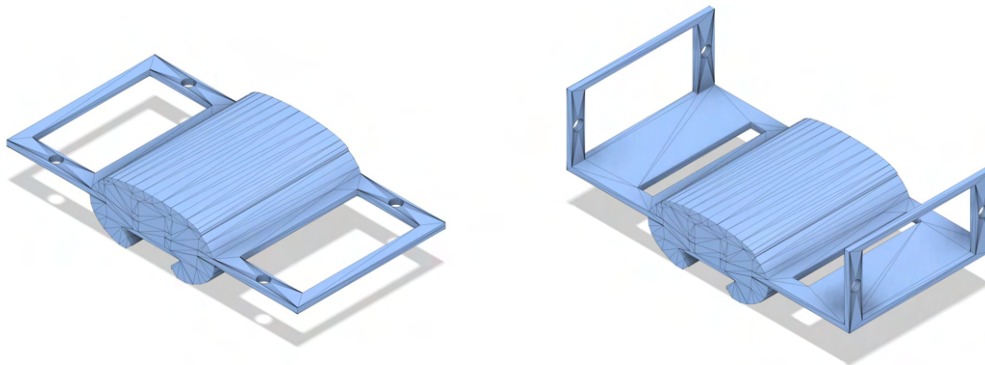


(b) Design of the *Phoenix Hand v2*'s gripper box.

Figure 7.10: Partial design of the *Phoenix Hand v2*.

The alterations of the gripper box are shown in Figure 7.11. The fitting mechanism remained the same, as it is intended for it to attach to the gauntlet, that is a copy of the one used in the *Phoenix Hand v2* design. The only alteration was a simple addition of a support where the servomotors can hang from.

The main problem found, especially whilst using the first prototype shown in Figure 7.11(a), is the interference that can be caused between the servos and the gauntlet. The



(a) Design of the first prototype gripper box.

(b) Design of the second prototype gripper box.

Figure 7.11: Design of the prototypes for the gripper box.

position of the servos is not ideal so, for the second prototype, shown in Figure 7.11(b), the servos were organized horizontally instead of vertically. This new position prevents interference between the servos and the rest of the prosthesis but the location of the support system is still problematic. When using this type of support system located in the gauntlet, the applied tension resultant of the rotation of the servos lead to an unexpected action equivalent to the wrist extension in addition to the flexion of the fingers, similar to what is shown in Figure 7.12. This motion is not desirable since it is realist nor beneficial when grasping objects.

This support system also leaves the servos, fragile components of the prosthesis, susceptible to damage and interference from the outside.

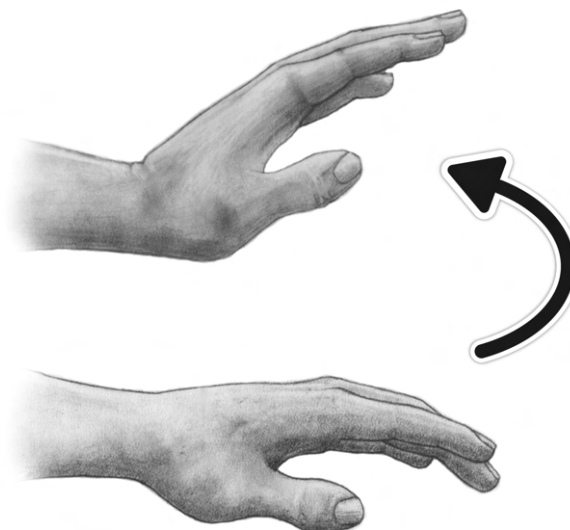


Figure 7.12: Simulation of the behaviour of the prosthesis when force is applied [73].

Due to the substitution of the rigid *PLA* material with new flexible material, the gripper box is also not able to connect with the same level of stability as previously. It is necessary to use a rigid material for the gauntlet piece and improve stability in favour of comfort, in order for the servo support system located in the wrist region to work.

Despite all efforts, the addition of the servomotor support system in the wrist region did not seem to benefit the prosthesis design, as a matter of fact, it negatively impacted the balance and comfort of the prosthesis. For that reason, it can be concluded that the wrist region is not adequate for the location of the servomotor support system, so the design returned to the original version.

7.1.3 Metacarpal Region Design

The majority of the prostheses on the market only perform power grasping movements without adapting to the shape of the object. Nevertheless, new 3D-printed prostheses models have mechanisms that enable the prosthetic hands to adapt to the object shape while grabbing it. When first developing the model, these mechanisms were taken into consideration and used to inspire the new model. Figure 7.13 shows the first draft of the metacarpal region, inspired by the *Nazree's Prosthetic Hand*, shown in Figure 5.4 of Chapter 5. This model had a new mechanism that improved anthropomorphism but had a low level of customization so there was a need to make a new model inspired by the *Nazree's Prosthetic Hand*.

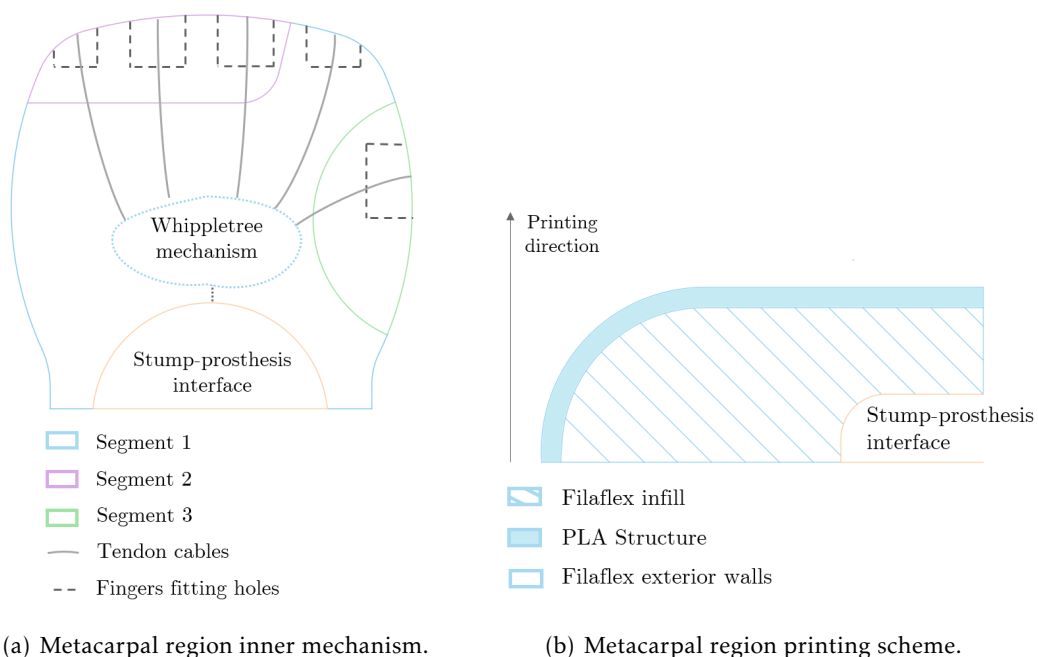
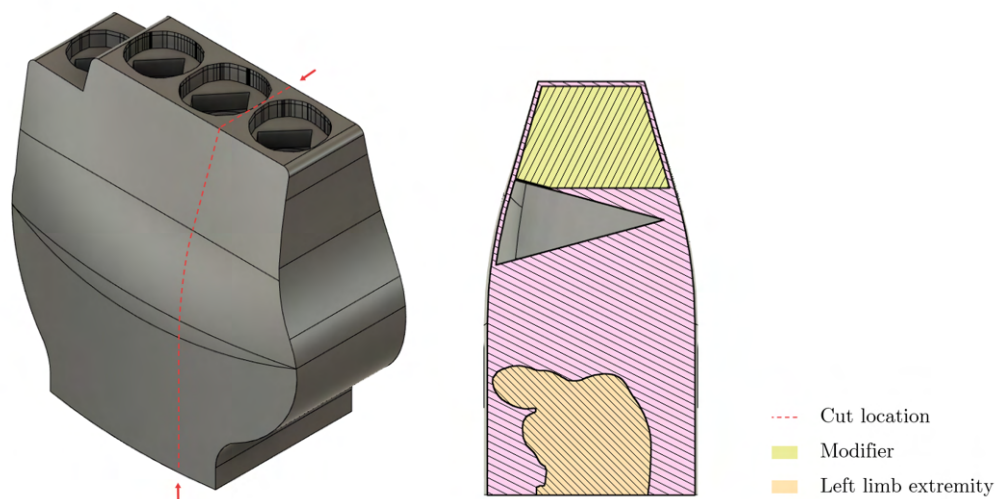


Figure 7.13: Draft of the metacarpal region structure, inspired in the *Nazree's Prosthetic Hand*. Segments 1 to 3 would be articulated to simulate the motion of the metacarpal region while gripping.

Several prototypes inspired by the new mechanism discussed previously were developed in Ana Oliveira's study [63]. The first change made from the *Nazree's Prosthetic Hand*, was moving the whippletree to the exterior, as used in the *Phoenix Hand v2*. Including all these mechanisms in the interior as well as creating space so the child could place the stump would be difficult would lower the level of customization significantly.

With this in mind, the first prototype of Ana Oliveira's study was developed, as shown in Figure 7.14, a simple prototype with a poor level of anthropomorphism and sharp edges. This prototype was made in order to produce a simple sketch of the organization of the space for the patient's stump and mechanism to simulate the behaviour of the metacarpal region of the hand. This prototype has already a rough sketch of a simple chamber that simulates the metacarpophalangeal joints. The design of this chamber allows for improvement in anthropomorphism without compromising its motion during the performance of the power grasp. Additionally, for better support of the finger pieces, an infill modifier was used in the top interior area of the prototype, resulting in a higher level of structure for the connection of the fingers.



(a) External design of the first prototype. (b) Inner design, cut along the sagittal plane of the metacarpal region, of the first prototype.

Figure 7.14: Design of the first prototype of the metacarpal region from Ana Oliveira's study [63].

The second prototype was of partial prints of the chamber portion of the metacarpal region with the objective of evaluating the anthropomorphism level of various chamber degrees. This adaptation of the prototype allows the metacarpal region to adapt to the object since in reality, the joints it simulates tend to move. In the study, it was concluded that the ideal prototype used chambers with 35° , as shown in Figure 7.15.

Ana Oliveira's study considered these prototypes enough to develop the ideal model [63]. After a variety of versions printed using different printing settings and printing positions, a final prototype shown in Figure 7.16 and Figure 7.17 was achieved.

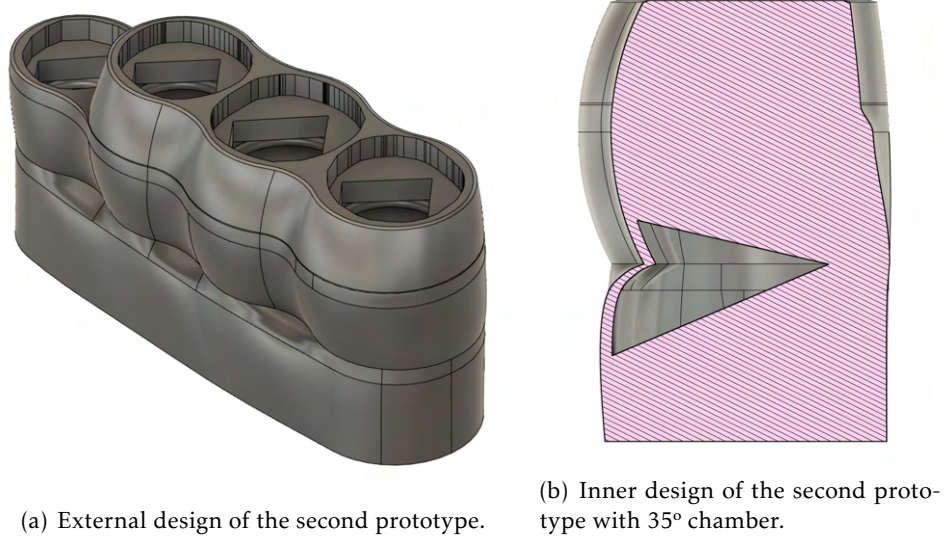


Figure 7.15: Design of the second prototype of the metacarpal region from Ana Oliveira's study [63].

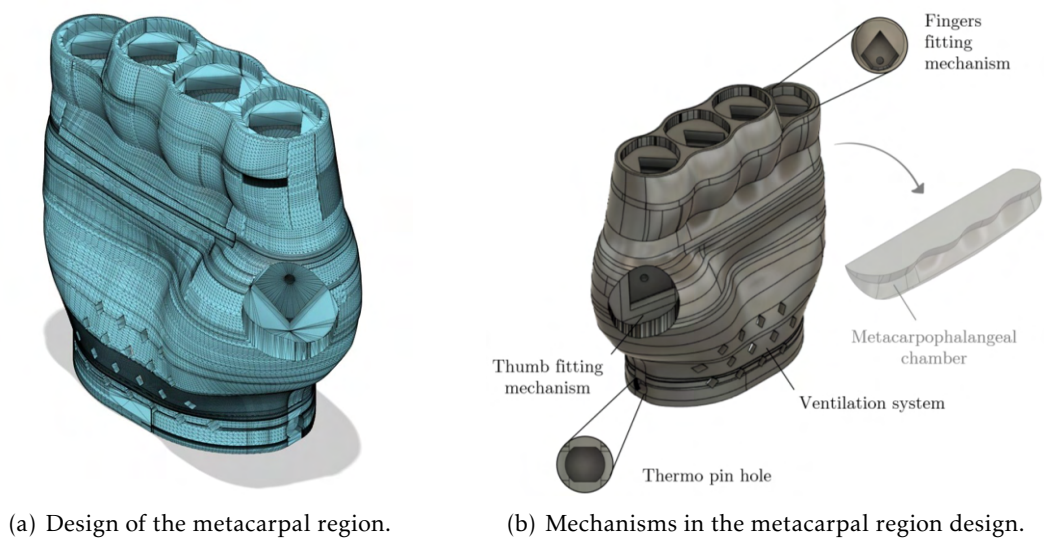
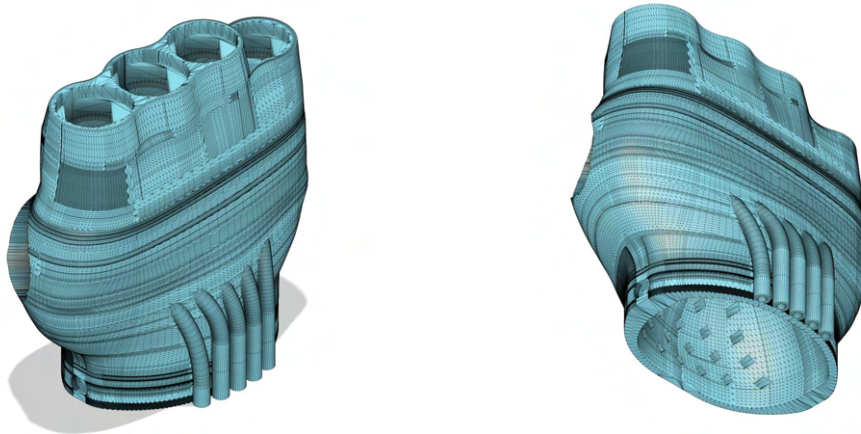


Figure 7.16: Final metacarpal region prototype from Ana Oliveira's study [63].



(a) Isometric view 1 of the design of the metacarpal region prototype.

(b) Isometric view 2 of the design of the metacarpal region prototype.

Figure 7.17: Different views of the design of the final metacarpal region prototype from Ana Oliveira's study [63].

This structure, although not entirely customised, achieved a high level of anthropomorphism, in the meantime, there were several aspects that needed to be improved and solved. The settings that were chosen produced a very faithful replication of the different tissues that compose the human hands though there were some printing defects. This model needs support enforcers during printing so the print does not collapse on itself, this is not a problem when using *PLA* but with *Filaflex* the printing quality is lower in these areas. Luckily, the areas where the support enforcer is needed are located on the bottom of the model so it does not ruin the design. Further improvements, such as increasing its functionality and enhancing some aesthetic features such as the wires conduction, were a must in order to improve the prosthesis.

The main problem found whilst using this prototype model is the same as the problem found in the original finger prototypes: the new filament used and its high flexibility can increase the difficulty of clearing the phalanges tunnels. Combining these new properties with the use of the new string material, passing the string through the canals becomes a problem. The canal model used in this prototype needs to be upgraded in order to make the assembly process more adequate. This was achieved by simplifying the canal system. The more straight the canal is, the less probable the wire is to get lost in the debris.

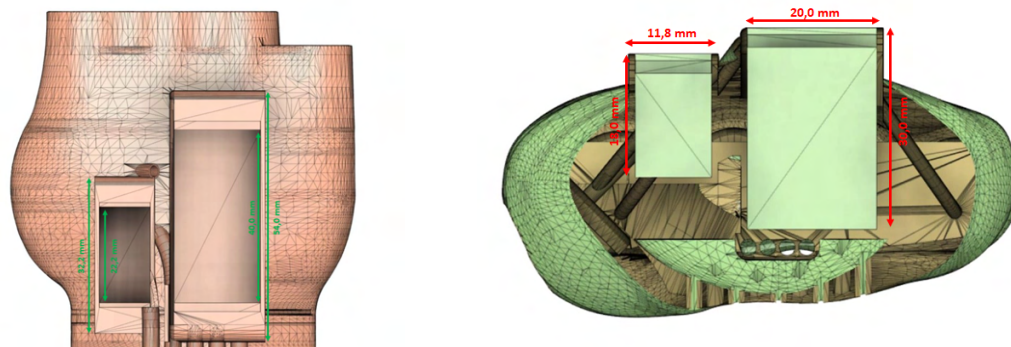
Just like in the wrist region design, the ideal printing parameters were achieved through trial and error. Functionality-wise, it was fundamental to consider the flexion of the metacarpophalangeal joints, which meant a high level of flexibility of the model. After a variety of tries, the ideal parameters that result in a high level of printing quality without interfering with the flexibility during the flexion of the metacarpophalangeal joint were achieved whilst using *Filaflex 60A* and an infill of 30%. After printing, the prototype initially seemed too flexible and incapable of achieving enough structure to

the prototype but the addition of some dense and rigid components, like servomotors, would give the ideal level of rigidity to the prosthesis.

7.1.3.1 Addition of the Servomotor Support System Prototype

As discussed in Section 7.1.2.1, the wrist area was not the adequate region for the location of the servomotors support system. The region of the prosthesis with the most available area for storage is the metacarpal region and, for that reason, a deeper understanding of the organization of the servomotor support system in the metacarpal region should be made.

The first prototype was achieved by carving a servomotor-shaped hole in the posterior region of the metacarpal region. The dimensions used for the servo hole should correspond to the real dimensions of the servo used. Due to the flexible properties of the material used, when inputting the dimensions of the servomotors there was no need to consider a size tolerance since the material adapts to the servo. It even secures the servo in place with more security. Figure 7.18 shows the dimensions used in the prototype developed during Section 7.4.1.3 with a *Tower Pro MG995-360°* and a *Tower Pro SG90-360°* servomotor side by side. When sizing the servo support system, there is a need for a special attention to leave enough space for both servos could rotate without colliding.



(a) Top view for the servomotor support system. (b) Front view for the servomotor support system.

Figure 7.18: Dimensions for the servomotor support system in the metacarpal region prototype.

Figures 7.19 and 7.20 show different views of the prototype for the metacarpal region that detail the new wiring system and the new servomotor support system. Due to the small size and simplicity of the servos this model works for most sizes of prostheses. The only limitation found whilst using this model is the need for the width to be at least 32 mm, so that the servomotor can fit.

This alteration on the prototype implied the need to alter the wiring system since the new servo support system covers the previous wiring canals. In Figure 7.21 it is shown

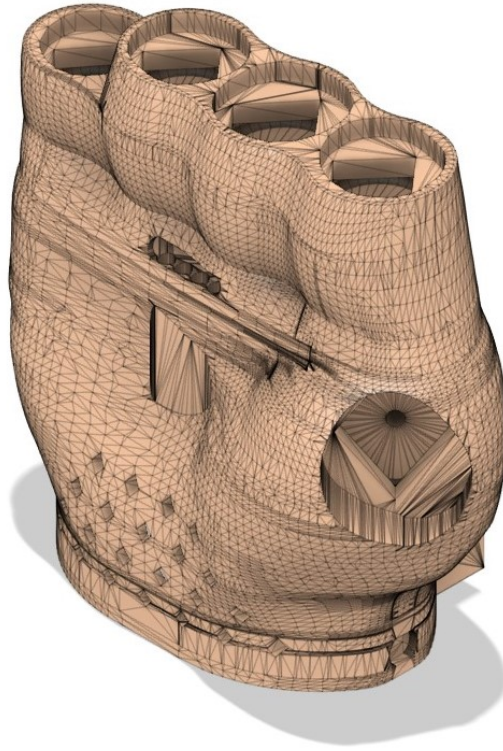
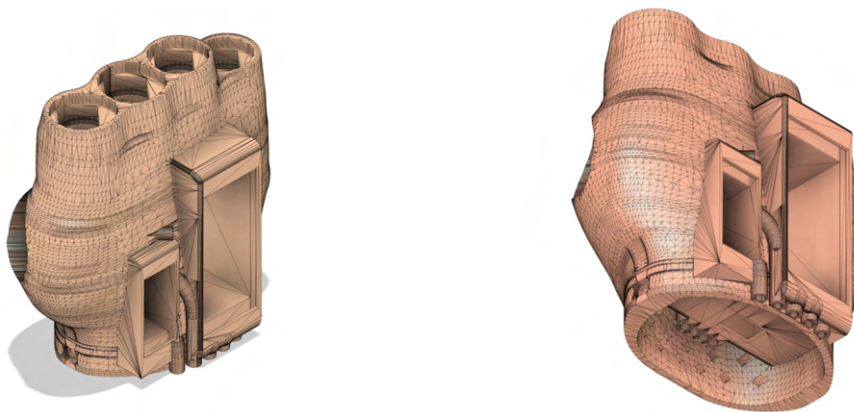


Figure 7.19: Design of the metacarpal region prototype.



(a) Isometric view 1 of the design of the metacarpal region prototype. (b) Isometric view 2 of the design of the metacarpal region prototype.

Figure 7.20: Different views of the design of the metacarpal region prototype.

the new wire system. It is composed exclusively by straight canals in order to facilitate the wiring. There is still residuals from the previous wiring system, due to the unnecessary difficulty of covering the wire canal but it has no influence in the functionality and flexibility of the new prosthesis. The same figure also shows how the prototype components were organized, more specifically, how the servo support system fits the prosthesis.

This new model does not have any influence on the flexion of the metacarpophalangeal joint. The servo support does not intersect with the chambers responsible for the flexion and only substitutes what previously was a solid area of the metacarpal.

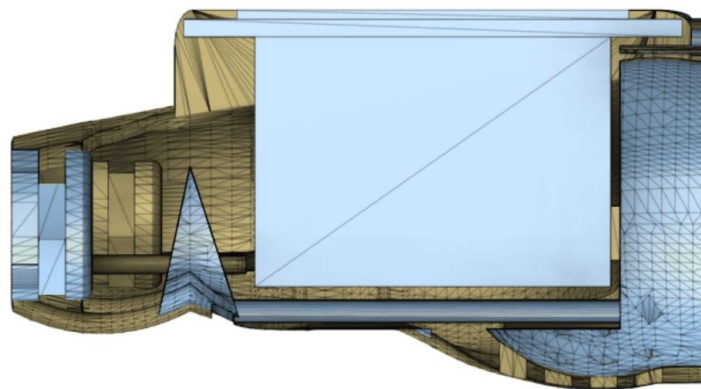


Figure 7.21: Design of the metacarpal region prototype with a cut along the sagittal plane.

This servo support system solves the main limitation found in Section 7.1.2.1. By using the servo in the metacarpal piece, the prosthesis does not simulate the wrist extension observed whilst using the prototypes of the gripper box. Whilst using this metacarpal region prototype, the only movements observed in the prosthesis are the flexion of the fingers and the flexion of the metacarpophalangeal joint, as intended.

A limitation of this support system is a lower level of customization and adaptability to different users. The scaling process does not have in consideration the fixed size of the servomotors, so the support also alters with the rest of the metacarpal piece. If the support system was separated from the metacarpal, it was only required to adapt the fitting mechanism. Since it is all in the same piece, it requires extra work to adapt the support to the new scale of the prosthesis.

7.2 Tuning of the Printing Parameters

The developed prosthesis is composed of a combination of flexible and rigid materials, *Filaflex* and *PLA*, respectively. During the development of the prosthesis, especially throughout the design of the fingers, several printing tests were required in order to determine the best printing parameters for *Filaflex*. It is clear that the filament manufacturing process, the composition of filament making, and the optimization of printing

process parameters from FDM additive manufacturing technology are the essential indicators in the quality evaluation. It is imperative to obtain high-quality components, improved material responses and improved properties.

Every aspect of factor and input parameters in the FDM engineering process affects the quality and mechanical properties of the final product. The definition of these parameters needs to be made considering the printing quality as well as the functionality of the fingers. The complete list of the final printing parameters, found to present the best printing quality is shown in Appendix C.

7.2.1 Influence of Layer Orientation

In order to evaluate if the layer orientation would compromise the appealing character of the prosthesis, fingers were printed horizontally and vertically. After comparing the two different methods, prints made horizontally were excluded due to its lack of quality, as shown in Figure 7.22. This parameter not only influences aesthetics but also the connectivity between the layers.



(a) Horizontal print test.

(b) Vertical print test.

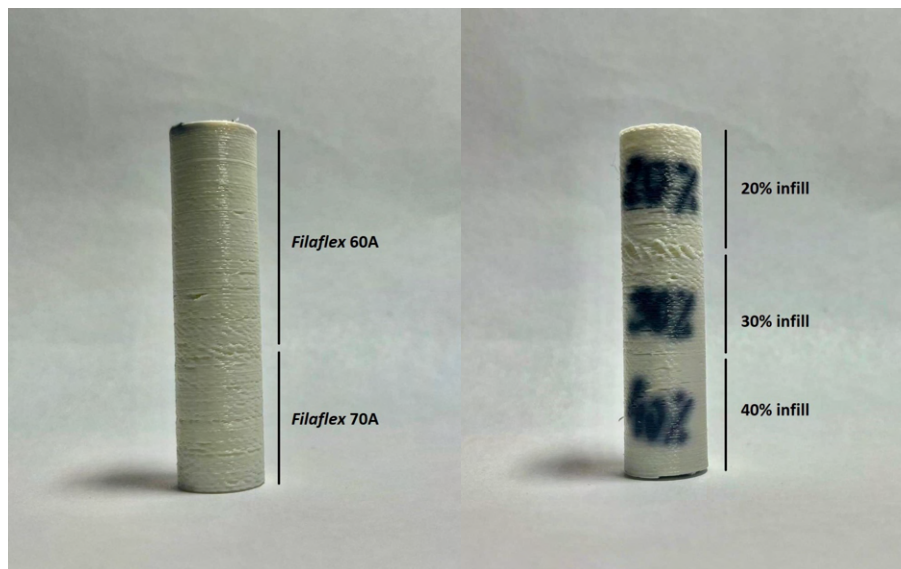
Figure 7.22: Results of the influence of layer orientation tests.

7.2.2 Switching Printing Parameters Mid Print

A variety of tests were performed using different types of *Filaflex* filament, *Filaflex 60A*, *Filaflex 70A* and *Filaflex 82A* more specifically, and different types of pairing combinations and parameters. Initially, the pairing of two filament models with different degrees of flexibility or using a variation of *infill* mid-print seemed more adequate since it allowed the finger to have a more robust structure in its fitting area and a more flexible structure towards the top of the finger. The *The Original Prusa i3 MK3S+* printer does not allow normally two filament prints but, since *Filaflex 60A* and *Filaflex 70A* have similar properties and equal printing parameters, a few tests were performed. These tests were

possible thanks to the *PrusaSlicer* software (version 2.5.0) that allows in the *Preview* menu to switch colours mid-print. This feature stops the print and allows for the user to unload the filament and switch to another with the same printing parameters.

Upon a few tests, it became evident this option was not reliable for the prosthesis since it produce small areas of less adhesion at the moments when a switch in the printing parameters or filament was made. This area is more evident when switching filaments mid-print but also noticeable when the *infill* is changed mid-print, as shown in Figure 7.23. The areas of lack of adhesion were mainly due to the fact that to switch filament, the print had to be paused, causing the print object to cool down and produce less adhesion between those layers when the print restarted. In the end, the final decision was to only use one set of parameters during each print due to the decrease in printing quality.



(a) Switch filament mid print test.

(b) Switch infill mid print test.

Figure 7.23: Results of the switching parameters tests.

7.2.3 Pull Tests

In view of the different printing results obtained when varying the filaments and printing properties, some tests were required in order to evaluate the quality of the models when using *Filaflex*. These tests were performed by printing the same finger model, namely the final prototype of the index finger, whilst using different printing parameters and a variety of filament models. The setup for these tests is shown in Figure ??

A previous dissertation started with a subjective analysis of the finger prototype print using different printing parameters and a conclusion on the optimal printing settings to produce the best printing quality was made. This analysis made evaluating the fingers' flexibility difficult as some fingers were too similar for the human sensibility to distinguish. Thus, with the purpose of choosing the model with the best printing quality and

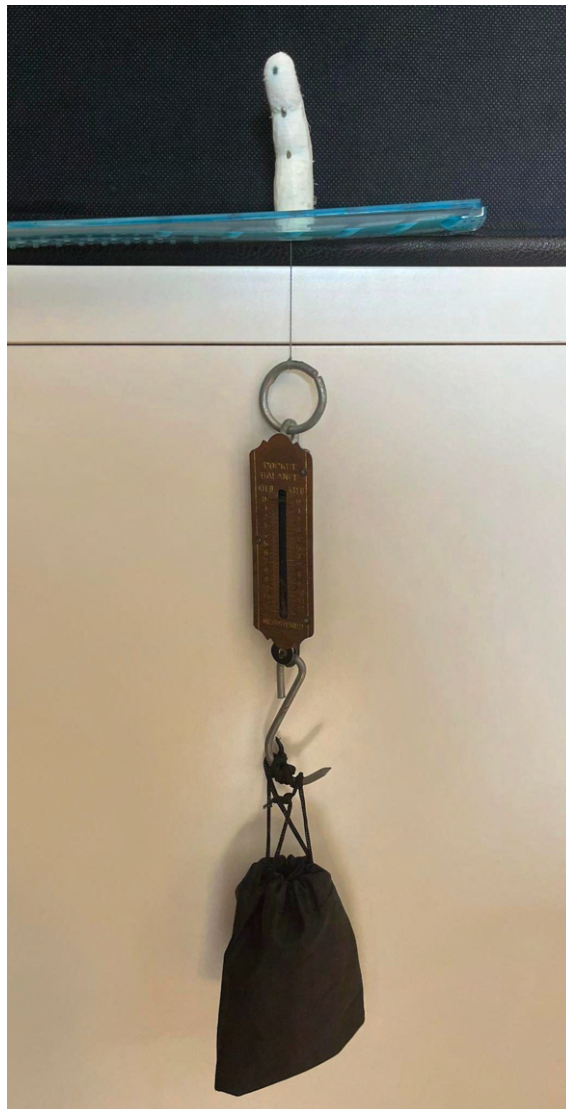


Figure 7.24: Picture of the pull test setup.

the pretended flexibility, there was a need to expose the printed models to pull tests, whilst always using the same filament model, more specifically the *Filaflex 82A*.

Using the results obtained, the previous thesis was able to conclude on the optimal printing parameters that produce the best printing quality and the ideal finger model that produces more flexibility, but this study lacked information when it came to a deeper understanding of the behaviour of the model with different filament models and densities. So, in this study, the same tests that evaluate flexibility were used in the final finger model, using the ideal printing parameters and two additional filament models, each more flexible than the one used previously, *Filaflex 60A* and *Filaflex 70A*. The collected data referring to these tests is presented in Appendix D.

Among all the print tests performed, some of them presented several printing defects or behaved in an unwanted way which made them invalid for the main goal of this study, which consists of creating a more realistic and appealing upper limb prosthesis. Therefore,

only the models referred in Appendix D were subjected to pull tests.

Through an eye test, it became obvious that the more dense the finger model was, which corresponds to more quantity of material on its infill, the better the printing quality and the more difficult it was to bend the finger. The conclusion on the relation between the flexibility and the quantity of material is backed up by the collected data through the pull test. When comparing two finger models printed using the same filament models and with two different percentages of infill, for example, two models printed with *Filaflex 60A* but one with 25% infill, shown in Figure 7.25, and the other with 50% infill, shown in Figure 7.26, whilst maintaining all the other printing parameters constant, it is possible to realise that the model with the higher percentage of infill requires a greater quantity of force to bend the same amount as the model with a lower percentage of infill.

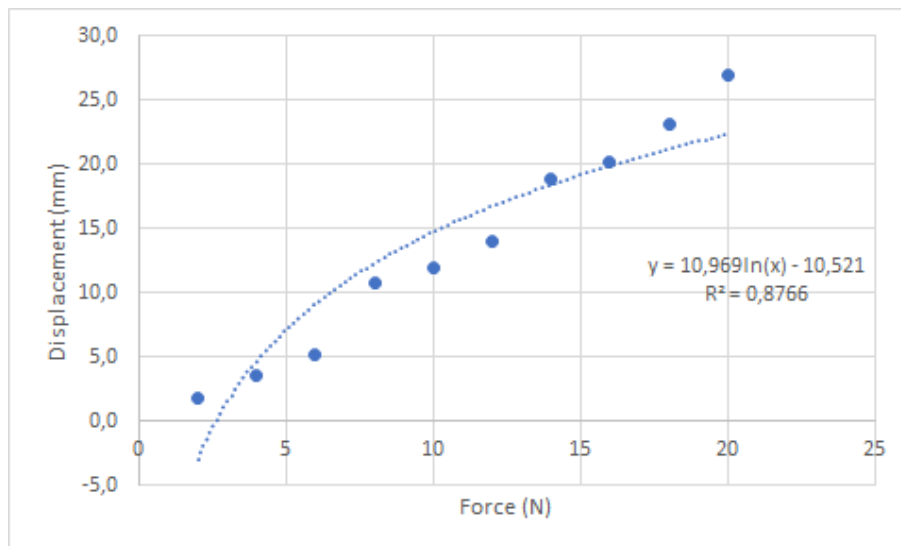


Figure 7.25: Behaviour of the model printed with *Filaflex 60A* and 25% infill.

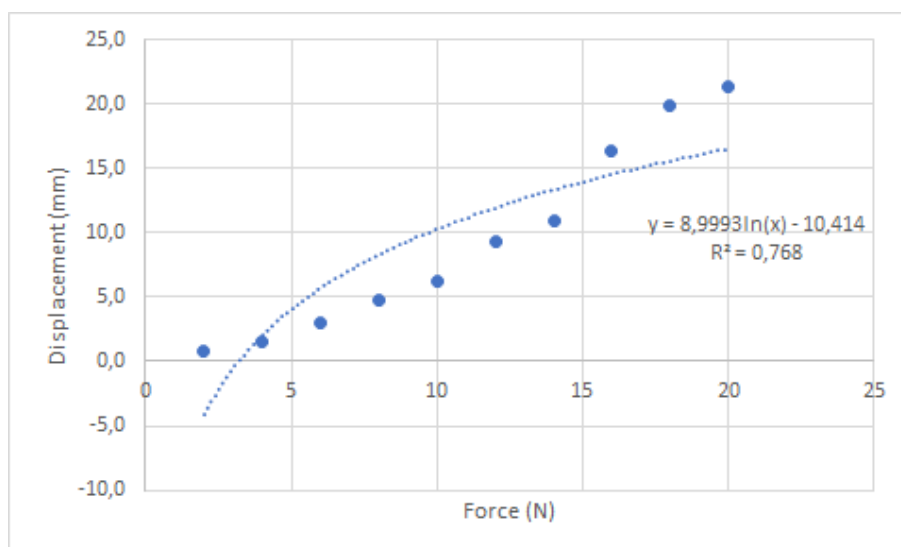


Figure 7.26: Behaviour of the model printed with *Filaflex 60A* and 50% infill.

By analysing the resultant plots of the pull tests, all of them present a logarithmic trendline, which reveals the behaviour of the material. This trendline means that the initial displacement is caused by a bigger amount of force, implying higher initial energy. Then, after overcoming a certain threshold, a minor amount of force leads to a bigger displacement. This behaviour was expected but it is the opposite of what would be desirable since it would be more beneficial to facilitate the movement of the finger in the beginning stage, followed by the application of higher forces to complete the flexion of the finger.

Although these print tests were also used to confirm the best printing parameters for better quality and resistance, its main goal was to, not only study the relation between infill and flexibility but also to quantify the force needed to bend a single finger. This information is of great importance in the later stage of the development of the prosthesis.

Another factor to consider is the resistance to the tension applied without breaking, which means better quality for the prototype. The mechanical properties of both *Filaflex 60A* and *Filaflex 70A* materials are around the same with no significant differences specially for low levels of applied tension. In both materials, the elongation at break is around the same value, with 900% for *Filaflex 60A* and 905% for *Filaflex 70A*. The stress at a low level of elongation, which is the case for this study, is also around the same for both materials, with 1 MPa for *Filaflex 60A* and 1,5 MPa for *Filaflex 70A*. The Table 7.1 shows the similar mechanical properties of both materials used in this study more in-depth. For this study and application, it is possible to see that the mechanical properties of the materials have no influence in this study in concrete, since for the parameters used, the values are similar enough to consider them equal.

Table 7.1: Mechanical properties of the materials used during this study.

Mechanical Properties	<i>Filaflex 60A</i>	<i>Filaflex 70A</i>	Unit
Hardness	63	70	Shore A
Tensile strength	26	32	MPa
Elongation at break	950	900	%
Stress at 20% elongation	1	1.5	MPa
Stress at 100% elongation	2.5	4	MPa
Stress at 300% elongation	4.5	6	MPa
Tear strength	40	45	N/mm
Abrasion loss	45	45	mm ³
Compression set 23°C / 72 hours	40	20	%
Compression set 70°C / 24 hours	25	39	%

In order to produce prostheses with the best print quality and properties, the perfect balance between flexibility and quality needs to be obtained. Thus, in view of these results, the final two sets of parameters which seem the more adequate for the prosthesis are the set printed using the filament model *Filaflex 60A* with 50% and the set printed

using the filament model *Filaflex 70A* with 25%. Both of these sets present the pretended flexibility but, coming back to the relation between the infill and print quality, the set recommended for the final prototype became the one printed in *Filaflex 60A* using an infill of 50%. After using both fingers printed with both materials for a long period of time, the prototype with a higher infill value also showed a higher level of endurance, with fewer tears and signs of rupture. This will lead to a better product that can be used for a longer period of time without needing repairs.

In general, the outcome of the printing tests is quite satisfactory and a more in-depth study of the other filament models and printing parameters does not seem relevant at the moment. The ideal behaviour, for the objective in mind, when developing the prosthesis using the recommended parameters is obtained with the filament model *Filaflex 60A* and an infill of 50% for the production of the finger pieces.

Although the pull tests were a great method to distinguish objectively which were the best set of parameters, there were some key points that need to be discussed. When performing this type of tests in order to assess the material properties, the tested objects should have a uniform geometry so only the material properties have influence in the object's behaviour. In this case, the finger's geometry is not uniform which may have an influence in the results. Additionally, the force application may have some influence and these facts could be a possible explanation for the algorithmic behaviour obtained. Moreover, even though the pull tests aimed to distinguish the best printing parameters, it is important to note that there were other factors that could not be controlled that could have compromised the printing results. The environment temperature during printing, which portion of the filament roll was being used are some of these factors. Finally, it is also important to highlight that the mass of the dynamometer, tab and bag were not accounted for since no significant displacement was noticeable with the application of their weight.

7.3 Integrated Hardware and Software for Myoelectric Control

Ema Lopes' study explored the option of using a single channel to identify dexterous movements using a fast and straightforward classifier [68]. In order to accomplish that, myoelectric signals were filtered, divided into time segments and features were extracted for further classification. The classification results obtained in the dissertation differed from those obtained in the literature due to limitations in the methodology and the number of channels used. Nevertheless, Ema Lopes' study overcame the drawbacks found in other articles and studies, mainly the use of many channels.

The overall results found in the study in question proved that using a single acquisition channel is sufficient to identify when the volunteer is performing a gesture or is at rest. Besides that, the results showed that each gesture is distinguishable from the rest position using a single channel, even if the gesture is a single finger movement or grasp.

The developed classifier was capable of achieving high offline accuracy percentages (accuracy >90%) but is expected to decrease through the other classifier levels (accuracy <90%), which means it is still not recommended to use a single channel for real-time classification.

One of the main reasons for this low accuracy percentage is the use of a low sample pool for the learning class of the classifier, which could be solved with more acquisitions. Nevertheless, other parameters, such as the electrode's position or the number of channels, should be tested to see if they can improve the classifier's quality. These further tests hope to improve the functionality of the myoelectric controller, by reducing of the misclassified classes. This study was more focused on changing the positions of the electrodes, and consequent effects, and integrating the classifier into the prosthetic model in order for the classifier result to become its input source.

7.3.1 EMG Signal Acquisition and Processing

As already stated in Chapter 4, the surface myoelectric signal is very sensitive to numerous external factors, such as changes in the position of the electrodes and the equipment's noise. These external signal sources and the nature of the signal degrade the classifier's performance, due to the influence of the noise in the features' values. Meaning a cleaner signal, without noise, would result in better classifier performance.

There are also other ways of improving the accuracy of the classifier, mainly by using specific pre-processing and processing techniques, which were discussed in Ema Lopes' study [68]. The classifier produced in Ema Lopes' study, ended with low classification rates (< 80%) obtained during online tests and it is expected for the rates to lower to below 50% in offline tests. Having classification rates lower than 90% is a risk to the user's safety, which decreases the functionality and robustness of the prosthesis. Improving the filtering of the signal in the pre-processing technique is the most critical way of improving the accuracy and classification performance. However, this study is more focused on the integration of electronic components into the prosthetic model. For that reason, only ways of improving the EMG signal acquisition, and indirectly improving the performance of the classifier, were studied.

The acquisition setup includes electrodes designed to record muscle activity in a non-invasive method, at surface level, and an acquisition system connected to a laptop. The myoelectric signals were recorded using a *BIOPAC Model MP-36* acquisition unit by ©BIOPAC, shown in Figure 7.27, with built-in universal amplifiers that record a wide range of physiological signals. The *BIOPAC* data acquisition system recorded raw EMG signals and saved them in a *.txt* file format for later analysis offline.

The information is received in one of the four available channels and connected through a USB cable to the *BIOPAC Lessons Student* software. To record the myoelectric signal, three *EL254* electrodes were used and placed on the surface of the skin in three different positions. For more accurate records, the electrodes incorporate liquid



Figure 7.27: BIOPAC Model MP-36 acquisition unit by ©BIOPAC [74].

electrolyte gel and moderately-high chloride salt concentration. These disposable electrodes are recommended for short-term recordings, such as surface *EMG*.

In the initial position of the acquisition electrodes, shown in Figure 7.28 and Figure 7.29, there is an overlap between the electrode and both the tendon distal regions of different flexor forearm muscles and the *flexor retinaculum* of the hand, resulting in the crosstalk phenomenon. This area chosen to acquire the *EMG* signal is not the most appropriate since the region chosen results in a weaker *EMG* signal, as shown in Figure 7.30, which can influence the accuracy of the *Machine Learning* classifier.

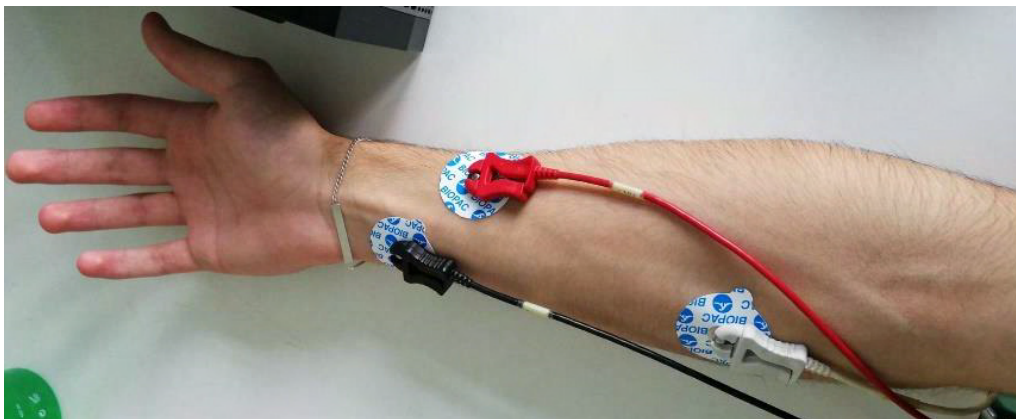


Figure 7.28: Picture of the original acquisition electrodes position.

In order to acquire the best possible signal, the *EMG* electrode should be placed at a proper location and its orientation across the muscle is important. Surface *EMG* electrodes should be placed between the motor unit and the tendinous insertion of the muscle, along the longitudinal mid-line of the muscle. A few requirements, such as keeping the distance between the centre of the electrodes or detecting surfaces between 1-2 cm and the longitudinal axis of the electrode parallel to the length of the muscle

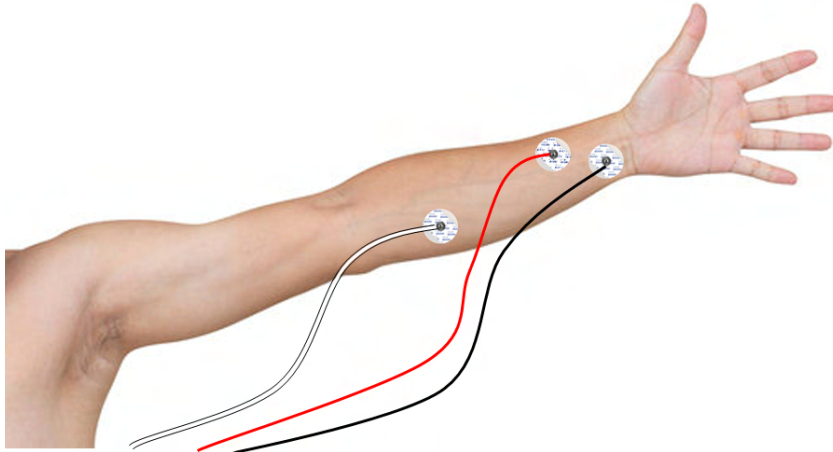


Figure 7.29: Original acquisition electrodes position.

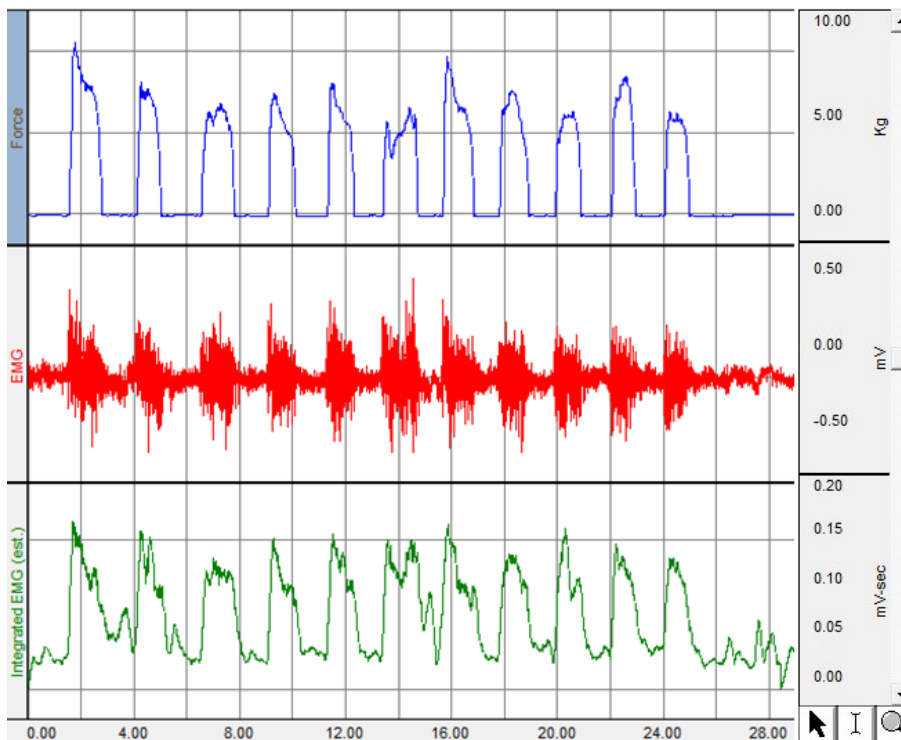


Figure 7.30: *Biopac Student Lab*® file using the old electrodes position.

fibres, can help improve the EMG signal. For that reason, the same protocol was followed using the new electrode positions. These acquisitions tested the signal quality with the electrodes positioned in the main muscle groups responsible for finger flexion. Most of them did not improve the EMG signal except for the position of the electrodes shown in Figure 7.31, which presented an improvement in the acquired EMG signal, as shown in Figure 7.32.

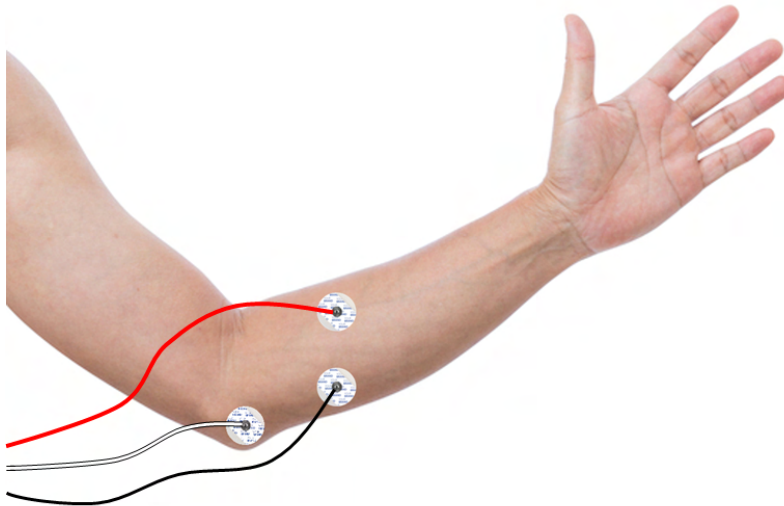


Figure 7.31: New acquisition electrodes position.

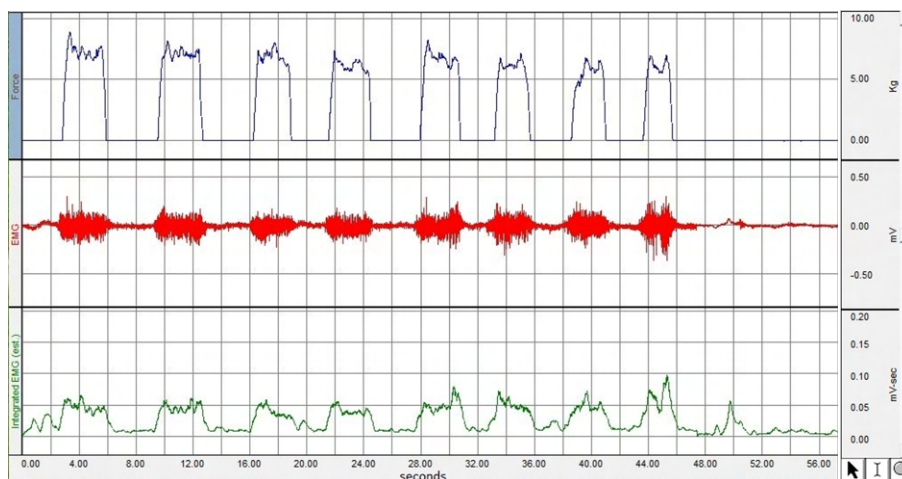


Figure 7.32: Biopac Student Lab® file using the new electrodes position.

The reference electrode was moved to the elbow region, which can improve signal quality, the other electrodes were also moved further back to the main body of the *flexor digitorum superficialis* muscle and the *flexor carpi radiialis* muscle, shown in Figure 7.33. These two new muscles chosen to evaluate the EMG signal were responsible for the finger and wrist flexion and abduction, respectively. With the electrodes in this new position, the mean force detected during the acquisition improved from around 2,37 kg per hand

flexion movement to around 3,08 kg. This difference does not hinder the use of the original acquisition files in the classifier but shows this new electrode position allows for better results. By moving the electrode position further back it also helps cover more patients with shorter residual limbs and loss of wrist function as well as allows more space for better organization of the electronic components of the prosthesis.



Figure 7.33: Main muscles responsible for finger flexion.

The other muscles tested for acquisition of the EMG signal were the *flexor digitorum profundus* and *flexor pollicis longus*, shown in Figures 7.34 and 7.35, respectively.

The *flexor digitorum profundus* is a muscle in the forearm that is responsible for flexing the fingers. It originates from the ulna and the interosseous membrane and inserts into the distal phalanges of the fingers. This muscle works in conjunction with the flexor digitorum superficialis to produce hand and finger movements. Although this muscle has an important role in the flexion of the fingers, it was not ideal for a surface EMG acquisition since it is located deep within the anterior compartment of the forearm, making its acquisition not suitable for this study.

The *Flexor pollicis longus* was the muscle that originated the worst EMG signal out of all the muscles tested. Beyond belonging to the deep flexors of the forearm, it also is



Figure 7.34: *Flexor digitorum profundus* muscle [77].



Figure 7.35: *Flexor pollicis longus* muscle [78].

responsible only for movements of the thumb such as gripping and pinching and not for the rest of the fingers. This produces a EMG of smaller mean force.

Another change made from Ema Lopes' study was decreasing the number of the hand gestures to be classified, from *spherical grip*, *tripod grip* and *index finger flexion* to just *spherical grip* and *index finger flexion*. The alteration made changed the output of movements classified as *tripod grip* to *rest*. This change was not made with the intent of improving the accuracy of the classifier, but due to the limitations of the new prosthesis model, which did not allow for a tripod-type grip. Nevertheless, by decreasing the number of actions for the recognition it is expected to lower the number of classification errors, due to its simpler nature.

7.3.2 Electronic Integration for Myoelectric Control

After receiving the *EMG* signal previously acquired, the classifier goes through a process of pre-processing the data and tries to recognise the action performed by following a sub-classification level system, where the input is the *EMG* signal's features and the output is the performed movement, as shown in Figure 7.36. The classifier starts by trying to

recognise if the volunteer performed any movement or was at rest, then it tries to recognize all gestures accurately, if not, it divides the classification into binary classifications so it can finally identify the movement performed.

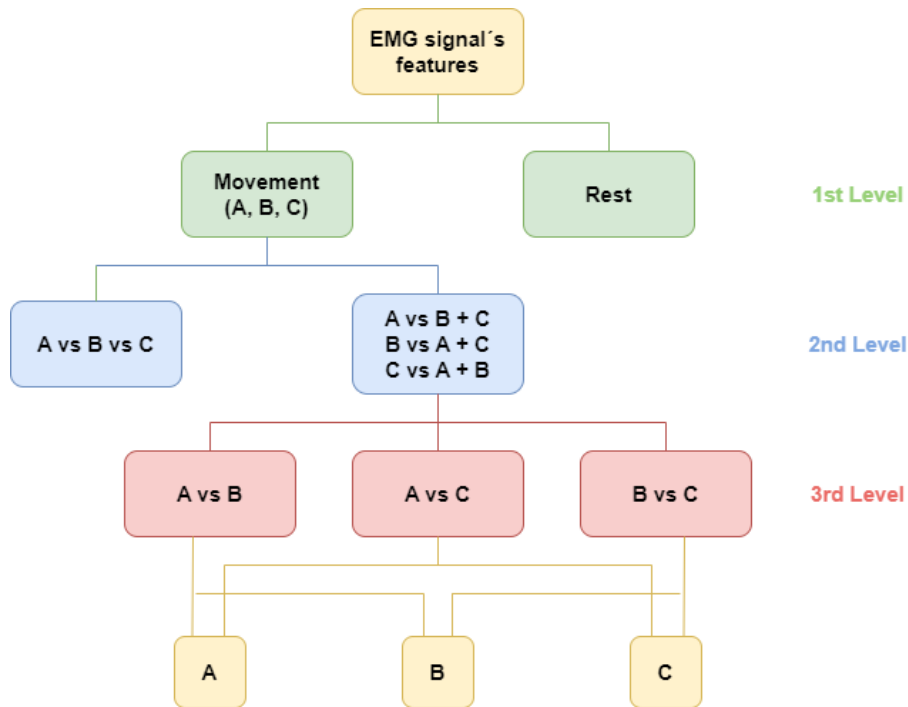


Figure 7.36: Scheme of the classification stages of Ema Lopes' classifier [68].

The *output* of the classifier can be used to induce a specific movement of the prosthesis. This is achieved with the combination of the *Python* script shown in Figure 7.37 and the classifier developed in Ema Lopes' study [68]. The scrip shown in Figure 7.37 communicates directly with the Arduino board through the *Serial Monitor* tool. The *Serial Monitor* tool is the connector between the computer and the Arduino that allows the control of the Arduino from the user's keyboard.

The result from the classifier is transmitted through the *Python* script as an input that elicits a response from a *sketch* that is uploaded to and run on an Arduino board. The Arduino *sketch* that induces the response from the prosthesis is shown in Figure 7.38. Connecting the Arduino-prosthesis device to the computer that induces the input source via a wireless connection was an important objective that significantly improved the functionality of the device. The addition of a Bluetooth module transmitter to the electronic circuit allows for this wireless connection. A HC-05 module is an easy-to-use Bluetooth Serial Port Protocol (SPP) module, designed for transparent wireless serial connection setup. Its addition into the Arduino *sketch* the inclusion of the `<SoftwareSerial.h>` library and the setup of the virtual serial port for the integration of the microcontroller into a Bluetooth network.

The *sketch* uses the *output* of the classifier as an *input* in the Arduino, associated with a predetermined response. Each cycle in the signal lasts for 20 milliseconds and for the

```
"""
Created on Mon Oct 10 17:02:58 2022
@author: Simão Gonçalves
"""

# arduino2Servo_userInput.py
import serial
import time

# Define the serial port and baud rate.
# Ensure the 'COM#' corresponds to what is shown
ser = serial.Serial('COM3', 9600)

def ser_rot():
    user_input = input("\n Type 1/2/quit : ")
    if user_input == "1":
        print ("action1 - flexion of all fingers")
        time.sleep(0.1)
        ser.write(b'1')
        ser_rot()
    elif user_input == "2":
        print ("action2 - point finger action")
        time.sleep(0.1)
        ser.write(b'2')
        ser_rot()
    elif user_input == "quit" or user_input == "q":
        print ("Program Exiting")
        time.sleep(0.1)
        ser.close()
    else:
        print("Invalid input. Type 1/2/quit : ")
        ser_rot()

time.sleep(2) # wait for the serial connection to initialize
ser_rot()
```

Figure 7.37: *Python* script to control an Arduino.

most of the time, the value is LOW. At the beginning of each cycle, the signal is HIGH for a time between 1 and 2 milliseconds. At 1 millisecond it represents 0 degrees and at 2 milliseconds it represents 180 degrees. In between, it represents a value from 0-180, as shown in Figure 7.39. Arduino uses a built-in function *servo.write(degrees)* that simplifies the control of the servos. There is a special case of continuous rotation servos. While a normal servo goes to a specific position depending on the input signal, a continuous rotation servo either rotates clockwise or counter-clockwise at a speed proportional to the signal. For example, *servo.write(0)* function will make the servomotor spin counter-clockwise at full speed, *servo.write(90)* will make the motor stop and *servo.write(180)* will turn the motor clockwise at full speed. For this study two different models of continuous rotation servos with different top speeds were used, so it was necessary to decrease the speed of the faster servo in order to match the top speed of the other servo.

```

// Include the Servo library
#include <Servo.h>
#include <SoftwareSerial.h>

SoftwareSerial WhaddaBT(0, 1); // creates a "virtual" serial port/UART
// connect BT module TX to 0
// connect BT module RX to 1

int servoPin3 = 3;      // the pin that the servo1-MG995 is attached to
int servoPin7 = 7;      // the pin that the servo2-SG90 is attached to
Servo Servo1;           // Create a servo object
Servo Servo2;
char incomingByte;      // a variable to read incoming serial data into

void setup() {
  WhaddaBT.begin(9600);
  WhaddaBT.print("Bluetooth connected! Please press 0 or 1 to turn servos.");

  // We need to attach the servo to the used pin number
  Servo1.attach(servoPin3);
  Servo2.attach(servoPin7);
}

void loop() {
  // see if there's incoming serial data:
  if (WhaddaBT.available()) {
    // read the oldest byte in the serial buffer:
    incomingByte = WhaddaBT.read();
    if (incomingByte == '1') { // action1 - flexion of all fingers
      Servo1.write(0);
      Servo2.write(75);
      delay(5000);
      Servo1.write(90);
      Servo2.write(90);
      delay(2000);
      Servo1.write(180);
      Servo2.write(105);
      delay(5000);
      Servo1.write(90);
      Servo2.write(90);
    }
    else if (incomingByte == '2') { // action2 - point finger action
      Servo1.write(0);
      delay(5000);
      Servo1.write(90);
      delay(2000);
      Servo1.write(180);
      delay(5000);
      Servo1.write(90);
    }
  }
  delay(100);
}

```

Figure 7.38: Arduino *sketch* to control servomotors movement.

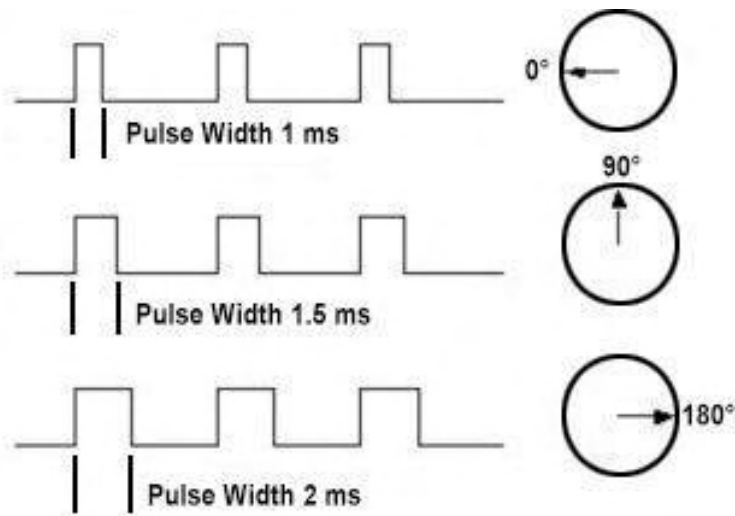


Figure 7.39: Electric signal control servomotor [79].

7.4 Motor Powered Components

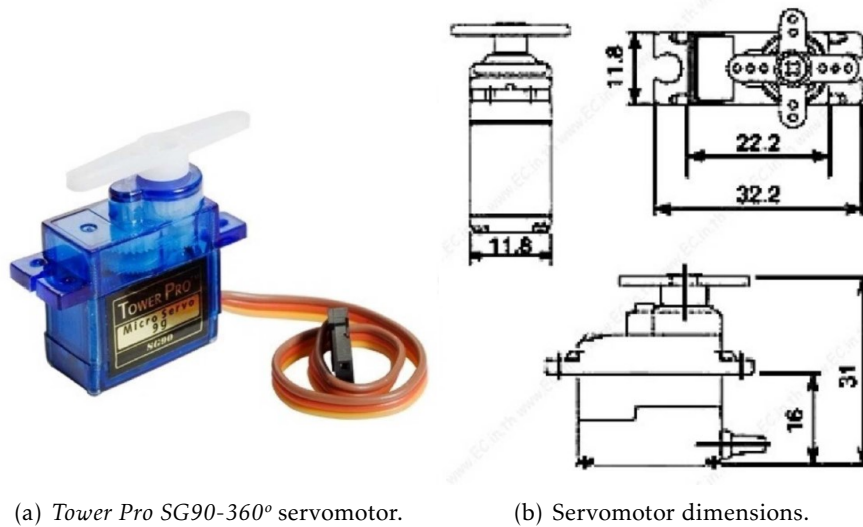
The robotic components of the prosthesis are designed for use in a *ATmega8* microcontroller that works together with the Arduino *sketch* shown in Figure 7.37. This process works using a simple principle of interfacing servos, whilst being powered by an external power supply.

When choosing the servomotor most adequate for the study, several factors need to be considered in order to optimize its functionality, such as size, weight, torque, price and if it has 180° or 360° rotation. It can easily be concluded that it is necessary a continuous rotation servomotor, in order words, a servomotor that can continuously rotate on its own. This allows the servo to roll the string that pulls the finger and work similarly to a fishing reel.

Through the results obtained in the pull tests and the conclusions reached, the force necessary to bend the finger prostheses is already known. In Appendix D, it is shown that the force necessary to bend the finger prostheses printed in *Filaflex 60A* and an infill of 50% is around 30 N, meaning it is necessary to apply a weight of around 3 kg, as shown in Table D.8. The process of choosing the servo with enough torque to exert the force necessary to completely bend the finger becomes now possible.

7.4.1 Parameters Identification of the Servomotor

The model *Tower Pro SG90-360°* servomotor is a tiny and lightweight servo with high output power. This kind of servo is one of the most commonly used and cheapest models, it is recommended for beginners, due to its simplicity and relative power. This servo can continuously rotate its 360 degrees and works just like the standard kinds but smaller. The dimensions and specifications are shown in Figure 7.40 and Table 7.2.

(a) *Tower Pro SG90-360°* servomotor.

(b) Servomotor dimensions.

Figure 7.40: *Tower Pro SG90-360°* servomotor and dimensions [80].Table 7.2: *Tower Pro SG90-360°* servomotor specifications [80].

Weight:	9 g
Dimension:	23.0 x 12.2 x 29.0 mm approx.
Stall Torque:	1.6kg-cm (4.8 V)
Rotation Angle:	360°
Operating Speed:	0.12 sec/60°
Operating Voltage:	4.8 V
Dead Band Width:	10 μ s
Temperature Range:	0°C - 55°C

It exists a vast quantity of available servos but the *Tower Pro SG90-360°* servomotor should be a priority when choosing which servo to use due to its low price, small dimensions and accessibility.

The chosen model needs to be a continuous rotation servo since it is not capable of pulling enough wire in a single 180° rotation. Nevertheless, it would be preferable to use a 180° rotation servo since its movements are significantly faster than a continuous rotation servo. A more complex servo could be able to also achieve the desirable faster speeds, similar to the *Tower Pro SG90-180°* servomotor, but other factors, such as weight, size and price, make it impossible to use. For that reason, simplicity should be a priority when deciding the servo to use in the model. The possible combinations of types and quantity of servos are immense, therefore several prototypes were made in order to achieve the best functionality possible.

7.4.1.1 First Prototype

The first prototype thought of was one that used five different *Tower Pro SG90-360°* servos, one attached to each finger. The *Tower Pro SG90-360°* servomotor has a torque of 1.6kg-cm at 4.8 V and the finger needs around 3kg of force applied in order for it to bend. The distance of the first pin in the adapter of the servo is 0,5 cm from the circular disc on the base motor. For that reason, the servo is going to be able to apply a weight of around:

$$1,6kg.cm * 1/0,5cm = 3,2kg$$

So, our design, shown in Figure 7.41, is successful and capable of working properly.

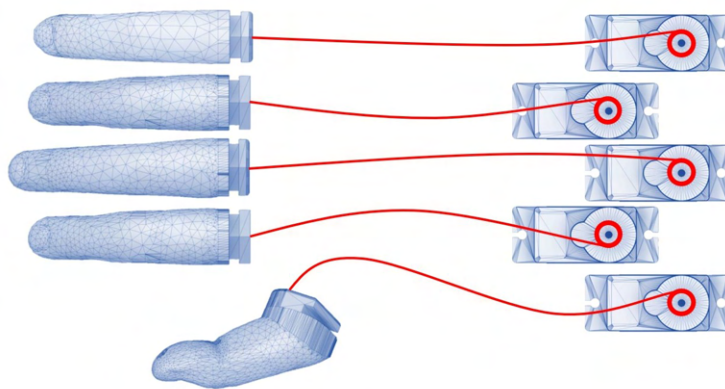


Figure 7.41: Design of the first prototype with five *Tower Pro SG90-360°* servos.

The main problem with this prototype is, whilst working with a limited amount of space in the forearm region, using five different servos becomes a difficulty. There is not enough space to organize all the necessary servos into the forearm piece, the only possible solution is developing a bigger structure capable of holding all five servos, which would impact negatively certain factors such as comfort and balance.

This new model uses a new way of wiring and drops the whipleretree mechanism, in order to improve functionality. Wiring the fingers individually instead of paring the index with the middle finger and the ring finger to the little finger, as on the original prototype, the mechanism shown in Figure 7.42, also makes the prototype lose the phenomenon of *enslaving*. This phenomenon consists of the involuntary force production by the fingers that were not explicitly involved in a force-production task [81], [82]. The *enslaving* happens because each finger is actuated by the activity of different muscles, which can act on different fingers. The neighbour's fingers are the more affected ones. The thumb is the most independent finger, followed by the index finger and the little finger. The ring and middle fingers are the ones that suffer the most *enslaving* effect. In view of this phenomenon, in the original model, the middle and ring fingers were connected to each other and the index was connected to the little finger [81], [83].

Being able to simulate the *enslaving* phenomenon increases the level of anthropomorphism but is a bonus to the prototype. Losing this phenomenon is not a step back

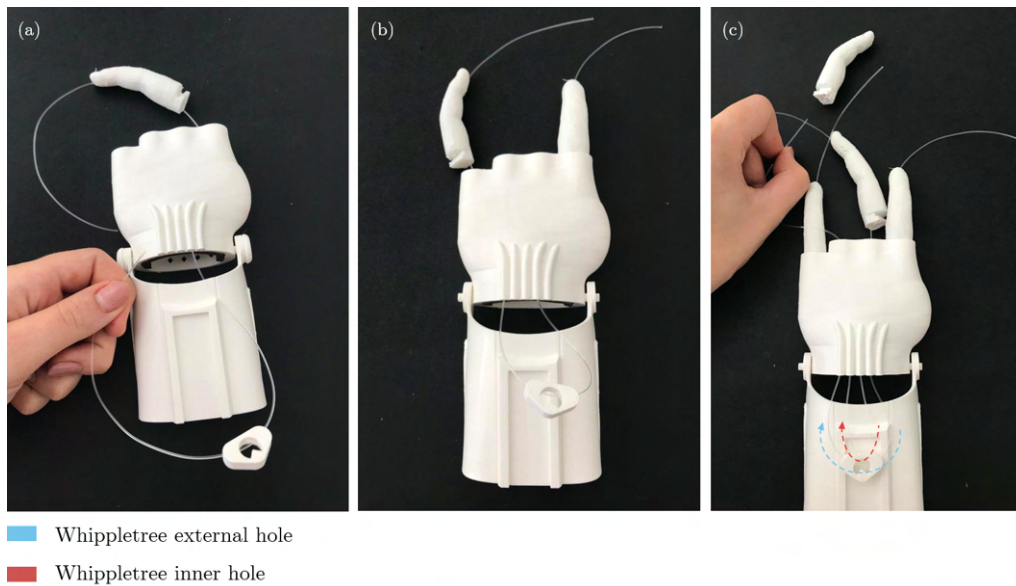


Figure 7.42: Whippletree mechanism assembly: (a) the strings connect the fingers and are inserted in distal-proximal order, then passed through the whippletree holes and inserted by doing the inverse path; (b) the fingers are fitted in the metacarpal region after being connected; (c) the index connects to the middle finger and the string passes through the whippletree external hole, while the middle connects to the ring finger and passes the string through the inner hole [63].

in quality, especially considering that in the movements simulated with this prototype, hand flexion and finger pointing action, there is not any level of *enslaving* [82]

7.4.1.2 Second Prototype

The first prototype was made using an excess of resources. Reducing the number of servos use, the weight and complexity of the forearm model became the main goal of the second prototype. Due to the different actions the prosthesis is intended to do, it became obvious the index finger needed to be attached to a different servo from the other fingers.

In this prosthesis model, the servomotor works as a fishing reel and for that reason, the distance of the center of gravity from the circular disc on the base motor does not need to be in the first pin in the adapter of the servo. The center of gravity can be pushed further back, to less than 0,25 cm from the center disc of the base motor. Having that in consideration, is servo is going to be able to apply more than a weight of:

$$1,6kg.cm * 1/0,25cm = 6,4kg$$

So, our design becomes capable of applying enough torque to bend two-finger models. In this prototype, shown in Figure 7.43, it is possible to reduce the number of servos down to three, one Tower Pro SG90-360° servo is connected to the index finger and the other two servos are connected to two different fingers. By reducing the number of servos,

the prosthesis becomes lighter, cheaper and it becomes easier to organise the electronic components in the forearm region.

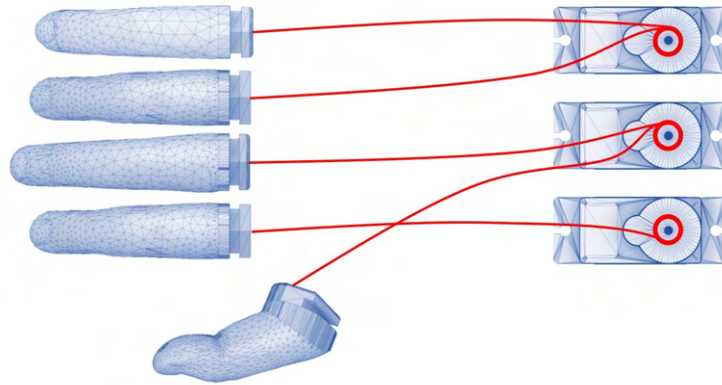


Figure 7.43: Design of the second prototype with three *Tower Pro SG90-360°* servos.

This prototype continues to be capable and work successfully. Nevertheless, it is still not the ideal model. The weight applied is too close to the stall torque which lowers the speed of the movement of the servos, making the action of closing and opening the hand a process too slow to be applied in the real world. The ideal model rotates in a faster way in order to better simulate the real-world movement.

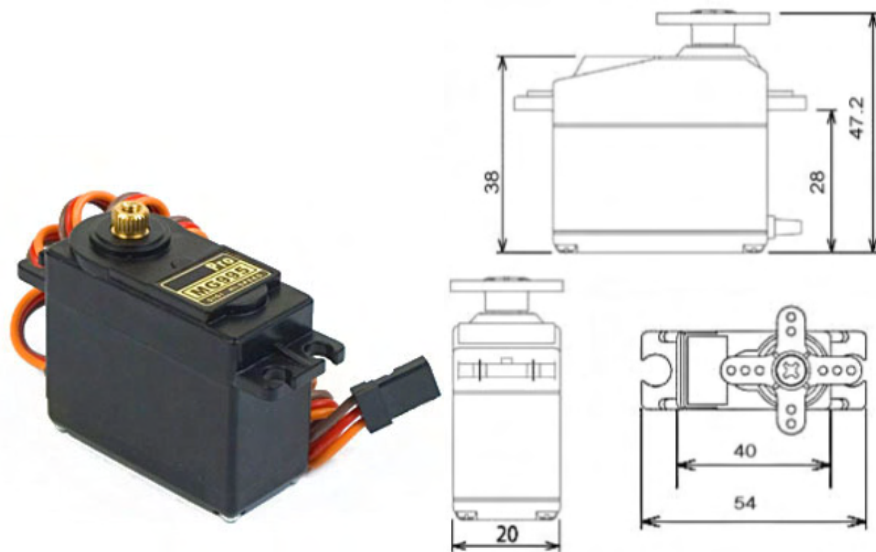
7.4.1.3 Third Prototype

The space in the prototype available for the organization of the servos is limited. The number of servos should then be the lowest possible and their size the smallest. Since the objective is for the prosthesis to accomplish hand flexion and pointing the index finger actions, the index finger needs to be connected separately to the other fingers. The rest of the fingers could be all connected to the same servo. Having that in consideration, the stronger servo should be able of applying a weight of:

$$3,0\text{kg} * 4 = 12,0\text{kg}$$

The model *Tower Pro MG995-360°* servomotor is a pricier and heavier servo model but with significantly higher torque. This high torque servo can also continuously rotate its 360 degrees. It allows any servo code, hardware or library to control it. The dimensions and specifications are shown in Figure 7.44 and Table 7.3.

This servomotor model is more towards the limit of the servo size allowed but a smaller servo with the same amount of torque would be more expensive or harder to find available in stores. Servos such as the *Turnigy TGY-MH958-360°* or the *Hitec HS-5645MG-360°*, shown in Figure 7.45, are both smaller in dimensions, especially in height when compare to the *Tower Pro MG995-360°* servomotor but in both cases, the servos are a bit heavier significantly more expensive, up to two times as much, and most importantly not in stock in the popular electronic shops in Portugal, such as *Mauser* and *PTRobotics*.

(a) *Tower Pro MG995-360°* servomotor.

(b) Servomotor dimensions.

Figure 7.44: *Tower Pro MG995-360°* servomotor and dimensions [84].Table 7.3: *Tower Pro MG995-360°* servomotor specifications [84].

Weight:	55 g
Dimension:	40.7 x 19.7 x 42.9 mm approx.
Stall Torque:	13kg-cm (6.0 V)
Rotation Angle:	360°
Operating Speed:	0.13 sec/60°
Operating Voltage:	4.8 V to 7.2 V
Dead Band Width:	5 μ s
Temperature Range:	0°C - 55°C

With this servo, the prototype has a bit more of the servo coming out of the metacarpal region, but during testing, it did not seem to affect the use of the prosthesis nor be susceptible to damage from the outside. During real-life use, the situation is not the same as during tests in the laboratory, so if the servo impacts negatively during the use of the prosthesis, the investment would be worth it and this servo model could be swapped with a different recommended model of smaller size.

As shown in the Table 7.3, the torque of this servo is high enough to pull the four fingers. For that reason, this prototype uses a single *Tower Pro SG90-360°* servomotor for the index finger and a *Tower Pro MG995-360°* servomotor for the rest of the fingers, as shown in Figure 7.46.

Using this model, this combination of servos not only occupies less space but also facilitates the organization in the metacarpal without affecting the level of functionality. This model was decided as the final model due to all of its advantageous features. This prototype takes a small step back in regards to aesthetics, due to the support box for the



(a) Turnigy TGY-MH958-360° servomotor [85].



(b) Hitec HS-5645MG-360° servomotor [86].

Figure 7.45: Alternative for the *Tower Pro MG995-360°* servomotor.

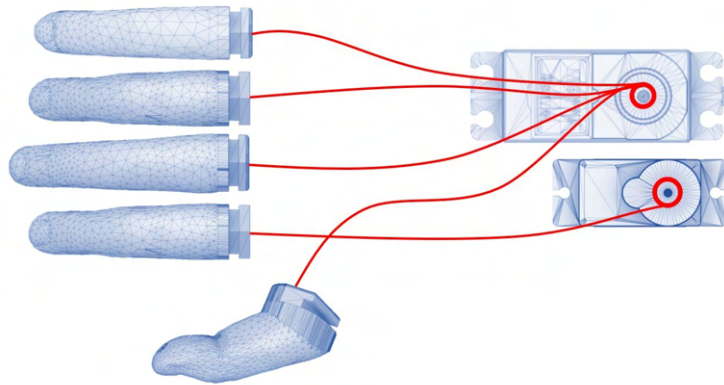


Figure 7.46: Design of the third prototype with a *Tower Pro SG90-360°* servo and a *Tower Pro MG995-360°* servo.

servos coming out a few millimetres from the posterior of the metacarpal. Nevertheless, this factor is insignificant when compared to the advances achieved in functionality. This model solves the main problems found until now and allows for the prosthesis to function with high quality without affecting the aesthetics significantly.

Connecting multiple servomotors to an Arduino seems easy at first but simply connecting the servos to the Arduino supply pins will not work correctly due to a lack of current to drive all the motors. The only solution is to connect an external power supply with an appropriate amount of current rating that can power all the servos. Looking at the datasheet of a *Tower Pro SG90-360°* servomotor and a *Tower Pro MG995-360°* servomotor, it is indicated a required input voltage of 4,8V to 6V and 3V to 7V, respectively. The Arduino UNO itself is not capable of feeding both the servos at the same time. The circuit requires an external power supply.

A normal alkaline battery (AA) will only provide 1,5V. So, it will be necessary to add a battery pack in series to get the required voltage. Using a battery pack of four normal alkaline batteries will give you a total of 6V at 500 mA/h. The duration of the battery

pack is not desirable but good enough for testing during this thesis.

7.5 Prosthesis Assembly and Functionality

During the course of this study, various similar prostheses were partially assembled and only the final prototype was completely built. This was in order to better manage certain resources, such as the servomotors. These partial builds allowed us to test different updates during the modelling stage. Small alterations were made during the modelling phase and the best way to test if the update worked or fitted in the prototype was by printing and testing the assembly and functionality. The final prosthesis was developed as a result of the analysis of the behaviour of the partial prints and assemblies.

This prosthesis is composed of fingers printed in *Filaflex 60A* and 50% infill and the metacarpal piece printed also in *Filaflex 60A* but in 30% infill, shown in Figure 7.47. Although the infill percentage in the metacarpal region is lower than for the fingers, the most flexible part of the prosthesis is the fingers. This is due to the addition of the servomotors causing an increase in stiffness to the metacarpal piece. Both regions of the prosthetic arm present, in general, a high level of cosmetic appearance.



(a) Final fingers vertically printed.

(b) Final metacarpal vertically printed.

Figure 7.47: Printed components for the final prosthesis prototype.

The thumb was the finger that presented a different morphology from the others. During the original design, some difficulties were already felt due to its different location and anatomical features. Unlike the other fingers, no curvature was added to the thumb as it was already present in the scanned model. This resulted in a different behaviour to an applied force and decreases in printing quality. Changes were tested in order to improve its features but due to the lack of experience, only simple alterations that present no improvements were made. For most of the thumb pieces, the cosmetic results are

satisfactory, with the only problem laying in the bottom part of the thumb, as shown in Figure 7.48. This lack of printing quality is caused by the necessary use of support enforcers. Two suggestions for improving the printing quality would be completely altering the morphology of the thumb in order not to need the support enforcers or using a filament other than *Filaflex*, such as PLA, for the support enforcers. As discussed previously, the lack of printing quality due to the removal of support enforcers is only evident when using flexible filaments.



Figure 7.48: Bottom view of the printed thumb for the final prosthesis prototype.

The rest of the fingers' morphology allows for an easier printing process that requires no support enforcers, generating a high printing quality, as shown in Figure 7.49. One of the additions to the finger design made in this study is the "bridge" that covers the most distal elliptic hole located in the middle of the distal phalanges, as shown in Figure 7.49(b). This feature was added with the intent of facilitating the process of tying the nylon string knot at the tip of the finger. Its addition is advantageous but due to the flexible properties of the material, this "bridge" can easily snap when force is applied. In practical tests made, it was concluded it would not be possible to withstand the tension when the servomotors would rotate. The solution found was using super-glue in the wire channel between the most distal interphalangeal joint and the tip of the finger. With this method, the final phalanges would lose their flexibility but would hold the nylon string in place in order to withstand the applied tension. This problem is only present due to the flexible properties of the *Filaflex* filament, prints of the finger piece made using PLA did not suffer from this same problem.

In this model, the high flexible properties of the material allow for the gauntlet piece to adapt to the user's arm without needing the moulding procedure required in previous models. The gauntlet piece that composes the wrist region, shown in Figure 7.50, was printed using *Filaflex 60A* and an infill of 20%. The moulding process was a complicated procedure since it required special attention in order to allow for the fitting of metacarpal and gauntlet piece. With this filament and properties, the gauntlet piece can be connected to the metacarpal region piece right after printing, without requiring any post-print handling. Despite of the high flexibility of the metacarpal piece, which also allow for more comfort, the stump-prosthesis interface should still be covered with self-adhesive



(a) Final index finger vertically printed.

(b) Final index finger vertically printed zoomed in.

Figure 7.49: Printed index finger for the final prosthesis prototype.

foam. This foam was placed in three different main spots of contact with the stump: on the distal region, posterior region and laterally.

Using flexible materials is advantageous in regards to comfort in the gauntlet region and on the stump prosthesis interface but it has negative effects in terms of structural stability of the connection between the metacarpal region and the forearm region. Due to its high flexibility, the areas where the pins fit are more susceptible to stretching and even rupture if enough weight is applied. Switching the prints of the pins and pin caps to *PLA* and an infill of 20%, instead of using *Filaflex*, helped significantly, since the extremities of the connection are rigid and will not stretch, but, during day-to-day activities, if the prosthesis suffers an impact or more weight is applied to the connection region, the pins could come off and break the prosthesis. Figure 7.51 shows a picture of the pins after being fitted in the metacarpal region piece.

In order to solve the previously discussed problems, the decrease in printing quality of the thumb, the knot snapping at the tip of the fingers and the metacarpal-gauntlet connection, the prints should be moved from the *Original Prusa i3 MK3S+*, which is a single extruder model printer, to a more advanced two extruder model printer. This different printer model can be useful since it allows for a print using multiple filament materials. Dual extruders are recommended for creating a specific type of part in a particular material [87]. These models are not only time-efficient but also allow for a

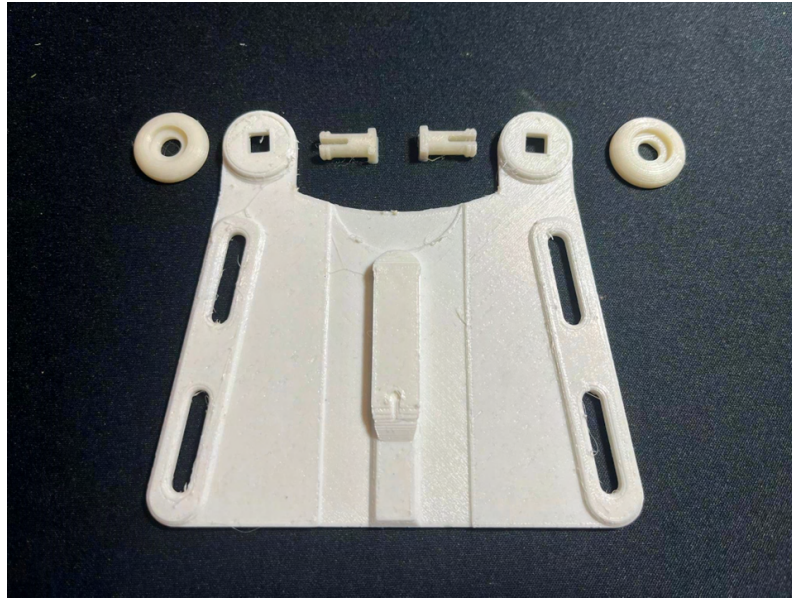


Figure 7.50: Printed components for the wrist region of the final prosthesis prototype.

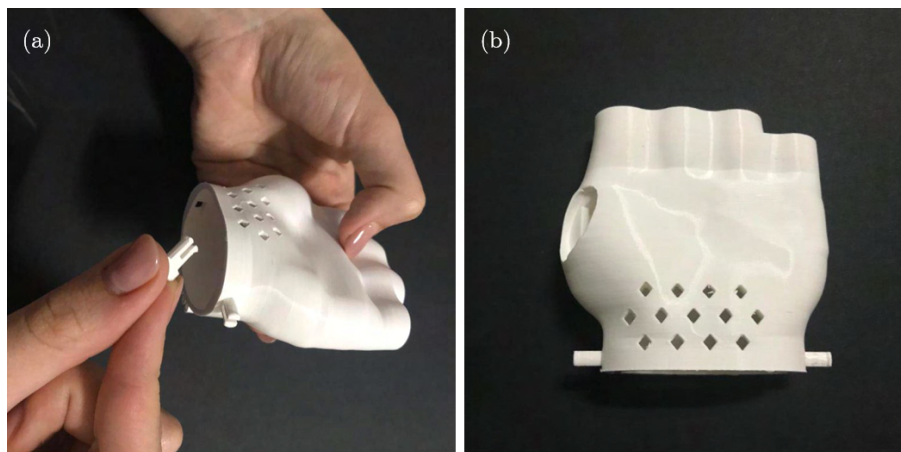


Figure 7.51: Fitting of the pins in the metacarpal region: (a) the pins are fitted from the inside of the stump-prosthesis interface in the counterbored holes; (b) pins after being fitted in the metacarpal region.

more accurate automatic alignment of soft and hard structures as they are produced, hence, avoiding certain scenarios when there was a need for manually combining the components post-printing [87], [88]. For this study, it would be especially advantageous to test prints of the metacarpal and gauntlet pieces using two different types of filaments, *Filaflex 60A* and *PLA*. The prosthetic model would improve its quality if these two specific parts were printed using a flexible material for most of its print but then switching to a rigid material in specific regions. Figure 7.52 shows the recommended print features using a dual extruder printer with *Filaflex 60A* and *PLA*. This feature should also be tested in the fitting area of the fingers, but it is believed it would not be as beneficial since it is the flexible properties of that area that facilitate the insertion and removal of the fingers in the metacarpal piece.

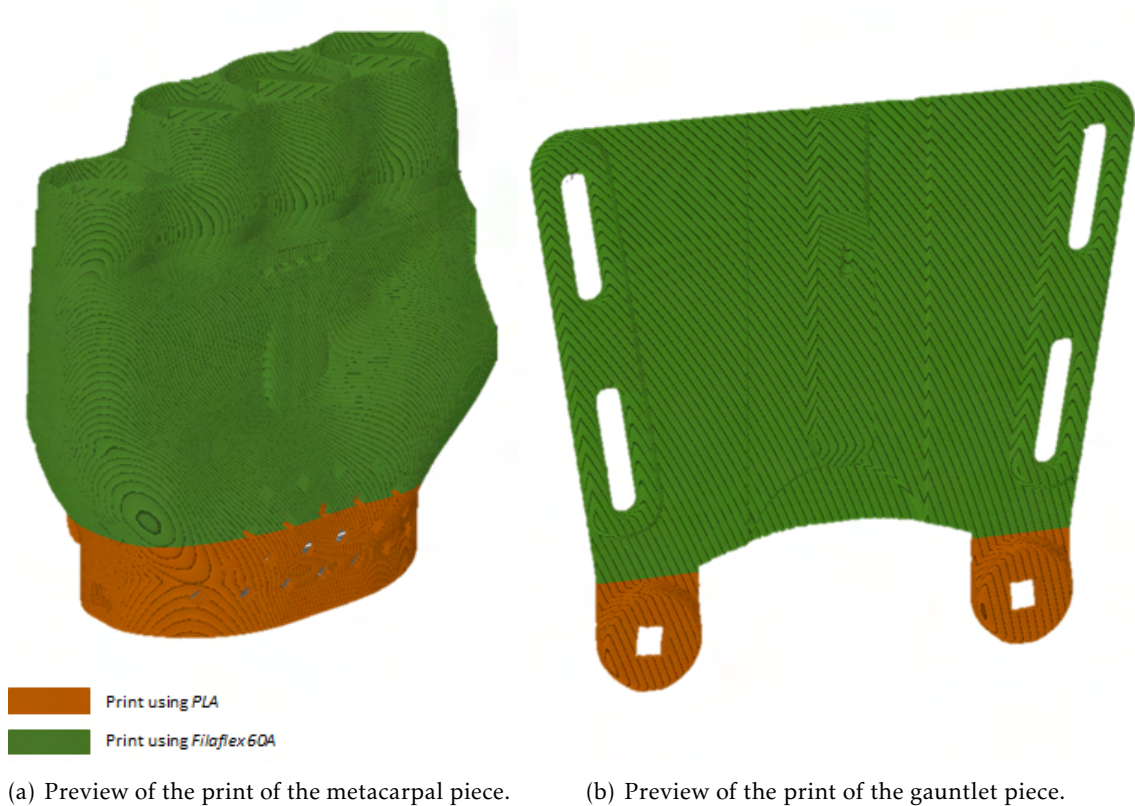


Figure 7.52: Suggestions of how to use a dual extruder printer for printing certain prosthesis pieces.

During the conduct of this study, the only printer available for use was the *The Original Prusa i3 MK3S+* by ©Prusa Research, a single extruder printer. In Section 7.2.2, it is shown the tests perform in order to evaluate if it was possible to perform a print whilst using two different filaments with a single extruder printer and it was concluded the printing quality suffers a significant downgrade in order to do so.

Towards the end of this study, the NOVA School of Science Technology (FCT NOVA) institute received a new model of a 3D-printer with a dual extruder, the *E2 3D Printer* by ©Raise3D, shown in Figure 7.53. This printer achieves its praise and best results whilst combining different materials with solidly proven build parameters. The unit lends itself to consistent part quality because the fully enclosed build environment limits internal variances and protects from the negative impact of external factors [89]. The *E2 3D Printer* by ©Raise3D features a high and stable print quality, versatility and high performance, as shown in the print examples of Figure 7.54, and it would be beneficial for the development of the prosthesis model to test different prints using its features that allow for high quality, two filament prints [89], [90].

Figure 7.55 presents the main prosthesis that was developed within the scope of this



Figure 7.53: Isometric view of the *E2 3D Printer* by ©Raise3D [89].

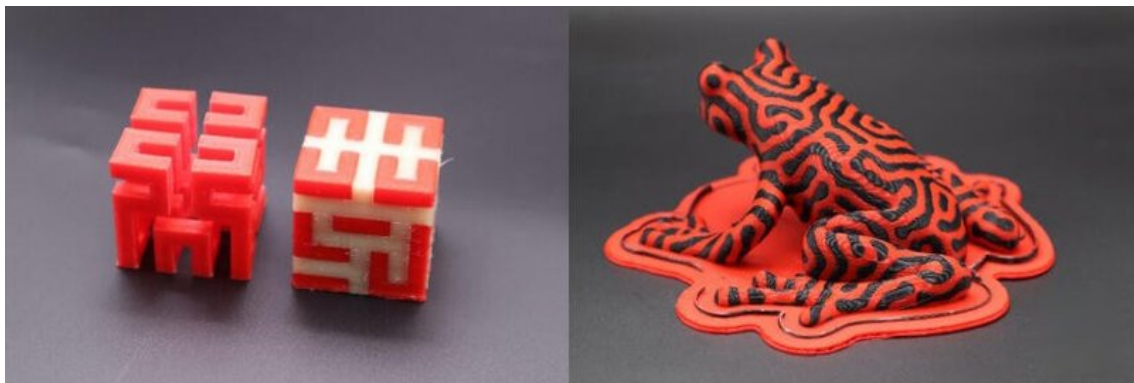


Figure 7.54: Examples of prints made with the *E2 3D Printer* using two different filaments [90].

study, fully assembled and composed by the printed components, shown in Figure 7.56, and the electronic components, shown in Figure 7.57. When handled, the parts printed revealed to be soft and comfortable to the skin.

When flexed, there was a slight bending of the fingers. However, this flexion was not enough to mimic the gripping motion of flexion of the metacarpophalangeal joints that was pretended. More tension was required to fully flex the prosthesis which was possible by the servomotors but not allowed by the wires used. The prosthesis had some level of functionality, allowing the flexion of the fingers in response to the classification of the grasping movement, as shown in Figure 7.58, and for the index pointing movement, as shown in Figure 7.59. This flexion does not fully mimic the gripping and pointing movement but there is enough level of anthropomorphism to be satisfied with the results.

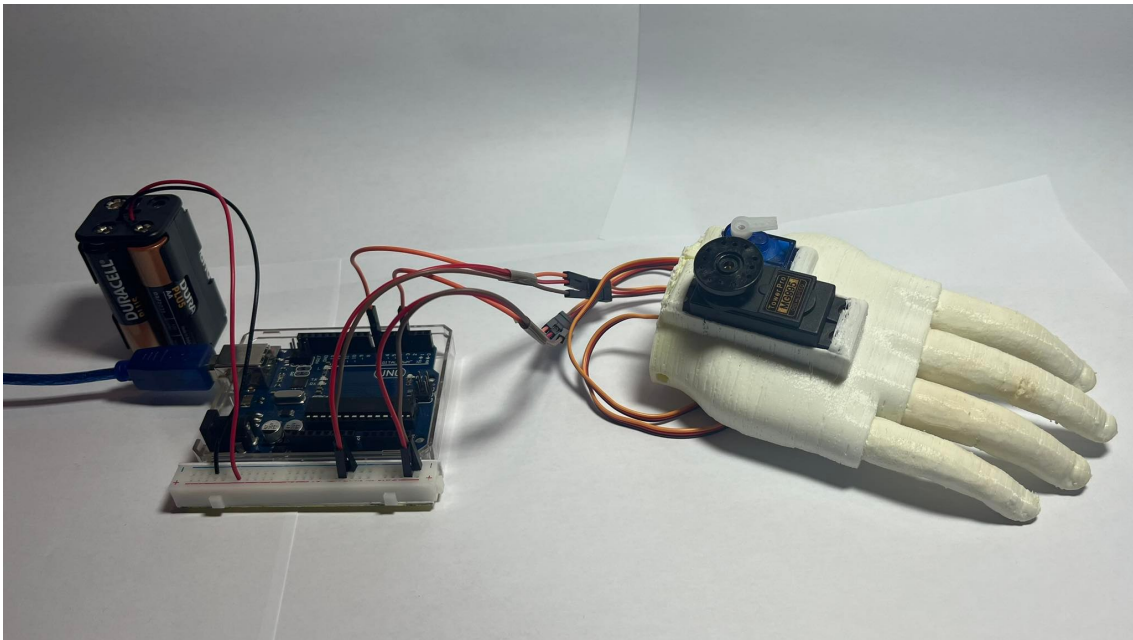


Figure 7.55: Final prosthesis model.

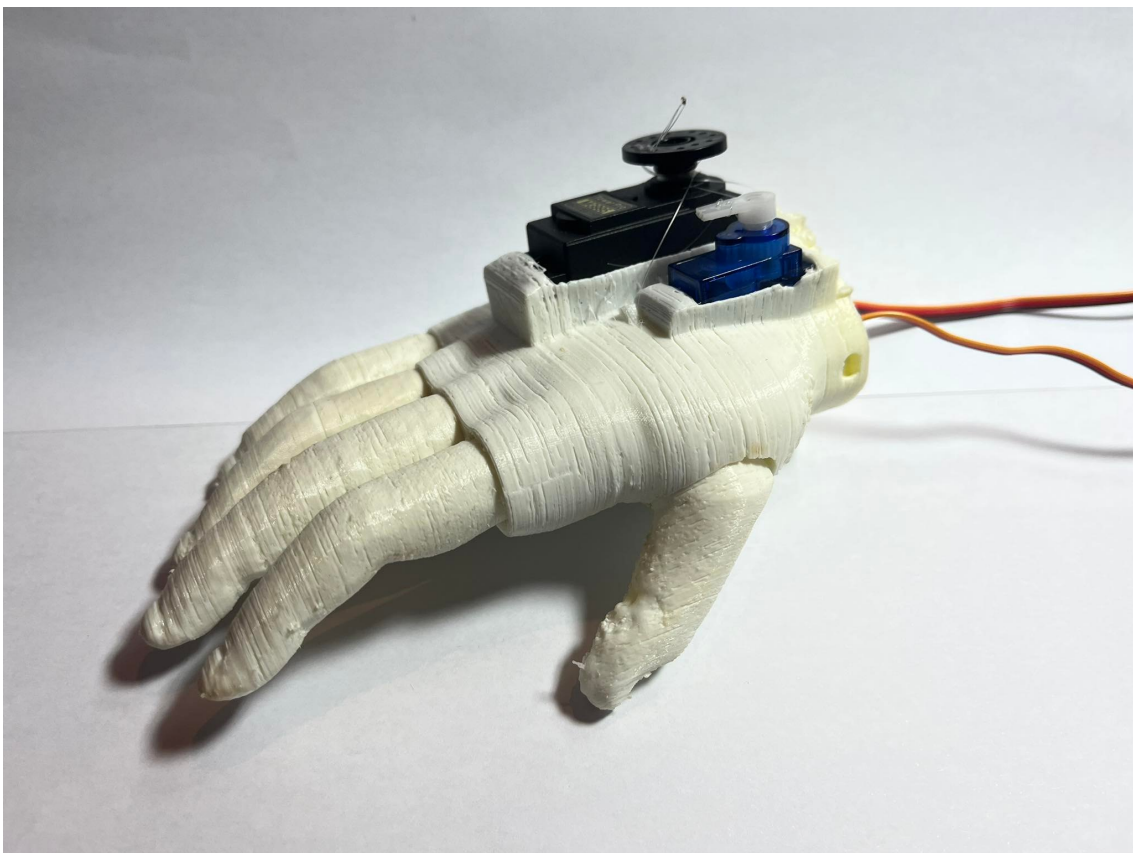


Figure 7.56: Printable components of the prosthesis fully assembled.

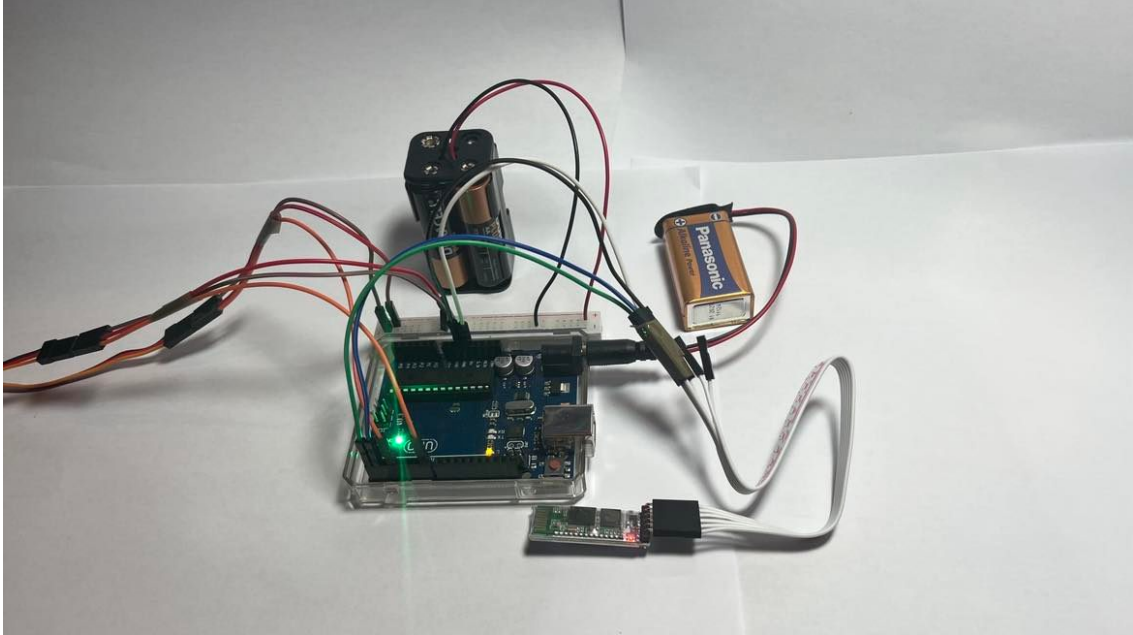


Figure 7.57: Electronic circuit used in the prosthesis model.

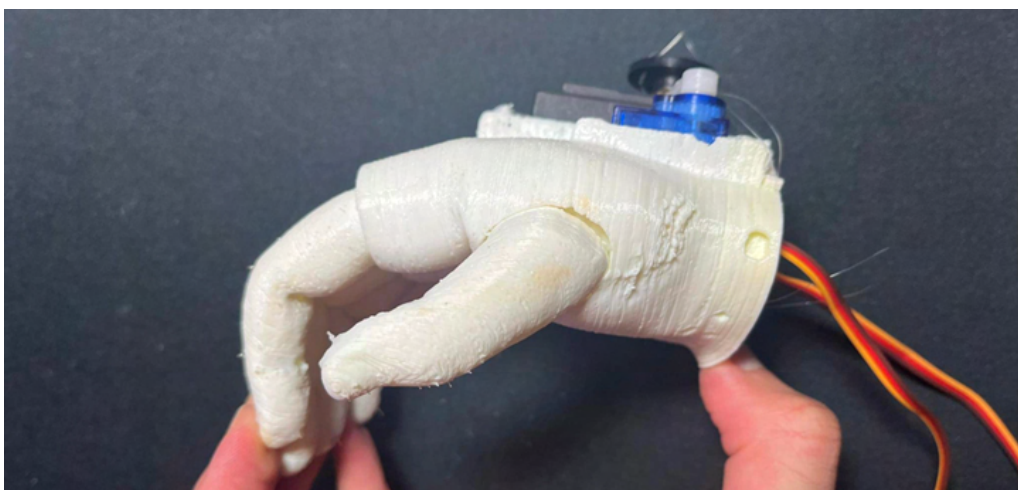


Figure 7.58: Gripping movement of the final prosthesis prototype.

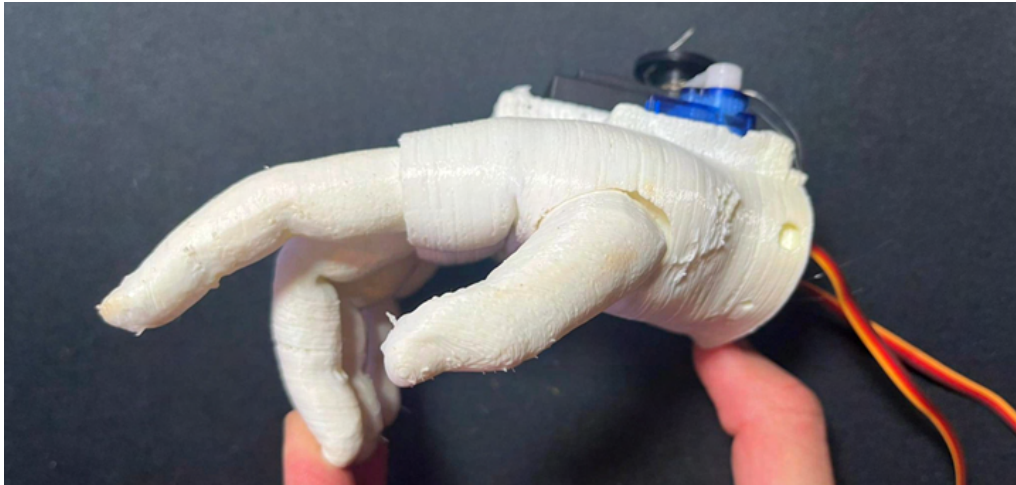


Figure 7.59: Index pointing movement of the final prosthesis prototype.

7.6 Prosthesis Evaluation

Throughout this study, several efforts were made in order to develop a body-powered hand prosthesis that would combine a more real and appealing cosmetic appearance together with a high level of functionality.

Regarding the cosmetic appearance, it is considered that this goal was successfully met, the prosthetic model has a high level of anthropomorphism and its colour matches the skin colour of the child. Maintaining the presence of the protuberances that simulate the hand creases and knuckles as well as the use of a flexible filament to mimic the hand's bones was a factor of extreme importance that was kept since it contributed to this high level of anthropomorphism, creating the idea of a real hand, especially when compared to other low-cost 3D-printed prostheses. Most of the limitations addressed in Ana Oliveira's study were solved and it was possible to incorporate Ema Lopes's study into the prototype, upgrading the prosthesis from a body-powered prosthesis into a myoelectric prosthesis, which were the main goals of this study.

The main drawback in the original design was addressed by upgrading the tensioning system from a completely external system in the wrist region to a partially internal in the metacarpal region. There is still a need for improvement, which can easily be achieved by a bigger investment in a smaller servomotor with the same torque, making the servo completely internal, but it did not seem necessary during this study. The original body-powered prosthesis also required the movement that simulates the wrist extension in order to tense, which is not a realistic behaviour when grasping an object. With this new model this problem is solved.

Another limitation addressed and solved during this study was the need for high-tensioning forces. This was solved by upgrading the filament to a more flexible one. This resulted in lower tensioning forces that also allowed for the evolution of the model from body-powered to electric.

Switching from a guitar string to a nylon string in the tensioning mechanism was one

of the solutions to lower the tension force required. This led to an increase in the difficulty of the assembly of the wiring system. This problem was already noticeable in the original model but now it is not as predominant. This was solved by reducing the number of curves in the wiring canals, simplifying the wiring system to just straight canals.

The improvement of the myoelectric classifier was not the main objective of this study, only its implementation into the prosthetic model. Nevertheless, this was achieved with the reduction of the number of classification classes and the improvement of the acquisition of the EMG signal, by switching the position of the electrodes.

Although most of the problems found in the previous studies were solved, some remained and new ones appeared. The flexion of the thumb and its printing quality were issues that remained unresolved. Switching from *Filaflex 70A* to *Filaflex 60A* helped reduce the tension force necessary to solve the issue in the other fingers, but the thumb remained unfazed. It is now believed that the issue lies in the thumb design and canal system rather than the flexibility of the finger. Its shape and the need for a support enforcer during printing is still also an issue that reduces the printing quality.

The new main problem found with this model is the need to design the servomotor support system from scratch every time the prosthesis is scaled, as shown in Figure 7.60. This is a long process that can delay the development of the product. This limitation is due to the fact the servo support system is built into the metacarpal region design. When scaling the prosthesis in order to adapt to the patient's needs, all dimensions in the metacarpal region design, however, the servomotor dimensions stay fixed. *Fusion 360 CAD* software (version 2.0.10940) and the *SolidWorks CAD 2021* software only allow for complete scaling of the part, both software programs do not allow for scaling of certain dimensions and fixating the rest. This is a minor inconvenience since it does not influence the functionality of the prosthesis and only extends the period of development of the prosthesis.

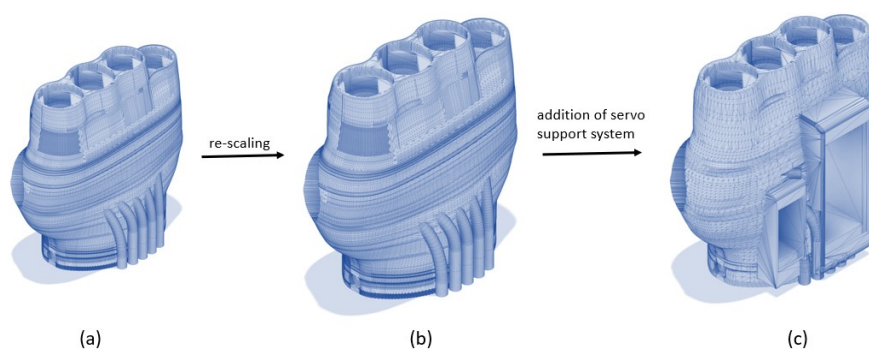


Figure 7.60: Process necessary every time the prosthesis is scaled: (a) original model, (b) scaled model, (c) scaled model with the servomotor support system.

The final prototype is functional in most aspects, with the exception of the flexion of the thumb. The prototype allows for a *python* file to receive a EMG signal previously recorded and processed in order to be saved in the correct format, classify its movement

and send the information to the Arduino board that acts accordingly and produces the respective movement. The prototype is still limited to only working for a few movements since the wire ends up snapping after a few uses. This hinders the use of the prosthesis in real life and requires constant repairs of the wiring system that allows the functionality of the prosthesis and its finger pieces. Since the wire is stuck in place using super-glue, every time the wire snaps it is not possible to only replace the wire, it requires a new set of fingers so the prosthesis can work again.

Despite all the aspects that need to be enhanced, even in terms of appearance and functionality, it is important to refer that the development process was the result of simultaneous, often conflicting, requirements of functionality, appearance and printability. Most of the decisions that were made during this study were the result of constant trade-offs. For example, increasing the printing quality would lead to a higher difficulty flexing the fingers; upgrading the servomotor would lead to more costs, more weight and less availability; switching to a smaller servomotor would lead to less torque, making it impossible to flex the fingers or a significantly more expensive servo. However, the resultant prosthesis, which consists of a prototype is considered a huge step in the field of 3D-printed prosthesis and an upgrade to the previous models.

When compared to other existing prostheses and the prototypes developed during Ana Oliveira´s study and Ema Lope´s study, several improvements can be pointed out, especially in functional terms. Aesthetically, the new model is not a big improvement on Ana Oliveira´s study but this model is capable of implementing the classifier developed by Ema Lopes´s study, upgrading the prosthetic device from body-powered to myoelectric. Although there are still a few functionality aspects to improve when compared to other prostheses in the market, there is a great belief that some of the developed concepts could lead to high levels of customisation, functionality and aesthetics it further improved.

7.6.1 Prosthesis Characteristics

The cosmetic appearance and functionality are two of the main user needs of a prosthesis. However, other aspects such as comfort and price are also important. In Table 7.4 information on the material cost, mass and printing time of the final prototype model is shown. In Appendix F it is presented a more in-depth informative table with the discriminated cost of each component that composes the final prototype prosthesis.

Table 7.4: Material cost, mass and total printing time of the final prosthesis prototype.

	Final Prosthesis
Material Cost (€)	59.81 €
Mass (g)	172,63 g
Printing Time (h:min)	26:10

In theory, the human hand weighs around 0.585% of its total body weight. For a

user of around 65kg, which is around the weight of the children for which this prosthetic model is destined, it means that the designed prosthesis needs to have less than 380.25g [91]. As shown in Table 7.4, the developed prototype is significantly lighter than the maximum weight. This means this prosthetic model can be used for a vast majority of young patients without worrying about the disparity of the weight of the prosthesis compared to the healthy hand.

By analysing Table 7.4 it is evident how beneficial 3D-printed prostheses are due to their light-weight and low cost. The obtained cost is significantly lower than most prostheses with a certain level of functionality in the market. This fact should be encouraging to further continue this study and reveals the promising character of 3D-printed prostheses, especially made from a flexible material. The major population benefiting from this prototype are children, given the necessity for regular replacement of the prosthesis with updated dimensions. The printing time is a bit above the common range of most 3D-printed prostheses, which usually take around 15 to 20 hours of printing time, but it is expected since *Filaflex* requires a slower print when compared to other materials, such as PLA. The printing time depends on the complexity of the model and the printing settings that influence the printing quality. This justifies the higher printing time when compared to the other, more rudimentary models.

Despite all upgrades and improvements, this prototype still has its limitations. The risks associated with the failure of the prototype, such as tension pin failure, finger failure, elastic tension failure, locking mechanism failure or electronic failures were not considered. The risks associated with this prosthesis can be moderate or higher since it can put at risk the user's safety and can lead to the damaging of the object or make the fingers useless. The resistance of the material was not tested but, towards the end of the study, small signs of degradation were starting to become noticeable. With this in mind, this device should not be used as a daily use prosthesis but has a training device in clinical environments. In this dissertation, the adaptability of the designed system to a wide range of sizes does not restrain the training to a specific user, which is an advantage in clinical background.

7.6.2 System Usability Scale Assessment

The SUS was the methodology chosen to measure the level of satisfaction of the final prototype produced in this study. The results of the two surveys presented, the standard SUS survey and the additional survey with specific questions about the developed prosthesis, are 97.5 and 100 out of 100, respectively, which classifies the prototype as "Excellent". However, it is important to mention that the survey was answered by the person responsible for the development of the prosthesis and not a real user, so there is a bit of bias, and the answers were given having in mind the initial expectations of the study.

Appendix E presents the answers to the SUS survey as well as the ten additional questions. The answers given reveal that, even though the prosthesis is not fully functional, the progresses, especially in terms of aesthetics, were notorious when compared to other 3D-printed myoelectric prosthesis.

Conclusion

This chapter presents an overview of the present study, in which the final considerations of the developed work are present, namely the major achievements and suggestions for future work.

8.1 Summary of the Study Achievements

Hands are an essential tool for human beings as they are used in most day-to-day activities. So losing a hand or even part of the upper limb will have a relevant influence on a patient's daily life and mental health. Prosthetic rehabilitation can help revert this scenario since it promotes the partial re-establishment of the limb's functionality, improving their quality of life. However, due to the prosthetic industry not being a very profitable industry that requires a lot of investment in the development stage, not all patients can afford a prosthesis that answers their basic needs. This is even more noticeable for children patients that are in their development stage and have growth spurts, which means frequent replacements for bigger prostheses.

The development of AM, has helped provide new and improved solutions for the main problems of the prosthetic field since it enables the production of these devices at a low cost. Nevertheless, the devices produce using AM methods still suffer from high rejection rates due to their rigidity, low level of functionality and toy-like appearance. Therefore, there is a need to invest in more flexible and realistic prosthetic models with a high level of functionality, whilst also ensuring other essential features such as comfort, low cost and customization.

Some prosthesis models built with flexible materials have started to appear, nonetheless, they are mostly cosmetic or restricted to body-powered models. Developing a functional electric or even myoelectric prosthesis would significantly contribute to advances in the prosthetic industry. The hypothesis of this study was that a more realistic, functional, comfortable and tailored hand prosthesis that implements a EMG signal classifier as the input source of the grip motions can be developed using AM and flexible materials, without compromising other features such as lightness, ease of repair and low-cost.

This study was the continuation of Ana Oliveira's study that design a prototype of a flexible body-powered prosthetic model and implementation of Ema Lopes' study, which developed a EMG signal classifier, in the prototype, upgrading the prosthesis into a myoelectric prosthetic prototype. The basis of this study was Ana Oliveira's prototype and its improvement. Design upgrades and adaptations were necessary due to the prosthesis' new needs and characteristics. During the progress of this study, several prototypes were made in order to test the newly generated concepts. These prototypes were resultant of simultaneous trade-offs between the printability, functionality, resistance, appearance and force needed to flex the finger models.

In order to produce the final prototype, firstly it was necessary to understand the behaviour of the models to different filaments and print properties. A proportional invertibility relation between the printing quality and the forces needed to bend the fingers was discovered which allowed to introduce of servomotors into the prototype. When choosing the servomotor, the servo had to have enough torque to bend the fingers, so choosing it was a matter of balance between the cost, availability, torque of the servomotor and printing quality of the finger pieces. The perfect balance was not found since the prosthesis did not reach the ideal level of functionality. Although it is difficult to flex the prosthesis, it is believed to be due to the tensioning system of the servo mechanism. The constriction on the finger movement is probably related to their morphological design, which needs to be improved, especially of the thumb.

Despite the low functionality of the designed prostheses, the final results were very satisfactory, especially when compared to other existent 3D-printed prostheses, such as *Raptor Reloaded*, and the previous prototypes in which the study continued from:

- The developed prosthesis uses a more flexible material that adapts to the user's forearm region shape, contributing to an increase in comfort, especially in the stump-prosthesis region.
- The prosthesis continues to use a realist approach to its design, making them more aesthetically appealing than other available prostheses found in *open-source* forums, such as *e-Nable* forum. By enhancing their aesthetic appearance, this type of prosthesis has a higher chance of acceptance. With the realist look, children will stop looking at the prostheses as a new toy and more like an instrument to help them in their day-to-day life. With the ageing of the user, the rejection rate will not decrease since the prosthesis is not of childish, unreal appearance.
- The functionality level and the functionality ceiling in this prosthesis increase significantly with the introduction of the electronic components and the connection with an EMG classifier. Although at this stage, the classifier succession rate is not desirable, with the introduction of amputated people in the volunteers' group the myoelectric signal processing would significantly improve.

- Like other 3D-printed prostheses, the developed devices are low-cost solutions, which makes them perfect for children since they are more likely to be damaged. This model allows for partial replacement of the damaged pieces without compromising the rest of the device, lowering the repair price, and the segmentation of the components helps in the assembly process, increasing their user-friendly character. The fast growth that is associated with children also does not affect the worth and investment of this type of prosthesis in children. Finally, these low production costs for prostheses will also benefit people with lower purchasing power that can not afford more expensive devices.
- The usage of flexible filament helps simulate the compliance of the hand's skin, achieving stronger grips and avoiding slips of objects. This feature is quite impacting for patients with acquired deficiencies who have a huge need to restore their sensory feedback.

The development of the present 3D-printed myoelectric hand prostheses has revealed several contributions to the scientific community as it may be one of the first steps for the evolution of these types of AM made prostheses. This device is capable of bringing benefits to patients with upper limb defects, not only restricted to children with congenital disorders that need to have their first contact with prosthetic devices but also, with the significant increase in functionality, to the traumatic amputees with less buying power.

8.2 Future Work

As with all studies and experiments, this dissertation has a few limitations that should be considered and addressed in future works. Future work should include:

- **Improvement of the functionality of the classifier:** this can be done through the reduction of the misclassified classes. In order to achieve satisfactory results perhaps one acquisition channel is not enough and there would be a significant improvement in the accuracy of the classifier after adding a second acquisition channel. Testing new electrodes' placements in different muscle groups, such as in extensor muscles, could increase signal detection and consequently the classification performance.
- **Improvement of the functionality of the designed prosthesis:** this might be done by improving the wiring, so it can withstand a higher tension force without the wire snapping, or changing the thumb morphology, so it can bend and have a behaviour similar to a real thumb and to the other finger designs. When designing these fingers designs, simulating the appearance of the fingers was key. This helps the cosmetic factor but it affects functionality. Designing a more articulated device that simulates the human skeleton whilst maintaining the cosmetic appeal is challenging but would significantly help overcome these limitations.

- **Enhancement of the cosmetic appearance:** although in Ana Oliveira's study significant achievements were achieved concerning this topic, in this study, with the addition of the servomotor support system in the metacarpal region piece and the restructure of the its wire system, there was a decline in the cosmetic appeal. The level of anthropomorphism of this structure could increase by making the servo support system fully or at least more internal, or creating a new mechanism. Altering the design of the thumb so, when printing, it does not require a support enforcer would improve the aesthetics of the prototype.
- **Upgrading the battery dependency:** the external power supply used for this study is enough for the testing stage of the project, it is enough to power the prosthesis for about 15 min. If this prosthetic devices are to be used in real-life scenarios it is essential to prolong the battery duration. Testing different types of external power supplies capable of powering the prosthetic device for a longer period of time should be the next step in the development of this prototype.
- **Testing with a dual extruder printer:** one of the limitations of this prototype is connected to the restriction of only using one type of filament during each print. Testing new methods of AM that allow for a combination of PLA and *Filaflex* in one printed piece would help overcome some of the problems, such as the low resistance to tension in the connection between the metacarpal piece and the gauntlet and the difficulty of tying the wire to the tip of the finger pieces. By using a more advanced printer model, better results would be achieved and the functionality of the prosthesis would improve.
- **Evaluation of the prosthesis:** the intention of this study was to evaluate this prosthesis in order to have a more in-depth understanding of its capabilities. However, due to its still relatively low functionality level, this was not possible. After improving functionality it is important to test the mechanical resistance and performance of the prototype. Resistance test where it was evaluated how much force the prototype can withstand, their maximum payload before it fails or breaks, were not able to be performed. After improving certain details, it also should be tested its grasping capabilities by measuring its grasping force.

Despite the limitations, the overall results satisfy the expectations. Improvements were achieved and significant upgrades in functionality were achieved with the evolution from a body-powered prosthetic device to a myoelectric prosthesis made from flexible materials. Finally, it is important to highlight the importance of this current study to be continued with the aim of keeping improving the functionality and customisation of this prosthetic model. This dissertation can contribute to advances in the prosthetic industry and in the implementation of new ideas and solutions in the development of prosthetic devices by improving the state of the art.

Bibliography

- [1] J. M. Lourenço, *The NOVAthesis L^AT_EX Template User's Manual*, NOVA University Lisbon, 2021. [Online]. Available: <https://github.com/joaomlourenco/novathesis/raw/master/template.pdf>.
- [2] K. Soyer, B. Unver, S. Tamer, and O. Ulger, *The importance of rehabilitation concerning upper extremity amputees: A systematic review*, 2016. DOI: 10.12669/pjms.325.9922.
- [3] K. S. Lee and M. C. Jung, *Ergonomic evaluation of biomechanical hand function*, 2015. DOI: 10.1016/j.shaw.2014.09.002.
- [4] D. Van Der Riet, R. Stopforth, G. Bright, and O. Diegel, "An overview and comparison of upper limb prosthetics", *IEEE AFRICON Conference*, 2013, ISSN: 21530033. DOI: 10.1109/AFRCON.2013.6757590.
- [5] T. R. Dillingham, L. E. Pezzin, and E. J. MacKenzie, "Limb amputation and limb deficiency: Epidemiology and recent trends in the united states", *Southern medical journal*, vol. 95, no. 8, pp. 875–884, 2002.
- [6] "Biomechanical analysis of users of multi-articulating externally powered prostheses with and without their device", *Prosthetics and Orthotics International*, vol. 43, no. 6, pp. 618–628, 2019, ISSN: 17461553.
- [7] J. P. Matos, E. Carolino, and R. Ramos, "Dados epidemiológicos sobre amputações realizadas em Portugal entre 2000 e 2015", *IV Jornadas de Ortoprotesia*, 2018. [Online]. Available: <http://hdl.handle.net/10400.21/8818>.
- [8] *Congenital Limb Abnormalities - Pediatrics - Merck Manuals Professional Edition*. [Online]. Available: <https://www.merckmanuals.com/professional/pediatrics/congenital-craniofacial-and-musculoskeletal-abnormalities/congenital-limb-abnormalities> (visited on 2022-02-09).
- [9] C. A. Goldfarb, N. Shaw, J. A. Steffen, and L. B. Wall, *The Prevalence of Congenital Hand and Upper Extremity Anomalies Based Upon the New York Congenital Malformations Registry*, 2017. DOI: 10.1097/BPO.0000000000000748.

- [10] M. Toda, T. Chin, Y. Shibata, and F. Mizobe, *Use of powered prosthesis for children with upper limb deficiency at Hyogo Rehabilitation Center*, 2015. DOI: 10.1371/journal.pone.0131746.
- [11] J. M. Zuniga, J. L. Peck, R. Srivastava, *et al.*, "Functional changes through the usage of 3D-printed transitional prostheses in children", *Disability and Rehabilitation: Assistive Technology*, vol. 14, no. 1, pp. 68–74, 2019, ISSN: 17483115. DOI: 10.1080/17483107.2017.1398279. [Online]. Available: <https://doi.org/10.1080/17483107.2017.1398279>.
- [12] "Limb deficiency and prosthetic management. 1. Decision making in prosthetic prescription and management", *Archives of Physical Medicine and Rehabilitation*, vol. 87, no. 3 SUPPL. Pp. 3–9, 2006, ISSN: 00039993. DOI: 10.1016/j.apmr.2005.11.022.
- [13] *Enabling The Future – A Global Network Of Passionate Volunteers Using 3D Printing To Give The World A "Helping Hand*. [Online]. Available: <https://enablingthefuture.org/> (visited on 2022-02-09).
- [14] J. ten Kate, G. Smit, and P. Breedveld, "3D-printed upper limb prostheses: a review", *Disability and Rehabilitation: Assistive Technology*, vol. 12, no. 3, pp. 300–314, 2017, ISSN: 17483115. DOI: 10.1080/17483107.2016.1253117. [Online]. Available: <http://dx.doi.org/10.1080/17483107.2016.1253117>.
- [15] R. M. Bongers, P. J. Kyberd, H. Bouwsema, L. P. Kenney, D. H. Plettenburg, and C. K. Van Der Sluis, "Bernstein's levels of construction of movements applied to upper limb prosthetics", *Journal of Prosthetics and Orthotics*, vol. 24, no. 2, pp. 67–76, 2012, ISSN: 10408800. DOI: 10.1097/JPO.0b013e3182532419.
- [16] A. B. Harris, *Human anatomy*, 5555. 1976, vol. 261, p. 10, ISBN: 9780072943689. DOI: 10.1038/261010c0.
- [17] J. D. Spratt, L. R. Salkowski, J. Weir, and P. H. Abrahams, *Imaging Atlas of Human Anatomy E-Book*. Elsevier Health Sciences, 2010.
- [18] *Structural Functional Birth Defects*. [Online]. Available: <https://birthdefects.org/structural-and-functional-birth-defects/> (visited on 2022-02-11).
- [19] C. J. Dy, I. Swarup, and A. Daluiski, "Embryology, diagnosis, and evaluation of congenital hand anomalies", *Current Reviews in Musculoskeletal Medicine*, vol. 7, no. 1, pp. 60–67, 2014, ISSN: 19359748. DOI: 10.1007/s12178-014-9201-7.
- [20] J. W. Seeds, R. C. Cefalo, and W. N. Herbert, "Amniotic band syndrome", *American Journal of Obstetrics and Gynecology*, vol. 144, no. 3, pp. 243–248, 1982, ISSN: 00029378. DOI: 10.1016/0002-9378(82)90574-9. [Online]. Available: [http://dx.doi.org/10.1016/0002-9378\(82\)90574-9](http://dx.doi.org/10.1016/0002-9378(82)90574-9).

- [21] “Amniotic band syndrome”, *Journal of Foot and Ankle Surgery*, vol. 37, no. 4, pp. 325–333, 1998, ISSN: 10672516. DOI: 10.1016/S1067-2516(98)80070-7. [Online]. Available: [http://dx.doi.org/10.1016/S1067-2516\(98\)80070-7](http://dx.doi.org/10.1016/S1067-2516(98)80070-7).
- [22] *Bridas amnióticas: o que são, causas e tratamento - Tua Saúde*. [Online]. Available: <https://www.tuasaude.com/bridas-amnioticas/> (visited on 2022-02-11).
- [23] *Limb Amputation: Reasons, Procedure, Recovery*. [Online]. Available: <https://www.webmd.com/a-to-z-guides/definition-amputation#1> (visited on 2022-02-11).
- [24] B. Maat, G. Smit, D. Plettenburg, and P. Breedveld, *Passive prosthetic hands and tools: A literature review*, 2018. DOI: 10.1177/0309364617691622.
- [25] C. Castellini, *Upper limb active prosthetic systems-overview*. INC, 2019, pp. 365–376, ISBN: 9780128146590. DOI: 10.1016/B978-0-12-814659-0.00019-9. [Online]. Available: <http://dx.doi.org/10.1016/B978-0-12-814659-0.00019-9>.
- [26] B. Phillips, G. Zingalis, S. Ritter, and K. Mehta, “A review of current upper-limb prostheses for resource constrained settings”, *Proceedings of the 5th IEEE Global Humanitarian Technology Conference, GHTC 2015*, pp. 52–58, 2015. DOI: 10.1109/GHTC.2015.7343954.
- [27] B. Dutra, “Metodologia para estimação de intenção de movimento e controle em tempo real de prótese mioelétrica de mão: Uma abordagem linear, preditiva e estocástica”, Ph.D. dissertation, 2018-07. DOI: 10.13140/RG.2.2.15508.19845.
- [28] F. Cordella, A. L. Ciancio, R. Sacchetti, *et al.*, “Literature review on needs of upper limb prosthesis users”, *Frontiers in Neuroscience*, vol. 10, no. MAY, pp. 1–14, 2016, ISSN: 1662453X. DOI: 10.3389/fnins.2016.00209.
- [29] W. J. Gaine, C. Smart, and M. Bransby-Zachary, “Upper limb traumatic amputees: Review of prosthetic use”, *Journal of Hand Surgery: European Volume*, vol. 22, no. 1, pp. 73–76, 1997, ISSN: 20436289. DOI: 10.1016/S0266-7681(97)80023-X.
- [30] *Additive manufacturing and 3D printing in manufacturing*. [Online]. Available: <https://www.i-scoop.eu/industry-4-0/additive-manufacturing-3d-printing/> (visited on 2022-02-13).
- [31] E. Tempelman, H. Shercliff, and B. N. van Eyben, *Manufacturing and design: understanding the principles of how things are made*. Elsevier, 2014.
- [32] L. E. Diment, M. S. Thompson, and J. H. Bergmann, “Three-dimensional printed upper-limb prostheses lack randomised controlled trials: A systematic review”, *Prosthetics and Orthotics International*, vol. 42, no. 1, pp. 7–13, 2018, ISSN: 17461553. DOI: 10.1177/0309364617704803.
- [33] *Generation of an STL File from 3D Measurement Data with User-Controlled Data Reduction*, 1999. DOI: 10.1007/s001700050049.
- [34] *Estereolitografia - Processo e Materiais | 3Dilla*. [Online]. Available: <https://pt.3dilla.com/impressora-3d/estereolitografia/> (visited on 2022-02-13).

- [35] *Sinterização Seletiva a Laser – O Processo* | 3Dilla. [Online]. Available: <https://pt.3dilla.com/impressora-3d/selective-laser-sintering/> (visited on 2022-02-13).
- [36] *Modelagem por Deposição Fundida - Tecnologia de Impressão 3D* | 3Dilla. [Online]. Available: <https://pt.3dilla.com/impressora-3d/fused-deposition-modeling/> (visited on 2022-02-13).
- [37] *ExOne | Binder Jetting Technology*. [Online]. Available: <https://www.exone.com/en-US/resources/case-studies/what-is-binder-jetting> (visited on 2022-02-13).
- [38] *Polyjet – Tecnologia de Impressão 3D* | 3Dilla. [Online]. Available: <https://pt.3dilla.com/impressora-3d/polyjet/> (visited on 2022-02-13).
- [39] M. J. Whittingham, R. D. Crapnell, E. J. Rothwell, N. J. Hurst, and C. E. Banks, “Additive manufacturing for electrochemical labs: An overview and tutorial note on the production of cells, electrodes and accessories”, *Talanta Open*, vol. 4, p. 100 051, 2021, ISSN: 26668319. DOI: 10.1016/j.talo.2021.100051. [Online]. Available: <https://doi.org/10.1016/j.talo.2021.100051>.
- [40] Z. Liu, Y. Wang, B. Wu, C. Cui, Y. Guo, and C. Yan, *A critical review of fused deposition modeling 3D printing technology in manufacturing polylactic acid parts*, 2019. DOI: 10.1007/s00170-019-03332-x.
- [41] “A review on recent advancements in fused deposition modeling”, *Materials Today: Proceedings*, vol. 27, no. xxxx, pp. 752–756, 2020, ISSN: 22147853. DOI: 10.1016/j.matpr.2019.12.036. [Online]. Available: <https://doi.org/10.1016/j.matpr.2019.12.036>.
- [42] *Original Prusa i3 MK3S+ | Original Prusa 3D printers directly from Josef Prusa*. [Online]. Available: https://www.prusa3d.com/category/original-prusa-i3-mk3s/?gclid=CjwKCAiA9aKQBhBREiwAyGP5lRBdYwCTD9wiqpg0euAybM5Qy9yaxPf14cwV-nAhEx_H5VTyFEA9RoC0EQQAvD_BwE (visited on 2022-02-13).
- [43] T. D. Ngo, A. Kashani, G. Imbalzano, K. T. Nguyen, and D. Hui, “Additive manufacturing (3D printing): A review of materials, methods, applications and challenges”, *Composites Part B: Engineering*, vol. 143, no. December 2017, pp. 172–196, 2018, ISSN: 13598368. DOI: 10.1016/j.compositesb.2018.02.012. [Online]. Available: <https://doi.org/10.1016/j.compositesb.2018.02.012>.
- [44] Y. E. Goldman, “Muscle contraction”, *Enzymes*, vol. 23, no. C, 2003, ISSN: 18746047. DOI: 10.1016/S1874-6047(04)80002-7.
- [45] S. Ebashi, M. Endo, and I. Ohtsuki, “Control of muscle contraction”, *Quarterly Reviews of Biophysics*, vol. 2, no. 4, pp. 351–384, 1969, ISSN: 14698994. DOI: 10.1017/S003358350001190.
- [46] D. Aitchison Smith, *Cooperative Muscular Activation by Calcium BT - The Sliding-Filament Theory of Muscle Contraction*. 2018, pp. 347–373, ISBN: 978-3-030-03526-6. [Online]. Available: https://doi.org/10.1007/978-3-030-03526-6_8.

- [47] C. Ibáñez, “Real-time EMG Control for Hand Exoskeletons”, p. 69, 2018.
- [48] M. Zahak, “Signal Acquisition Using Surface EMG and Circuit Design Considerations for Robotic Prosthesis”, *Computational Intelligence in Electromyography Analysis - A Perspective on Current Applications and Future Challenges*, 2012. DOI: 10.5772/52556.
- [49] J. Wang, L. Tang, and J. E Bronlund, “Surface EMG Signal Amplification and Filtering”, *International Journal of Computer Applications*, vol. 82, no. 1, pp. 15–22, 2013. DOI: 10.5120/14079-2073.
- [50] J. P. van Vugt and J. G. van Dijk, “A convenient method to reduce crosstalk in surface EMG. Cobb Award-winning article, 2001.”, *Clinical neurophysiology: official journal of the International Federation of Clinical Neurophysiology*, vol. 112, no. 4, pp. 583–92, 2001, ISSN: 1388-2457. [Online]. Available: <http://linkinghub.elsevier.com/retrieve/pii/S1388245701004825><http://www.ncbi.nlm.nih.gov/pubmed/11275529>.
- [51] D. Farina, C. Cescon, and R. Merletti, “Influence of anatomical, physical, and detection-system parameters on surface EMG.”, *Biological cybernetics*, vol. 86, no. 6, pp. 445–456, 2002, ISSN: 03401200. DOI: 10.1007/s00422-002-0309-2.
- [52] A. Fleming, N. Stafford, S. Huang, X. Hu, D. P. Ferris, and H. H. Huang, “Myoelectric control of robotic lower limb prostheses: A review of electromyography interfaces, control paradigms, challenges and future directions”, *Journal of Neural Engineering*, vol. 18, no. 4, 2021, ISSN: 17412552. DOI: 10.1088/1741-2552/ac1176.
- [53] D. G. Madusanka, L. N. Wijayasingha, R. A. Gopura, Y. W. Amarasinghe, and G. K. Mann, “A review on hybrid myoelectric control systems for upper limb prosthesis”, *MERCon 2015 - Moratuwa Engineering Research Conference*, vol. 3, pp. 136–141, 2015. DOI: 10.1109/MERCon.2015.7112334.
- [54] Y. M. Wong and G. Y. Ng, “Surface electrode placement affects the EMG recordings of the quadriceps muscles”, *Physical Therapy in Sport*, vol. 7, no. 3, pp. 122–127, 2006, ISSN: 1466853X. DOI: 10.1016/j.ptsp.2006.03.006.
- [55] *What is EMG sensor, Myoware and How to use with Arduino? - Latest Open Tech From Seeed*. [Online]. Available: <https://www.seeedstudio.com/blog/2019/12/29/what-is-emg-sensor-myoware-and-how-to-use-with-arduino/> (visited on 2023-02-23).
- [56] C. Calderon-Cordova, C. Ramirez, V. Barros, P. A. Quezada-Sarmiento, and L. Barba-Guaman, “EMG signal patterns recognition based on feedforward Artificial Neural Network applied to robotic prosthesis myoelectric control”, *FTC 2016 - Proceedings of Future Technologies Conference*, no. December, pp. 868–875, 2017. DOI: 10.1109/FTC.2016.7821705.

- [57] *The geniuses who invented prosthetic limbs - BBC Future*. [Online]. Available: <https://www.bbc.com/future/article/20151030-the-geniuses-who-invented-prosthetic-limbs> (visited on 2023-01-31).
- [58] P. Hernigou, “Ambroise Paré IV: The early history of artificial limbs (from robotic to prostheses)”, *International Orthopaedics*, vol. 37, no. 6, pp. 1195–1197, 2013, ISSN: 03412695. DOI: 10.1007/s00264-013-1884-7.
- [59] K. S. Tanaka and N. Lightdale-Miric, “Advances in 3D-printed pediatric prostheses for upper extremity differences”, *Journal of Bone and Joint Surgery - American Volume*, vol. 98, no. 15, pp. 1320–1326, 2016, ISSN: 15351386. DOI: 10.2106/JBJS.15.01212.
- [60] *e-NABLE Devices Catalog - e-NABLE*. [Online]. Available: <https://hub.e-nable.org/s/e-nable-devices/wiki/page/view?title=Phoenix+v2+Hand> (visited on 2022-02-13).
- [61] *Nazree’s Prosthetic Hand | 3D CAD Model Library | GrabCAD*. [Online]. Available: <https://grabcad.com/library/nazree-s-prosthetic-hand-1> (visited on 2023-02-23).
- [62] F. C. B. Dias Pinheiro, “Development of a Functional Upper Limb Prosthesis”, no. May, p. 8, 2018.
- [63] A. Oliveira, C. Quaresma, and B. Soares, “Development of a 3D-printed body-powered prosthesis with flexible materials”, *Advances and Current Trends in Biomechanics*, pp. 294–298, 2021. DOI: 10.1201/9781003217152-65.
- [64] *Ottobock worldwide – innovations that move people | Ottobock SE Co. KGaA*. [Online]. Available: <https://www.ottobock.com/en/> (visited on 2022-02-13).
- [65] *bebionic | Ottobock US*. [Online]. Available: <https://www.ottobockus.com/prosthetics/upper-limb-prosthetics/solution-overview/bebionic-hand/> (visited on 2022-02-13).
- [66] *Michelangelo prosthetic hand | Ottobock US*. [Online]. Available: <https://www.ottobockus.com/prosthetics/upper-limb-prosthetics/solution-overview/michelangelo-prosthetic-hand/> (visited on 2022-02-13).
- [67] P. Golder and D. Mitra, *Product Design and Development*. 2018, pp. 171–172, ISBN: 9780078029066. DOI: 10.4337/9781784718152.00017.
- [68] U. D. E. Lisboa, “Development and Optimization of a Low-Cost Myoelectric Upper Limb Prosthesis Ema de Matos Castanheira e Lopes”, 2022.
- [69] A. Ullah, S. Ali, I. Khan, M. A. Khan, and S. Faizullah, “Effect of analysis window and feature selection on classification of hand movements using EMG signal”, *Advances in Intelligent Systems and Computing*, vol. 1252 AISC, no. September, pp. 400–415, 2021, ISSN: 21945365. DOI: 10.1007/978-3-030-55190-2_30. arXiv: 2002.00461.

- [70] M. Zahak Jamal, "Signal Acquisition Using Surface EMG and Circuit Design Considerations for Robotic Prosthesis", *Intech*, vol. 11, no. tourism, p. 13, 2016, ISSN: 17187729. DOI: 10.5772/52556. [Online]. Available: <https://www.intechopen.com/books/advanced-biometric-technologies/liveness-detection-in-biometrics>.
- [71] *System Usability Scale (SUS) | Usability.gov*. [Online]. Available: <https://www.usability.gov/how-to-and-tools/methods/system-usability-scale.html> (visited on 2023-01-17).
- [72] *Measuring and Interpreting System Usability Scale (SUS) - UIUX Trend*. [Online]. Available: <https://uiuxtrend.com/measuring-system-usability-scale-sus/> (visited on 2023-01-17).
- [73] L. Takayama, G. S. A. D. Merino, E. A. D. Merino, L. J. Garcia, J. M. Cunha, and S. C. Domenech, "Hand tool project requirements: the case of banana cultivation and its physical demands (OWAS)", *Product Management Development*, vol. 13, no. 2, pp. 119–130, 2015. DOI: 10.4322/pmd.2015.012.
- [74] *Data Acquisition, Loggers, Amplifiers, Transducers, Electrodes | BIOPAC*. [Online]. Available: <https://www.biopac.com/> (visited on 2023-03-17).
- [75] *Flexor digitorum superficialis: Origin, insertion, action | Kenhub*. [Online]. Available: <https://www.kenhub.com/en/library/anatomy/flexor-digitorum-superficialis-muscle> (visited on 2023-03-17).
- [76] *Flexor digitorum superficialis: Origin, insertion, action | Kenhub*. [Online]. Available: <https://www.kenhub.com/en/library/anatomy/flexor-digitorum-superficialis-muscle> (visited on 2023-03-17).
- [77] *Flexor digitorum superficialis: Origin, insertion, action | Kenhub*. [Online]. Available: <https://www.kenhub.com/en/library/anatomy/flexor-digitorum-superficialis-muscle> (visited on 2023-03-17).
- [78] *Flexor digitorum superficialis: Origin, insertion, action | Kenhub*. [Online]. Available: <https://www.kenhub.com/en/library/anatomy/flexor-digitorum-superficialis-muscle> (visited on 2023-03-17).
- [79] F. A. Bernardini, M. T. da Silva, J. M. Abe, L. A. de Lima, and K. Miatluk, "Analysis of the Displacement of Terrestrial Mobile Robots in Corridors Using Paraconsistent Annotated Evidential Logic $E\tau$ ", no. November, pp. 167–175, 2020. DOI: 10.5121/csit.2020.101115.
- [80] TowerPro, "Datasheet SG90 9g Micro Servo", *Cytron Technologies*, pp. 3–5, 2018. [Online]. Available: http://www.ee.ic.ac.uk/pcheung/teaching/DE1_EE/stores/sg90_datasheet.pdf<https://datasheetpdf.com/pdf-file/791970/TowerPro/SG90/1>.

BIBLIOGRAPHY

- [81] Z. M. Li, S. Dun, D. A. Harkness, and T. L. Brininger, "Motion enslaving among multiple fingers of the human hand", *Motor Control*, vol. 8, no. 1, pp. 1–15, 2004, ISSN: 15432696. DOI: 10.1123/mcj.8.1.1.
- [82] C. Hager-Ross and M. H. Schieber, "Quantifying the independence of human finger movements: Comparisons of digits, hands, and movement frequencies", *Journal of Neuroscience*, vol. 20, no. 22, pp. 8542–8550, 2000, ISSN: 02706474. DOI: 10.1523/jneurosci.20-22-08542.2000.
- [83] M. Flückiger, T. Grosshauser, and G. Tröster, "Precision finger pressing force sensing in the pianist-piano interaction", *SMC 2016 - 13th Sound and Music Computing Conference, Proceedings*, pp. 137–142, 2019.
- [84] ALLDATASHEETCOM, "MG995 High Speed Servo Actuator",
- [85] *Turnigy TGY-MG958 Composite Digital Metal Gear Servo - Digiware Store*. [Online]. Available: <https://digiwarestore.com/en/servo/turnigy-tgy-mg958-composite-digital-metal-gear-servo-713217.html> (visited on 2023-03-17).
- [86] *HS-5645MG High Torque, Metal Gear Digital Sport Servo | HITEC RCD USA*. [Online]. Available: <https://hitecrd.com/products/servos/sport-servos/digital-sport-servos/hs-5645mg/product> (visited on 2023-03-17).
- [87] "A Scientist's Guide to Buying a 3D Printer: How to Choose the Right Printer for Your Laboratory", *Analytical Chemistry*, vol. 92, no. 22, pp. 14 853–14 860, 2020, ISSN: 15206882. DOI: 10.1021/acs.analchem.0c03299.
- [88] M. L. Smith and J. F. Jones, "Dual-extrusion 3D printing of anatomical models for education", *Anatomical Sciences Education*, vol. 11, no. 1, pp. 65–72, 2018, ISSN: 19359780. DOI: 10.1002/ase.1730.
- [89] DEVELOP3D, *Raise3D E2 Review - DEVELOP3D*. [Online]. Available: <https://develop3d.com/3d-printing/raise3d-e2-review-3d-printer/> (visited on 2023-01-16).
- [90] D. M. S. T. 3. Shop, *Review", 3D Printers Online Shop Top3DShop.com "Raise3D E2 3D Printer*. [Online]. Available: <https://top3dshop.com/blog/raise3d-e2-3d-printer-review> (visited on 2023-01-16).
- [91] H. M. McHenry, "Body size and proportions in early hominids", *American Journal of Physical Anthropology*, vol. 87, no. 4, pp. 407–431, 1992, ISSN: 10968644. DOI: 10.1002/ajpa.1330870404.

Additional Details on the Concept Development

This Appendix presents a more detailed description of the methodology used in this study, which was inspired in the Product Design and Development methodology [67]. Figure A.1 presents the long version of the flowchart that illustrates the development process of the prosthesis.

APPENDIX A. ADDITIONAL DETAILS ON THE CONCEPT DEVELOPMENT

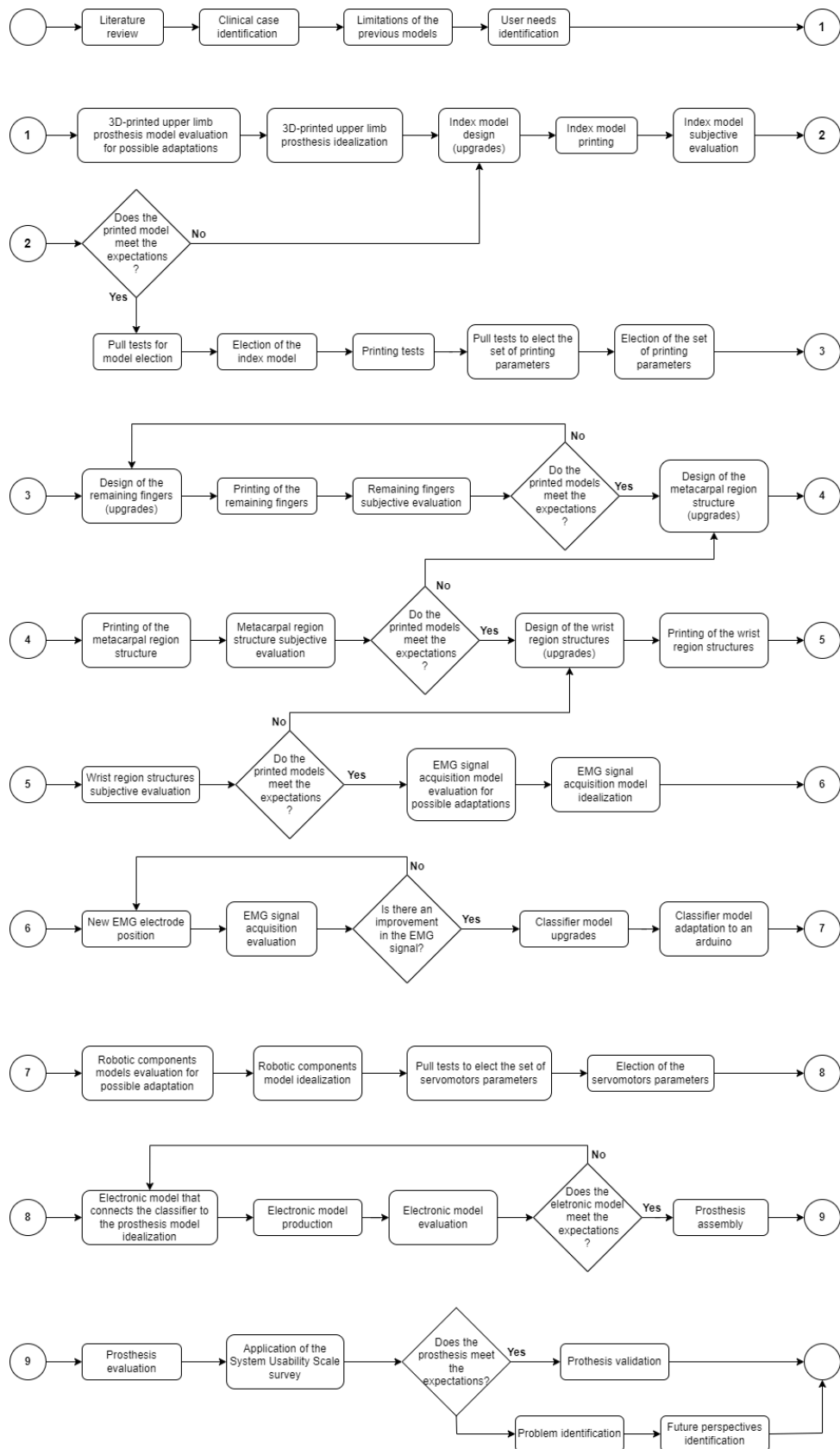


Figure A.1: Extended methodology flowchart

Filament Technical Data Sheet

This Appendix presents the technical data sheet provided by Recreus, the filaments manufacturer, for both *Filaflex 60A Pro* and *Filaflex 70A*. It is recommended to upload the printing profiles to the chosen slicer software, which in this study is the *PrusaSlicer* software (version 2.5.0). Printing settings not shown in those files should be left untouched.

TECHNICAL DATA SHEET

FILAFLEX 60A 'PRO'

Description

Filaflex is a Thermoplastic Polyether-Polyurethane elastomer with additives that allow high printability in FDM printers. Filaflex® has a remarkable hydrolysis resistance, high resistance to bacteria and low temperature flexibility properties in printed parts.

Physical properties	Value	Unit	Test method according to
Material density	1.07	g/cm ³	DIN EN ISO 1183-1-A

Mechanical properties	Value	Unit	Test method according to
Hardness	63	Shore A	DIN ISO 7619-1 (3s)
Tensile strength	26	MPa	DIN 53504-S2
Elongation at break	950	%	DIN 53504-S2
Stress at 20% elongation	1	MPa	DIN 53504-S2
Stress at 100% elongation	2.5	MPa	DIN 53504-S2
Stress at 300% elongation	4.5	MPa	DIN 53504-S2
Tear strength	40	N/mm	DIN ISO 34-1Bb
Abrasion loss	45	mm ³	DIN ISO 4649-A
Compression set 23°C / 72 hours	40	%	DIN ISO 815
Compression set 70°C / 24 hours	25	%	DIN ISO 815

Printing properties	Recommended
Printing temperatures	215 - 235°C
Printing speed	20 - 30 mm/s
Hot-bed temperature	21°C
Optimal layer height	0.2 mm
Minimal nozzle diameter	0.4 mm or higher
Retraction parameters	3.5 - 6.5 mm (speed 20 - 160 mm/s)

TECHNICAL DATA SHEET
FILAFLEX 70A ULTRA-SOFT
Description

Filaflex is a Thermoplastic Polyether-Polyurethane elastomer with additives that allow high printability in FDM printers. Filaflex® has remarkable abrasion resistance, higher tolerance to hydrolysis failure, high resistance to bacteria and low temperature flexibility properties in printed parts.

Physical Property	Value	Unit	Test method according to
Material density	1,08	g/cm ³	ISO 1183

Mechanical Property	Value	Unit	Test method according to
Hardness	70	shore A	DIN ISO 7619-1 (3s)
Tensile strength	32	MPa	DIN 53504-S2
Elongation at break	900	%	DIN 53504-S2
Stress at 20% elongation	1,5	%	DIN 53504-S2
Stress at 100% elongation	4	%	DIN 53504-S2
Stress at 300% elongation	6	%	DIN 53504-S2
Tear strength	45	N/mm	ISO 34-1
Abrasion resistant	45	mm ³	ISO 4649
Compression set 23°C/72 hours	20	%	ISO 815
Compression set 70°C/24 hours	39	%	ISO 815
Tensile strength after storage in water at 80°C for 42 days	20	Mpa	DIN 53504-S2
Elongation at break after storage in water at 80°C for 42 days	900	%	DIN 53504-S2
Notched impact strength (Charpy)n at +23°C	nb	kJ/m ²	ISO 179

Thermal Property	Value	Unit	Test method according to
Glass Transition Temperature 10°C/min	-50	°C	ISO 11357-1/-2
VST Vicat Softening Temperature	84	°C	Método Vicat A: 10 Nw, 120°C/h

Printing Proprieties	Recommended
Printing temperatures	215-235°C
Printing speed	20-40 mm/s
Hot-bed temperature	0-40°C
Retractions	3,5-6,5mm (speed 20 - 40mm/s)

Recommended Printing Parameters

This Appendix presents the printing settings recommended for the development of this project. The printing parameters were tested in a previous study with the aim of concluding on the best set of parameters that combine a good printing quality with low forces needed to flex the prosthesis. The printing parameters have shown to be good enough for the project in hand and were used during the whole duration of the project. Figure C.1 presents the print settings for the *The Original Prusa i3 MK3S+* printer and Figure C.2 recommended the filament settings for the best printing quality and properties using *Filaflex 60A* . Printing settings not shown in the Figures should be left untouched.

APPENDIX C. RECOMMENDED PRINTING PARAMETERS

Layer height

- Layer height: • mm
- First layer height: • mm

Vertical shells

- Perimeters: • (minimum)
- Spiral vase:

Recommended object thin wall thickness for layer height 0.20 and 2 lines: 0.60 mm , 3 lines: 0.87 mm , 4 lines: 1.15 mm , 5 lines: 1.43 mm , 6 lines: 1.71 mm

Horizontal shells

- Solid layers: Top: • Bottom: •
- Minimum shell thickness: Top: • mm Bottom: • mm

Top shell is 0.8 mm thick for layer height 0.2 mm. Minimum top shell thickness is 0.28 mm.
Bottom shell is 0.8 mm thick for layer height 0.2 mm. Minimum bottom shell thickness is 0.28 mm.

Infill

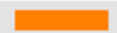
- Fill density: • %
- Fill pattern: •
- Length of the infill anchor: • mm or %
- Maximum length of the infill anchor: • mm or %
- Top fill pattern: •
- Bottom fill pattern: •

Speed for print moves

- Perimeters: • mm/s
- Small perimeters: • mm/s or %
- External perimeters: • mm/s or %
- Infill: • mm/s
- Solid infill: • mm/s or %
- Top solid infill: • mm/s or %
- Support material: • mm/s
- Support material interface: • mm/s or %
- Bridges: • mm/s
- Gap fill: • mm/s
- Ironing: • mm/s

Figure C.1: Print Settings parameters used in the *PrusaSlicer* software.

Filament

- Color: • 
- Diameter: • mm
- Extrusion multiplier: •
- Density: • g/cm³
- Cost: • money/kg
- Spool weight: • g

Temperature

- Nozzle: First layer: • °C Other layers: • °C
- Bed: First layer: • °C Other layers: • °C

Enable

- Keep fan always on: •
- Enable auto cooling: •

If estimated layer time is below ~20s, fan will run at 50% and print speed will be reduced so that no less than 20s are spent on that layer (however, speed will never be reduced below 15mm/s).
 During the other layers, fan will always run at 30% except for the first 3 layers.

Figure C.2: Filament Settings parameters used in the *PrusaSlicer* software.

Pull Tests

This Appendix presents the protocol defined to evaluate some of the developed prototypes of the fingers. This protocol developed with the aim of testing the flexibility of different designs as well as assess the best printing parameters that would lead to higher level of functionality. This Appendix also presents the drawings of the finger support and horizontal tab designed for the pull tests protocols as well as the values of several pull tests that were made. This values can be consulted in Tables D.1 up to D.14.



Pull Tests Protocol

Study Description:

This protocol was established within the scope of a Biomedical Engineering Master Thesis aiming to develop a body-powered hand prosthesis with flexible materials by Additive Manufacturing. This study is taking place on NOVA School of Science and Technology in partnership with *Patient Innovation*.

The main goal of this study is to improve the cosmetic appearance and increase flexibility of 3D-printed body-powered prosthesis through the replacement of the stiff material that composes *e-Nable* prostheses. This material will be replaced by a combination of rigid and flexible materials in order to give these prostheses a more real-life appearance.

For this purpose, it was necessary to determinate the optimal materials combination as well as analyse some of the existent prostheses. The identification of the user's needs is crucial to determine the prosthesis specifications and therefore create some concepts aiming to identify the best model to develop. Concerning concepts generation and selection, it was desired a high level of customization, especially regarding to the size of printed hand when compared to the sound hand. Establishing sensory feedback was also a concern.

Finally, as a result of the created concepts several prototypes for testing and concept validation were designed, according to Product Design and Development methodology.



Data Collection Goals:

The presented protocol describes the methodology for the pull tests used to evaluate the printed fingers in terms of force needed to bend each finger model.

The prosthesis development was divided into three main design stages. Fingers were the first components to be addressed as there were previous studies about them. During this stage, only the index was designed. After validating the index design, its design could be used in the other fingers. During this study, several different models were developed. However, only some of them were subjected to pull tests.

During the design of the fingers, several printing tests were also performed in order to find the best printing quality. However, despite all efforts, it was quite difficult to determine the best printing parameters, which combine a good printing quality and low bending forces, so more tests were required. These additional tests had the goal of selecting the material model and infill properties that produce the finger prototype with ideal behaviour.

Thus, the main goal of this protocol is to determine which printing parameters will be used on index model, by measuring the necessary force to bend those fingers. Following this methodology allows to evaluate the fingers objectively, avoiding errors from a subjective assessment.



Methodology Principle:

This protocol measures the force needed to bend each finger model. Metallic cylinders with different masses will be applied to the fingers, generating different forces and causing the finger to bend. Consequently, the fingertip suffers an approximately vertical displacement that is measured with a dial gauge. The measures stop when the weight applied to the finger reaches 2 000g.

The dynamometer weight as well as the weight of the tissue bag used to place the weight will increase the applied force. Both the dynamometer and the tissue bag must be weighed, so the real applied force is known. This force is given by the following equation, where m_{bag} , m_{din} and m are the masses of the tissue bag, dynamometer and metallic cylinders, respectively, and g , the gravitational constant:

$$W = (m_{bag} + m_{din} + m) \cdot g$$

However, it is expected that the W value and the value measured from the dynamometer do not present significant differences.

Methodology

The present protocol was developed considering the laboratory environment and conditions. Regarding the main goals of this protocol, the methodology does not need to be very strict nor need the usage of expensive equipment.

The only requirement needed to test the fingers was an elevated structure where the fingers could be fixed, and its wire could be pulled vertically. For the present study, a support that can be fixed by screws to the available elevated structure was designed as well as a horizontal tab, so the contact with the tab fitted into the top of the dynamometer. The fingers are then fixed to a fitting hole. Figure 1 shows the 3D printed designed support and the horizontal tab, also 3D printed with *PET*.



Figure 1. Designed structures for the present protocol: (a) finger support; (b) horizontal tab.

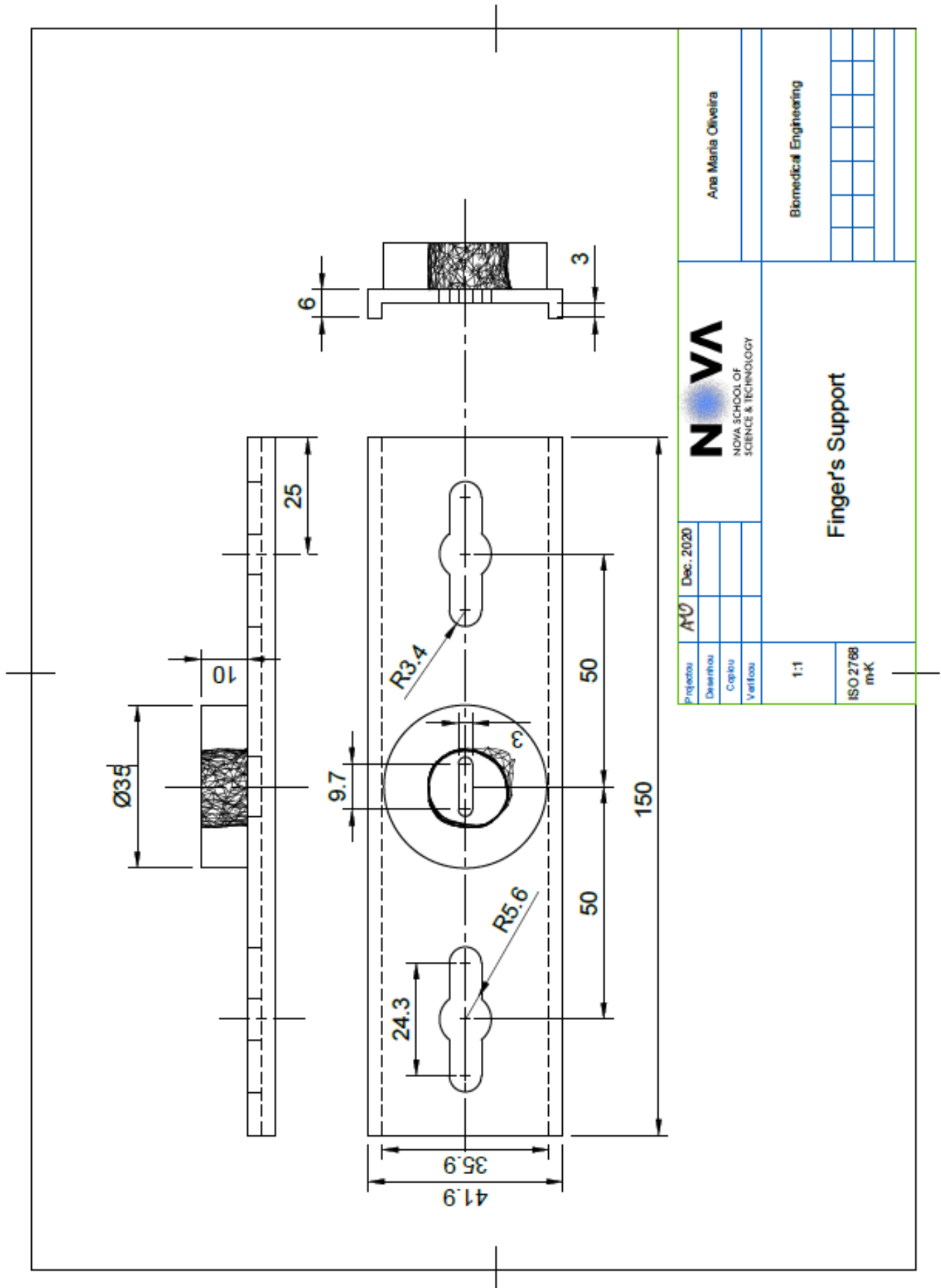


Materials:

- Finger support;
- Acoustic guitar string, E and B (40 *cm* for each finger);
- 2 screws and respective nuts and washers;
- Small nuts;
- Dial gauge;
- Dynamometer;
- Light tissue bag;
- Pliers;
- Weights.

Procedures:

1. Weight the tissue bag and dynamometer and register values. Repeat this step two more times and calculate the mean value of their weights.
2. Fix the finger's support to the elevated structure using the screws and respective nuts. For this study $M8 \times 50$ screws were used,
3. Pass the metal wire through the finger and lock it at the top by wrapping the wire's tip around the small nut with the pliers' help.
4. Insert the finger at the finger's support, making sure the wire passes through the support's hole.
5. Fix the horizontal tab at the top of the dynamometer.
6. Fix the dynamometer at the other end of the wire. If necessary, use the pliers once more.
7. Tie the tissue bag to the dynamometer's far end.
8. Fix the dial gauge at the elevated structure. Its pointer must be placed at its maximum displacement and simultaneously touching the horizontal tab. Make sure the dial gauge is calibrated.
9. Place the weights inside the tissues bag, starting at 200*g* and then adding 200*g* at a time until the weight of 2 000*g* is reached. For the present study, the available metallic cylinders had masses between 100*g* and 800*g*. Higher mass values were obtained by combining cylinders. If between two values the finger reaches the maximum bending capacity, measure the medium value between the last two values.
10. Read the dynamometer's value as well as the marked value in the dial gauge for each added weight and register the values read. Repeat this step three in total for each finger.



Projectou	AVO	Dec. 2020
Desenhou		
Copiou		
Verificou		

NOVA
NOVA SCHOOL OF
SCIENCE & TECHNOLOGY

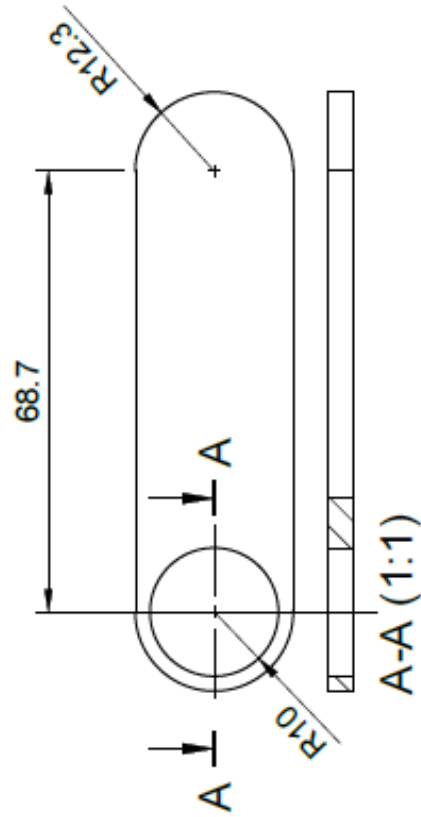
Ana Maria Oliveira

Biomedical Engineering

Finger's Support

1:1

ISO 2768
mK



Projecto:	AMU	Dec. 2020	NOVA		Ana Maria Oliveira
Desenho:			NOVA SCHOOL OF SCIENCE & TECHNOLOGY		Biomedical Engineering
Capitulo:			Horizontal Tab		
Verificou:					
1:1					
ISO 2768 m-K					

Table D.1: Pull tests results of the model printed with *Filaflex 60A* and 25% infill

Force (N)	Measurements (mm)				Mean	Displacement (mm)			
	1st	2nd	3rd	Mean		1st	2nd	3rd	Mean
2	63,0	63,5	63,2	63,2	2,0	1,5	1,8	1,8	
4	61,3	62,0	61,0	61,4	3,7	3,0	4,0	3,6	
6	60,0	59,5	60,0	59,8	5,0	5,5	5,0	5,2	
8	54,0	54,5	54,0	54,2	11,0	10,5	11,0	10,8	
10	53,0	53,0	53,0	53,0	12,0	12,0	12,0	12,0	
12	51,0	51,0	51,0	51,0	14,0	14,0	14,0	14,0	
14	46,0	46,0	46,5	46,2	19,0	19,0	18,5	18,8	
16	45,0	44,5	45,0	44,8	20,0	20,5	20,5	20,2	
18	41,5	42,0	42,0	41,8	23,5	23,0	23,0	23,2	
20	38,0	38,0	38,0	38,0	27,0	27,0	27,0	27,0	

Table D.2: Predicted behaviour of the model printed with *Filaflex 60A* and 25% infill

Force (N)	Measurements (mm)	Mean (y = 0 mm)
2	-2,92	1,88
4	4,69	9,49
6	9,13	13,93
8	12,29	17,09
10	14,74	19,54
12	16,74	21,54
14	18,43	23,23
16	19,89	24,69
18	21,18	25,98
20	22,34	27,14
22	23,38	28,18
24	24,34	29,14
26	-	-
28	-	-
30	-	-

Table D.3: Pull tests results of the model printed with *Filaflex 60A* and 30% infill

Force (N)	Measurements (mm)				Mean)	Displacement (mm)			Mean
	1st	2nd	3rd			1st	2nd	3rd	
2	64,0	64,5	64,0	64,2	1,0	0,5	1,0	0,8	
4	62,5	62,0	62,0	62,2	2,5	3,0	3,0	2,8	
6	60,0	60,0	60,0	60,0	5,0	5,0	5,0	5,0	
8	57,0	57,5	57,0	57,2	8,0	7,5	8,0	7,8	
10	56,0	56,0	56,0	56,0	9,0	9,0	9,0	9,0	
12	53,0	53,5	50,5	52,5	12,0	11,5	14,5	12,7	
14	50,0	50,0	50,5	50,5	15,0	15,0	15,0	15,0	
16	45,5	46,5	46,0	46,3	18,5	18,5	19,0	18,7	
18	44,5	44,0	43,5	44,0	20,5	21,0	21,5	21,0	
20	41,0	40,0	40,5	40,5	24,0	25,0	24,5	24,5	

Table D.4: Predicted behaviour of the model printed with *Filaflex 60A* and 30% infill

Force (N)	Measurements (mm)	Mean (y = 0 mm)
2	-4,18	0,80
4	3,48	7,80
6	7,58	11,90
8	10,48	14,80
10	12,73	17,05
12	14,57	18,89
14	16,13	20,45
16	17,48	21,80
18	18,67	22,99
20	19,73	24,05
22	20,70	25,02
24	21,57	25,89
26	22,38	26,70
28	23,13	27,45
30	23,83	28,15

Table D.5: Pull tests results of the model printed with *Filaflex 60A* and 40% infill

Force (N)	Measurements (mm)				Mean	Displacement (mm)			
	1st	2nd	3rd	Mean		1st	2nd	3rd	Mean
2	64,0	63,0	64,0	63,7	1,0	2,0	1,0	1,3	
4	63,0	62,5	63,0	62,8	2,0	2,5	2,0	2,2	
6	60,0	60,0	60,0	60,0	5,0	5,0	5,0	5,0	
8	58,0	57,5	58,0	57,8	7,0	7,5	7,0	7,2	
10	54,0	54,0	53,5	53,8	11,0	11,0	11,5	11,2	
12	53,0	53,0	53,0	53,0	12,0	12,0	12,0	12,0	
14	50,0	50,5	50,0	50,2	15,0	14,5	15,0	14,8	
16	45,0	45,0	45,0	45,0	20,0	20,0	20,0	20,0	
18	41,0	41,0	41,5	41,2	24,0	24,0	23,5	23,8	
20	40,0	40,0	40,0	40,0	25,0	25,0	25,0	25,0	

Table D.6: Predicted behaviour of the model printed with *Filaflex 60A* and 40% infill

Force (N)	Measurements (mm)	Mean (y = 0 mm)
2	-3,92	1,30
4	3,50	8,72
6	7,84	13,06
8	10,92	16,14
10	13,31	18,53
12	15,26	20,48
14	16,91	22,13
16	18,34	23,56
18	19,60	24,82
20	20,73	25,95
22	21,75	26,97
24	22,68	27,90
26	23,54	28,76
28	24,33	28,76
30	-	-

Table D.7: Pull tests results of the model printed with *Filaflex 60A* and 50% infill

Force (N)	Measurements (mm)				Mean	Displacement (mm)			
	1st	2nd	3rd	Mean		1st	2nd	3rd	Mean
2	64,0	64,5	64,0	64,2	1,0	0,5	1,0	0,8	
4	63,5	63,5	63,5	63,5	1,5	1,5	1,5	1,5	
6	62,0	62,0	62,0	62,0	3,0	3,0	3,0	3,0	
8	60,0	60,5	60,0	60,2	5,0	4,5	5,0	4,8	
10	59,0	59,5	58,0	58,8	6,0	5,5	7,0	6,2	
12	56,0	55,5	55,5	55,7	9,0	9,5	9,5	9,3	
14	54,0	54,0	54,0	54,0	11,0	11,0	11,0	11,0	
16	49,0	48,5	48,5	48,7	16,0	16,5	16,5	16,3	
18	45,0	45,5	45,0	45,2	20,0	19,5	20,0	19,8	
20	43,5	44,0	43,5	43,7	21,5	21,0	21,5	21,3	

Table D.8: Predicted behaviour of the model printed with *Filaflex 60A* and 50% infill

Force (N)	Measurements (mm)	Mean (y = 0 mm)
2	-4,18	0,80
4	2,06	7,04
6	5,71	10,69
8	8,30	13,28
10	10,31	15,29
12	11,95	16,93
14	13,34	18,32
16	14,54	19,52
18	15,60	20,58
20	16,55	21,53
22	17,40	22,38
24	18,19	23,17
26	18,91	23,89
28	19,57	24,55
30	20,19	25,17

Table D.9: Pull tests results of the model printed with *Filaflex 70A* and 25% infill

Force (N)	Measurements (mm)				Mean	Displacement (mm)			
	1st	2nd	3rd	Mean		1st	2nd	3rd	Mean
2	64,0	64,0	64,0	64,0	1,0	1,0	1,0	1,0	
4	63,0	62,5	63,0	62,8	2,0	2,5	2,0	2,2	
6	59,0	59,0	59,0	59,0	6,0	6,0	6,0	6,0	
8	57,0	57,5	57,5	57,3	8,0	7,5	7,5	7,7	
10	55,5	55,0	55,5	55,3	9,5	10,0	9,5	9,7	
12	53,5	53,5	54,0	53,7	11,5	11,5	11,0	11,3	
14	52,0	21,5	51,5	51,7	13,0	13,5	13,5	13,3	
16	49,5	49,0	49,0	49,2	15,5	16,0	16,0	15,8	
18	47,0	46,0	46,0	46,3	18,0	19,0	19,0	18,7	
20	45,0	44,5	44,5	44,7	20,0	20,5	20,5	20,3	

Table D.10: Predicted behaviour of the model printed with *Filaflex 70A* and 25% infill

Force (N)	Measurements (mm)	Mean (y = 0 mm)
2	-2,26	1,00
4	3,64	6,90
6	7,09	10,35
8	9,54	12,80
10	11,44	14,70
12	13,00	16,26
14	14,31	17,57
16	15,45	18,71
18	16,45	19,71
20	17,35	20,61
22	18,16	21,42
24	18,90	22,16
26	19,58	22,84
28	20,21	23,47
30	20,80	24,06

Table D.11: Pull tests results of the model printed with *Filaflex 70A* and 30% infill

Force (N)	Measurements (mm)				Mean	Displacement (mm)			
	1st	2nd	3rd	Mean		1st	2nd	3rd	Mean
2	65,0	65,0	64,5	64,8	0,0	0,0	0,5	0,2	
4	63,5	64,0	64,0	63,8	1,5	1,0	1,0	1,2	
6	62,0	62,0	62,5	62,2	3,0	3,0	2,5	2,8	
8	59,5	60,0	60,0	59,8	5,5	5,0	5,0	5,2	
10	57,5	57,5	57,5	57,5	7,5	7,5	7,5	7,5	
12	56,0	55,0	56,0	55,7	9,0	10,0	9,0	9,3	
14	53,0	53,0	53,5	53,2	12,0	12,0	11,5	11,8	
16	50,0	50,0	49,5	49,8	15,0	15,0	15,5	15,2	
18	48,0	48,5	48,0	48,2	17,0	16,5	17,0	16,8	
20	46,0	47,0	47,0	46,7	19,0	18,0	18,0	18,3	

Table D.12: Predicted behaviour of the model printed with *Filaflex 70A* and 30% infill

Force (N)	Measurements (mm)	Mean (y = 0 mm)
2	-3,73	0,20
4	2,03	5,96
6	5,40	9,33
8	7,80	11,73
10	9,65	13,58
12	11,17	15,10
14	12,45	16,38
16	13,56	17,49
18	14,54	18,47
20	15,42	19,35
22	16,21	20,14
24	17,60	20,87
26	18,22	22,15
28	18,79	22,72
30	19,33	23,26

Table D.13: Pull tests results of the model printed with *Filaflex 70A* and 40% infill

Force (N)	Measurements (mm)			Mean	Displacement (mm)			Mean
	1st	2nd	3rd		1st	2nd	3rd	
2	65,0	65,0	65,0	65,0	0,0	0,0	0,0	0,0
4	65,0	65,0	65,0	65,0	0,0	0,0	0,0	0,0
6	64,0	64,5	64,0	64,2	1,0	0,5	1,0	0,8
8	64,0	63,5	63,5	63,7	1,0	1,5	1,5	1,3
10	62,5	62,5	62,0	62,3	2,5	2,5	3,0	2,7
12	62,0	62,0	62,0	62,0	3,0	3,0	3,0	3,0
14	61,0	61,0	61,0	61,0	4,0	4,0	4,0	4,0
16	59,5	60,0	60,0	59,8	5,5	5,0	5,0	5,2
18	58,0	59,5	58,5	58,7	7,0	5,5	6,5	6,3
20	57,0	57,0	57,0	57,0	8,0	8,0	8,0	8,0

Table D.14: Predicted behaviour of the model printed with *Filaflex 70A* and 40% infill

Force (N)	Measurements (mm)	Mean (y = 0 mm)
2	-6,29	0
4	-2,36	0
6	-0,06	0,80
8	1,56	2,42
10	2,83	3,69
12	3,86	4,72
14	4,74	5,60
16	5,49	6,35
18	6,16	7,02
20	6,76	7,62
22	7,30	8,16
24	7,79	8,65
26	8,24	9,10
28	8,66	9,52
30	9,05	9,91

| E

System Usability Scale

The following document presents the surveys that were used to obtain the feedback about the prosthetic model, as well as the corresponding results.

System Usability Scale

Study Description:

This survey is being within the scope of a Biomedical Engineering Master Thesis aiming to develop a myoelectric a myoelectric hand prosthesis with flexible materials by Additive Manufacturing. This study is taking place on NOVA School of Science and Technology in partnership with *Patient Innovation*.

The main goal of this study was to improve the cosmetic appearance and functionality of 3D-printed body-powered prostheses through the replacement of the stiff material that composes *e-NABLE* prostheses. This material was replaced by a combination of rigid and flexible materials in order to give these prostheses a more real-life appearance.

For this purpose, it was necessary to determine the optimal materials combination as well as to analyse some of the existent prostheses. The identification of the user's needs was crucial to determine the prosthesis specifications and therefore create some concepts aiming to identify the best model to develop. Concerning concepts generation and selection, it was desired a high level of customization, especially regarding to the size of the printed hand when compared to the sound hand. Establishing sensory feedback was also a concern.

Finally, as a result of the created concepts, several prototypes for testing and concept validation were designed, according to Product Design and Development methodology.

Data Collection Goals:

The prosthetic device developed during this study was based on a single clinical case, a child selected from the *Patient Innovation* program “*Dar a Mão*” in order to simplify the course of this research. However, this survey may could be applied to other patients with similar lesions in further studies with a similar methodology.

The present survey has the main goal of evaluating the usability of the prosthesis developed during this study, whereby it is pretended to obtain the feedback of the child and his family. Additionally, the prosthesis functionality as well as their aesthetic appearance, the production cost, weight and the total printing time will also be evaluated.

Thus, in order to assess the level of satisfaction, it will be used a survey with an usability scale, the *System Usability Scale (SUS)*. This is a standard tool that allows to measure the usability of a wide variety of products or even services. It is composed by ten questions with five response options that go from “Strongly Agree” to “Strongly Disagree”, which correspond to a 5 to 1 scores, respectively. These responses are then converted to a score that will correspond to the evaluation in terms of usability.

Finally, an additional survey with ten questions that follow the SUS logic will be presented. However, those questions were adapted to the features of the designed prosthesis, which can be used in further identical studies.

System Usability Scale

1 – Strongly disagree | 5- Strongly agree

- | | 1 | 2 | 3 | 4 | 5 |
|---|---|---|---|---|---|
| 1. I think that I would like to use this device frequently. | | | | | X |
| 2. I found the device unnecessarily complex. | X | | | | |
| 3. I though the device was easy to use. | | | | | X |
| 4. I think that I would need the support of a technical person to be able to use this device. | X | | | | |
| 5. I found the various functions in this device were well integrated. | | | | | X |
| 6. I thought there was too much inconsistency in this system. | X | | | | |
| 7. I would image most people would learn to use this system very quickly. | | | | X | |
| 8. I found the system very cumbersome to use. | X | | | | |
| 9. I felt very confident using the system. | | | | | X |
| 10. I needed to learn a lot of things before I could get going with this system. | X | | | | |

System Usability Scale – Additional Questions

1 – Strongly disagree | 5- Strongly agree

- | | 1 | 2 | 3 | 4 | 5 |
|--|---|---|---|---|---|
| 1. I found the aesthetic appearance of the prosthesis appealing to its daily use. | | | | | X |
| 2. The prosthesis is quite similar to a toy. | X | | | | |
| 3. The prosthesis is quire similar, in aesthetical terms, to a human hand. | | | | | X |
| 4. I think that the prosthesis is easily breakable. | X | | | | |
| 5. I think that the fitting of the prosthesis is uncomfortable. | | | | | X |
| 6. I think that the fitting of the prosthesis is very intuitive. | X | | | | |
| 7. I found the prosthesis' operating mode complicated. | | | | X | |
| 8. I found the system very cumbersome to use. | X | | | | |
| 9. I think that the prosthesis would be good complement for the daily living activities. | | | | | X |
| 10. This prosthesis might consist of a restriction for the daily living activities. | X | | | | |

Prosthesis Costs

The present Appendix presents the discriminated cost of the developed prostheses' material. The total values include the cost of all the components needed to construct the prostheses, including printing supports and electronic material. The cost of all prototypes made during the present study were not considered. Tables F.1 to F.3 present the discriminated cost of the final prototype of the prosthesis, that uses one *MG995-360 micro servo* and a *SG90-360 micro servo*.

APPENDIX F. PROSTHESIS COSTS

Table F.1: Discriminated cost of the printing components for the final prototype of the prosthesis.

Components	Printing Time	Weight	Cost
Index finger	01:58	7,21 g	0,18 €
Little finger	01:44	5,75 g	0,14 €
Middle finger	02:19	8,67 g	0,22 €
Ring finger	01:58	7,21 g	0,18 €
Thumb	01:44	7,13 g	0,18 €
Metacarpal region	13:14	57,23 g	1,43 €
Wrist region	02:54	13,23 g	0,33 €
Pins and Pincaps	00:20	2,2 g	0.05 €
Total:			2,71 €

Table F.2: Discriminated cost of the electronic components for the final prototype of the prosthesis.

Components	Quantity	Weight	Cost
Arduino UNO R3	1	25g	12.12 €
Jumper wire Dupont male-to-male 150mm	10	-	0.75 €
Mini-Breadboard	1	13.1g	1.37 €
Towerpro MG995-360 servo motor 3..7.2V DC	1	55g	12.36 €
Towerpro SG90-360 servo motor 4.8V..6V DC	1	9g	3.57 €
Whadda hc-05 Bluetooth Transmitter Module	1	-	18.05 €
Total:			46.85 €

Table F.3: Discriminated cost of the extra material required for the final prototype of the prosthesis.

Components	Quantity	Cost
Duracell Plus AA Battery 1,5V LR6	4	3.04 €
4xAA (2/2) Battery Support	1	0.52 €
Nylon threads	-	1.90 €
Super glue	1	4.79 €
Total:		10.25 €

